Bi-layer diaphragm walls: Experimental and numerical analysis.

DOCTORAL THESIS

Doctoral thesis by:
Luis Segura-Castillo

Directed by:
Antonio Aguado de Cea
Alejandro Josa

Barcelona, September 2013

Universitat Politècnica de Catalunya
Departament d´Enginyeria de la Construcció

Acta de qualificació de tesi doctoral

Curs acadèmic:

Nom i cognoms
_____

Programa de doctorat
_____

Unitat estructural responsable del programa
_____

Resolució del Tribunal

Reunit el Tribunal designat a l'efecte, el doctorand / la doctoranda exposa el tema de la seva tesi doctoral titulada

_____

_____.

Acabada la lectura i després de donar resposta a les qüestions formulades pels membres titulars del tribunal, aquest atorga la qualificació:

☐ NO APTE   ☐ APROVAT   ☐ NOTABLE   ☐ EXCEL·LENT

(Nom, cognoms i signatura)		(Nom, cognoms i signatura)	
President/a		Secretari/ària	
(Nom, cognoms i signatura)	(Nom, cognoms i signatura)	(Nom, cognoms i signatura)	
Vocal	Vocal	Vocal	

_____, _____ d'/de _____ de _____

El resultat de l'escrutini dels vots emesos pels membres titulars del tribunal, efectuat per l'Escola de Doctorat, a instància de la Comissió de Doctorat de la UPC, atorga la MENCIÓ CUM LAUDE:

☐ SÍ   ☐ NO

(Nom, cognoms i signatura)	(Nom, cognoms i signatura)
Presidenta de la Comissió de Doctorat	Secretària de la Comissió de Doctorat

Barcelona, _____ d'/de _____ de _____

Dedicado a Juancito, papá y Pocho.
Tres pilares en mi vida. Que se han
ido, dejando una huella en mi corazón

ACKNOWLEDGEMENTS - AGRADECIMIENTOS

Comienzo agradeciendo a las dos personas que hicieron posible esta tesis y, en general, esta experiencia. De lo general a lo particular, primero, Antonio Aguado, una persona con una visión global excelente, y segundo, Alejando Josa, detallista y meticuloso. Juntos conforman un equipo magnifico que se complementa casi a la perfección. Gracias por el tiempo, paciencia y sabiduría que me han dedicado.

Agradezco la financiación brindada por el Ministerio de Educación y Ciencia a través del proyecto BIA2010-17478: Procesos constructivos mediante hormigones reforzados con fibras. Al Programa de FPU del Ministerio de Educación por la financiación para la realización del doctorado (AP2010-3789). A Aguado por la financiación al comienzo de la tesis a través del proyecto: CTT-8062. Y al Instituto de Estructuras y Transporte de la Universidad de la República (Uruguay), por el constante apoyo recibido.

Al personal del Laboratorio de Tecnología de Estructuras, en especial Jorge Cabrerizo, por su ayuda durante la campaña experimental. Mi recuerdo a Luis Agulló, que empapaba el ambiente con su alegría. A todos los compañeros de doctorado: André, Francisco, Francesc, Albert, Nayara, Ju, Izelman, Sandra, Pau, Ana, Ahmed, Amin, Liao, Nacho, Catalina, Luca, Yohei, Renan, Júlia. Un agradecimiento especial a Sergio, que estuvo siempre dispuesto y abierto, desde el primer al último día, a dar una mano; y otro a Ricardo, con quien la lucha se trasladó también fuera de la uni.

Agradezco al IET y la FING de la UdelaR, que me han dado la oportunidad de hacer mis primeras armas en esta carrera, en especial, a Gemma, Berardi, el Guti, y Atilio, que me han incentivado y apoyado desde el comienzo y hasta el final de esta aventura que ahora culmina. Al equipo de PERMASTOP, en especial a Raúl Suarez, con quien compartimos días de lucha a pie de obra.

A todos mis compañeros de piso. Gracias Bea, Andrea (gran compañero de lucha, hoy perdido en la batalla), David, Jada y Maribel. Pero principalmente a Elena y Mar, que me recibieron, cuidaron, animaron, mimaron e hicieron posible un comienzo genial de esta aventura. Hicieron que a mi llegada a esta nueva vida me sintiera como en casa, gracias a ustedes Aragó fue mi hogar. …hasta que llegó Coralinda a poner orden... aunque, en estos años, hemos podido descubrir, con alegría, que debajo de esa Coraza, hay un Corazón.

Mucha gente grande en Barcelona. Oriol y Mireia (que también intentaron hacerme bailar); Tommy, Lea, Maco (me hicieron sentir más cerco del barrio); Roberto y Alba (y sus verduras orgánicas!); Susana (siempre en el aire). A Gerard (el orco de la montaña), Maria Isabel (la presidenta), Alejo, Martha Alejandra (te visitaré en Celaya, Guanajuato, Méjico!) y Jorge, un gran grupo. Matías, el Borges chileno, nuestros proyectos recién comienzan. Ita, siempre al firme para ver o hacer rock!

A la flía en Uruguay, mamá, Lauri, Valen, Moni, Marga, el piti, Daisy (que se la re jugó con el título!), Walter, Shirly, Carla, Bruno, Martina y la poripocha!!! Y la flía en Europa: Martina y Francis, Maia, Marcelo, Sara y Violeta, María y Jorge, que me bancaron en más de un viaje.

A las barras incondicionales de Uruguay, que en algún u otro momento estuvieron para alentar. Toda la cadena de Letizia, que siempre tiró pa arriba (Silvina, Isabel, Pedro, Gime, Regi, Vale y Sebas, Mati y Pame, Henry, Piti, Antonio, Sabri, Fito, Ichu, Damian, Pepe, Geral, Naty, Nadia, Javi rock y Pilar) y la gente más civilizada, Mari y Sebas, Juampi, Sofi y Andres, Niky, Vero y Fede, Joaquín, Ceci y Crufi, Gago, Martín y

Dani, y Maxi y Gabi. Gracias Ani, por tu tiempo por aquí. Gracias a toda la familia Coscia. Omar, tus correos fueron un cable directo con el paisito, al igual que las novedades y fotos (y hasta algún libro) que me tiraba Mario de vez en cuando.

Thanks to Simon and Chris, for the opportunity to live the great academic, personal and Olympic experience in Loughborough! The two big lofbra guys, Dave (A.M.) & James (A.K.), you make a wonderful team, hope to see you soon. Pratesinha bonina, thanks for the long nights of wine, laugh and crazy talks. And F., please, remember!

Por último, quiero destacar a personas especiales. A pesar de la distancia, la vida, el tiempo y el espacio, tienen un lugar importante en mí, en algún lugar de mi corazón, y me ayudaron a avanzar en este proyecto sabiendo que más cerca o más lejos siempre estaban ahí. Isaac, desde el comienzo hasta el fin! (miro con ternura la manga de mi camiseta). Flo, una guerrera de la vida, armada con su alegría. Gracias por compartirla conmigo. Silvana, gracias por todos los almuerzos, y por guiarme en los senderos de esta existencia espiritual. Vic, gran compañera de la vida. Fabián, creo que hablamos 3 veces en estos 4 años, pero cada una de esas veces, me sentí en el parque de los niños con un rosado glamour, te extraño. Veronika, I enjoyed and grew with you, thank for all what we have lived together. Leo, el mejor compañero de viaje. Giulia, *ambarabà ciccì coccò*! Abus, gracias por estar siempre esperándome con un café con leche y galletitas. Poly, te quiero! Angel, *Navegar e preciso viver nao e preciso*. Nuestros botes no van juntos, pero se cruzan soplados por los mismos vientos. Caro, siempre ahí, al firme, Beleza! Marga, que me ha sabido malcriar en cada visita, aguantar todos mis llamadas pre-viajes, y hacerme sentir que siempre estaba cerca. Lulu, alma hermana, gracias por estar cerca e iluminar mi vida con tus reflexiones y, sobre todo, con tu sonrisa, alimento de mi alma.

Esta tesis está dedicada a la memoria de tres grandes, que forjaron gran parte de lo que soy. Mi viejo sembró la semilla de la curiosidad por la vida, me enseñó a dudar, a mirar con ojo crítico la vida. Con Juancito exploramos y explotamos en discusiones metafísicas existenciales. Ese huracán de ideas, sentimientos y pasiones que eran el, e hicieron temblar mis cimientos. Pocho es un faro de luz, que sigue iluminando, marcando el rumbo al que quiero ir, en el que la calidad humana está por encima de todo. A los tres, Gracias.

SUMMARY

Leakage is a widespread problem associated with the construction of diaphragm walls whenever they are erected in water-bearing ground. The aim of the present research is to develop a new type of slurry wall: the bi-layer diaphragm wall (BL), which main objective is to tackle the aforementioned problem. The method to construct it is based on an existing solution: casting a second waterproof concrete layer against the diaphragm walls. In the BL technique, the second layer is made of steel fibre reinforced concrete (SFRC) sprayed over the conventional diaphragm wall (called Mono-Layer diaphragm wall (ML) in this thesis), including a waterproof admixture. The central idea is to maximize the functional attributes of the second layer, allowing it to play a structural role in addition to the waterproofing function.

The proposed methodology is based on a combination of experimental works and numerical tools. A design method for the BL walls, which is based on an uncoupled structural-section model, is proposed. The method is later used to carry out different comparisons with ML walls and an exhaustive parametric analysis of the construction processes involved in the walls construction. The experimental campaign comprised test at two levels. At element level, the structural response of walls built in a real building located in Barcelona was studied and, at section level, the bond strength between concretes of cores extracted from the abovementioned walls was measured.

The model at structural level, which is based on a finite element model, was contrasted with the results obtained in the experimental walls. The sectional analysis is taken from the specialized literature. With the complete structural-section model, the BL walls are analysed. The study shows that the main flexural resistance is provided by the first layer (the conventional diaphragm wall), providing the SFRC layer a secondary flexural resistance.

For the geometrical ranges of the elements considered in the thesis (35 cm to 60 cm width first layer, and 10 cm width second layer) the increase in the cross-section ultimate bending resistance when it is strengthened by the SFRC layer is between 8% and 15%. This increase allows a reduction in the steel reinforcement of the first layer (up to 7.0% of the total flexural reinforcement) and, to some extent, it also collaborates with a displacement reduction (reducing up to 7.3% of the maximum displacements). It was also found that the spraying sequence is a crucial parameter to be able to take advantage of the SFRC collaboration, and specific indications are described.

Good concrete to concrete bond strength was obtained for the extracted cores. The average shear strength value measured for each age (2, 6 and 35 days) was always above 1.0 MPa for the different cases. Beyond the local test performed, a monolithic behaviour was observed at element level in the experimental walls.

A similar final material consumption was observed between the BL walls and the combined consideration of a ML wall and an external waterproof system. The consideration of the technology cost entails a higher construction cost for the BL technique. However, it is still an interesting option under particular circumstances, like space limitations or if continuous maintenance costs want to be avoided in the future.

In general terms it can be said that the research herein presented lay the foundation for the development of the bi-layer diaphragm wall technique, which is a promising solution for the leakage problem of diaphragm walls. Nonetheless, more studies are needed to be able to fully use these types of walls as a standard

technique, e.g. a detailed cost study and sustainability analysis, debonding risk, waterproofing capability and above all more full scale experimental cases.

RESUMEN

Un problema habitual en la construcción de pantallas continuas en terrenos con presencia de agua es la existencia de filtraciones. El objetivo de esta tesis busca resolver este problema mediante el desarrollo de un nuevo tipo de pantalla: la pantalla bi-capa (BL, por sus siglas en inglés). El método para construir estos muros se basa en una solución existente: realizar una segunda capa de hormigón impermeable sobre los muros pantalla. En las pantallas BL, la segunda capa se realiza con hormigón con fibras de acero (SFRC) proyectado sobre las pantallas convencionales (llamadas ML en esta tesis) e incluyendo a su vez una adición impermeabilizante. La idea central es maximizar las funciones de la segunda capa, asignándole un rol estructural, además de la función impermeabilizante.

La metodología propuesta se basa en la combinación de trabajos experimentales y herramientas numéricas. Se propone un método de diseño para las pantallas BL basado en modelos estructura-sección desacoplados. Posteriormente se utiliza este método para realizar diferentes comparaciones con pantallas ML y un análisis paramétrico exhaustivo de distintos procesos constructivos involucrados en la construcción de las pantallas BL. La campaña experimental realizada comprende dos niveles: a nivel elemento, se estudió la respuesta estructural de pantallas construidas en un edificio real ubicado en Barcelona; a nivel seccional, se midió el nivel de adherencia entre ambas capas de hormigón mediante testigos extraídos de las pantallas antes mencionadas.

El modelo a nivel estructural, basado en elementos finitos, se contrastó con los resultados experimentales obtenidos. El modelo seccional se tomó de la bibliografía estudiada. Con el modelo estructura-sección completo se analizaron las pantallas BL. El estudio muestra que la principal resistencia flexional es aportada por la primera capa (el muro pantalla convencional), siendo secundario el aporte de la capa de SFRC.

Para el rango de elementos considerados en esta tesis (35 cm a 60 cm de espesor de primera capa y 10 cm de segunda), el incremento de la resistencia última a flexión cuando se considera el aporte de la capa de SFRC, está entre 8% y 15%. Este incremento permite una reducción en el acero de refuerzo de la primera capa de hasta un 7.0% del total del acero de flexión y, hasta cierto punto, también colabora con una reducción en los desplazamientos (alcanzando reducciones de hasta un 7.3% del desplazamiento máximo). Se observó también que la secuencia de proyección es un factor clave a la hora de aprovechar la colaboración extra aportada por la capa de SFRC. Indicaciones específicas se describen a este respecto.

Se obtuvo una buena resistencia de adherencia entre hormigones para los testigos extraídos. La resistencia media medida a cada edad (2, 6, y 35 días) estuvo siempre, para los distintos casos, por encima de 1.0 MPa. Más allá de los ensayos puntuales, se observó un comportamiento monolítico a nivel elemento para las pantallas BL experimentales.

Se obtuvo un consumo final de materiales similar entre pantallas BL y la consideración conjunta de una pantalla ML más un sistema impermeabilizante externo. Considerar los costos tecnológicos conlleva un costo constructivo mayor para las pantallas BL. Sin embargo, ésta es aún una opción interesante bajo consideraciones particulares, como limitaciones del espacio subterráneo interior o si se desean evitar costos continuos de mantenimiento.

En términos generales, se puede decir que la investigación aquí presentada sienta las bases para el desarrollo de la técnica de muros pantalla bi-capa, la cual es una solución prometedora para el problema de las filtraciones en pantallas. No obstante, son necesarios más estudios para poder usar plenamente este tipo de pantallas de forma habitual, e.g. estudios de sostenibilidad detallados, evaluación del riesgo de desprendimiento de la segunda capa, capacidad impermeable y, sobre todo, más ensayos experimentales a escala real.

TABLE OF CONTENTS

LIST OF FIGURES

LIST OF TABLES

CHAPTER 1.   INTRODUCTION

1.1. MOTIVATION

An extended underground infrastructure is nowadays needed in large cities to achieve a sustainable development (Bobylev, 2006). The compact city strategy, which aims an efficient use of space, specially below ground level, is one of the possible paths to allow it (Durmisevic, 1999). Moving activities of lesser social importance (traffic or parking) underground is useful in order to reduce noise pollution and polluting emissions, protecting the urban environment, ancient buildings, and parks (Rönkä, Ritola, & Rauhala, 1998). At the same time, placing some functions (e.g. leisure and recreational activities; traffic facilities: tunnels and car parking; technical maintenance facilities: sewage treatment or power plants) underground, free aboveground space that can be addressed to recreation and social activities (Durmisevic, 1999).

There are mainly two methods of building underground structures: (a) excavation in an open cut from ground level; and (b) mining or boring in tunnels. These methods must be implemented without affecting existing buildings and infrastructures adjacent to the construction site and minimizing the alterations to the daily activities of the city. In this city scenario, where ground deformations must usually be controlled to avoid damage to existing buildings, the diaphragm wall technique represents a particularly viable solution when the first of the abovementioned options is used (Rodriguez Liñan, 1995).

Diaphragm walls (also called *slurry walls*) (EN 1538, 2010) started being constructed in Italy in the 1950s (Ou, 2006; Puller, 1994). A synthetized definition of the technique was given by El Hussieny (El Hussieny, 1992), describing the diaphragm walls as "*artificial membrane of finite thickness and depth, constructed in the ground by means of a process of trenching, with the aid of a fluid support*". This is, with a dragging tools a narrow trench is excavated. While the excavation takes place a stabilizing fluid (bentonite slurry) is introduced. When the excavation is complete the reinforcement cage is introduced into the trench and the concrete is cast by tremie pipes, displacing and allowing recovery and recycling of the stabilizing fluid from the bottom up.

Although their basic principle reminds the same, the technique has been developed, improving the methods and equipment (e.g.: different types of dragging tools are now available: drilling bit, hydrophraise (or hydrofrase), trenchcutter, hydraulic grab, mechanical grab, clamshell; improved stability of the cutting face of the excavation; reduced leakages at panel vertical joints; allowance of force transmission between panels; improved bracing and anchoring systems), turning it into a competitive solution for deep excavation works. Moreover, the functionality of diaphragm walls has also widened, being nowadays used as retaining walls, load bearing walls, cut-off walls, or a combination of the aforementioned.

Despite the technical advances, the technique still presents some drawbacks. One widespread problem associated with this construction technique is leakage whenever the walls are erected in water-bearing ground (Puller, 1994), being their waterproof capacity a source of debate since the first walls of this type were built. Although leakage in the walls can occur for several reasons (detailed in (Puller, 1994)), the main one is that generally, the joints between panels develop cracks which provide a path for water ingress and, therefore, have certain degree of permeability (Brown & Bruggemann, 2002; EN 1538, 2010; ICE, 2007; Puller, 1994). As an example, three diaphragm wall joints can be seen in Fig. 1, where (a) the union of panels present a tilt, (b) water leakage appeared during construction, and (c) the water leakage appeared after the structure had been completed.

Fig. 1 - Typical defects of diaphragm walls in joints between panels.

Temporary stop-end is the usual system used in joints to connect the panels (Brown & Bruggemann, 2002). Even if there is a thin layer of bentonite in the joints, which usually have an acceptable degree of waterproofness, the deflections in the wall during the excavation process create paths that allow a water flow (Ou & Lee, 1987). Several methods have been developed to improve the joints against leakages, like water stop joints (Puller, 1994) or end-plates (overlapping joint) (El-Razek, 1999; Ou & Lee, 1987).

Notwithstanding the efforts made to achieve waterproofness, there is a general consensus among contractors and researchers that there is no effective technique to make joints fully watertight (ICE, 2007; Puller, 1994; Wong, 1997), especially if there is a high water table in the exterior of the walls. Accordingly, ICE guide states that a complementary waterproof system should be added if a good level of watertightness is needed (ICE, 2007). With this porpoise, several techniques have been developed to prevent or repair the existence of leaks (Puller, 1994).

A usual technique is to repair the affected areas as they are detected, injecting a chemical grout into the problematic cracks and joints, or directly chipping and restoring the element with a more waterproof mortar (also called *grouting* (Wong, 1997)). In a similar way, a cement or chemical grout can be injected in the soil behind the wall, in the areas where leakage is observed (Puller, 1994). (El-Razek, 1999) reported having successfully used this solution in a diaphragm wall project in Alexandria. However, leakage usually appears only over lengthy periods and at different times and areas of a wall (see **Fig. 1c**), even becoming worse with time (Wong, 1997), which may result in extensive repair works over indefinite periods that require several sessions, causing problems for both owners and contractors.

Another solution consists of casting an additional layer of mortar or concrete on the interior face of the walls (also called *tanking*), which is also a common way to make walls of bored piles watertight (Wong, 1997). As it can be seen in **Fig. 1**, it is not strange that deviations from true verticality occur in the panels as they are constructed. A favourable effect of this technique is that the second layer evens the surface when irregularities caused by panel deviations are detected.

Few publications were found reporting this solution. For example, (Li, Ju, Han, & Zhou, 2008) used it as a way to study tensile creep in concrete. Two arranges for the connection between linings that reflect different possibilities to be used in a real underground structure were studied: (a) continuous design, which connect both layers with extruding reinforcements; and (b) sliding design, which put an impermeable sheet in between both concrete layers. Meanwhile, (Sherif & Kudsi, 1975) performed a risk analysis on a double wall, aiming to quantify the cracking probability, which would lead to leaks.

Since the publication of codes that define three grades of waterproofing protection for underground structures (e.g. (BS 8102, 2009) or its previous versions) it became common practice in the United Kingdom (and spread to other countries like USA or Germany) to deal with the waterproof problem by constructing an inner wall separated by a cavity (Puller, 1994). In this system, the water is directed to an inferior deposit and pumped out from there. The solution is referred as *false wall* (Wong, 1997), or *drained cavity* (BS 8102, 2009).

Nowadays, drained cavities are extensively used. However, this solution loses significant volume because of the construction tolerances and the cavity. In some cases, the extra space required may have a crucial influence in the final project value. For example, if an inner leaf 15 cm wide separated by a cavity 10 cm wide is considered (neglecting construction tolerances), 25 cm in contact with every diaphragm wall would be lost. In a vehicles parking basement, the additional space would represent the difference to afford a parking place intended for a luxury car. In addition to the space lost, a drained cavity may, in the worst case, hide dangerous leakages and even structural problems (Puller, 1994).

In below-grade structures in general, it can be said that leakages are originated mainly by poor design and workmanship rather than the selection of materials. Therefore the key to avoid leakages resides in the design and implementation (Shohet & Galil, 2005). Beyond the waterproof method, the early selection of the type of wall, the construction sequence, and the temporal and permanent use of the retaining structure have a positive effect on the final cost. Hence, client, designer, and contractor should all be involved in the project at an early stage (Gaba, Simpson, Powrie, & Beadman, 2003). A holistic vision of the project requirements should be adopted to achieve optimization, in which the costs of material consumption, the final dimensions of the wall, maintenance requirements, and construction complexity should all be evaluated throughout its entire life cycle. Furthermore, to achieve sustainable design the best strategy is to consider environmental aspects also right from the start of the design process (Kurk & Eagan, 2008).

1.2. THESIS OBJECTIVES

The aim of the research was to develop a new type of slurry wall: The bi-layer diaphragm wall. The method to construct it is based on the tanking solution described above, where a second waterproof layer is casted against the diaphragm walls.

The bi-layer diaphragm wall is made of two bonded concrete layers poured and then sprayed, in separate stages. The first is a conventional Reinforced Concrete (RC) diaphragm wall. Once this wall attains the necessary strength, soil within the perimeter is excavated and removed, and the second layer, this time of sprayed Steel Fibre Reinforced Concrete (SFRC) with a waterproof additive, is applied. The solution is schematically presented in **Fig. 2**.
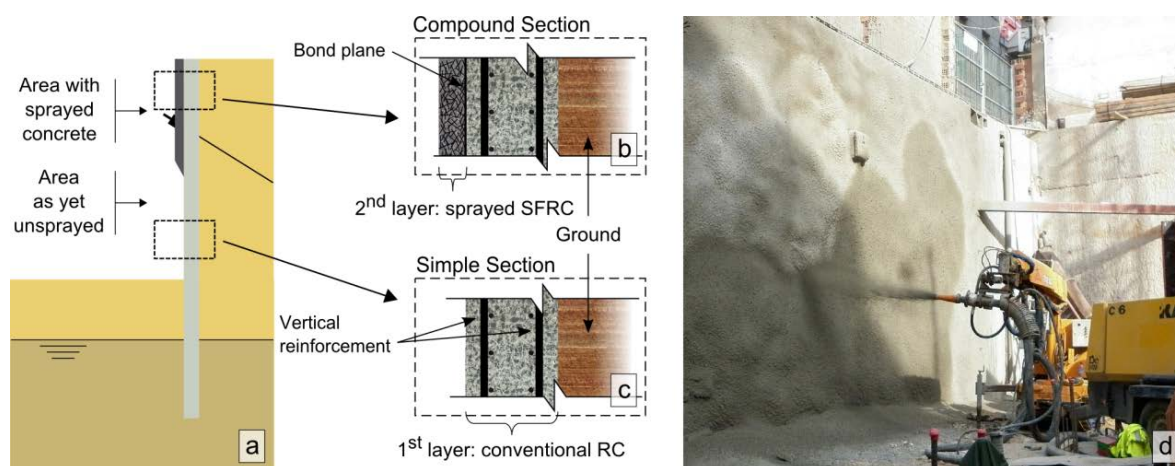
Fig. 2 - Bi-layer diaphragm walls. a) general scheme; b) compound section; c) simple section; and d) spraying of an experimental wall.

The idea is to maximize the functional attributes of the second layer, allowing it to play a structural role, in addition to its initial intended purpose (waterproofing). Due to the structural role of the second layer, the thickness and reinforcement of the first layer may be reduced, becoming an attractive structural solution if the waterproofness is also considered.

The objectives of the research were:

O1.   Corroborate the viability of the proposed solution.

O2.   Assess the bond strength reached between the concrete layers.

O3.   Assess the structural behaviour of the bi-layer diaphragm walls.

O4.   Develop an overall flexural design model (structural and sectional level).

O5.   Quantify the efficiency of the method when compared with equivalent conventional diaphragm wall alternatives.

O6.   Study the influence of the different constructions processes related to this type of walls.

O7.   Disseminate the results.

1.3. THESIS BACKGROUND

As it was seen in the previous section, many and diverse disciplines have to be combined in order to materialize this new structural element. The more important ones are shown in **Fig. 3**, where some of the interconnections are schematically represented.
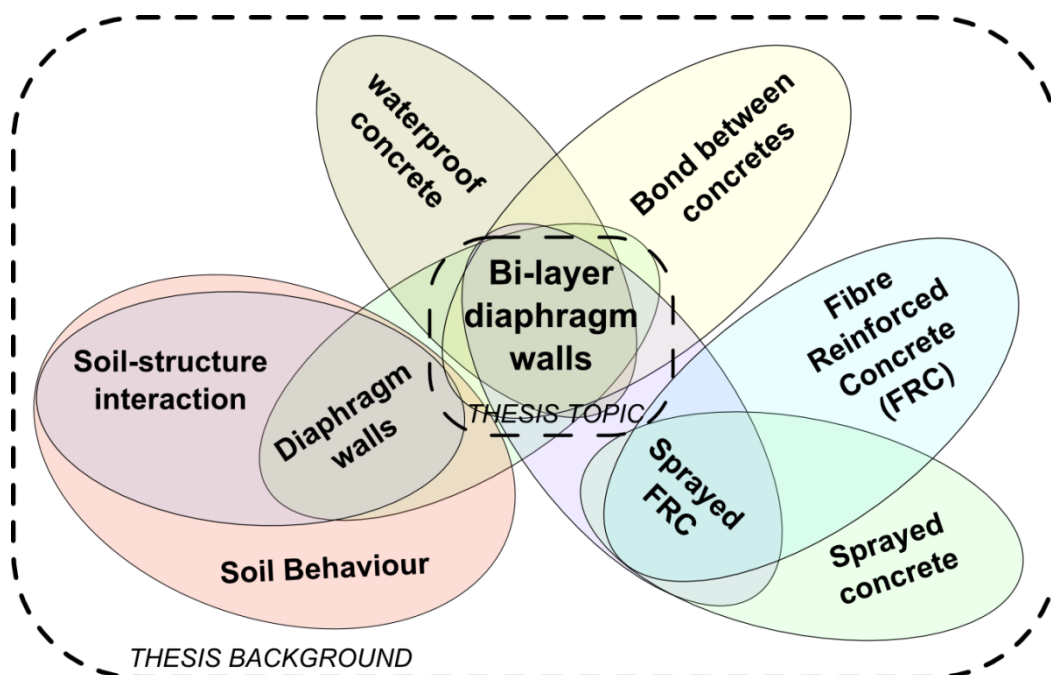
Fig. 3 - Main knowledge areas needed to materialize the bi-layer diaphragm walls

A brief introduction to these topics, which conforms the background of the thesis is presented in this section with the following aims: a) define the terminology used in the thesis; b) summarize key points in every topic; and c) guide the reader into specialized bibliography.

1.3.1. Diaphragm walls

A definition of diaphragm wall has already been given in previous sections together with a small description of the technique. There are several books addressing this structural element (e.g. (Schneebeli, 1981; Xanthakos, 1979)) and also a European code related to it (EN 1538, 2010).

Diaphragm walls are classified as flexible in the group of the excavation retaining structures, as its deformation influences in the general behaviour of the element and therefore in the way the element is designed. In this group it can also be found the following types of walls: sheet pile wall, soldier pile wall (also called: king post wall), contiguous bored pile wall, and secant bored pile wall.

The walls can be further classified in accordance with different criteria like its structural configuration under construction (e.g. cantilever, anchored, braced; top-down construction, island excavation, or zoned excavation) (Ou, 2006). In the first of them (cantilever), the structure stability depends entirely on the passive earth pressures, while in the others the stability is also given by one or several propping lines. Furthermore, the propped walls are usually sub-classified in walls with one prop level, or multiple prop levels.

The prop support system may be temporal (e.g. bracing, temporal anchors, ring wales) or permanent (e.g. beams or slabs, permanent anchors), and its use depends on the construction sequence adopted. A complete description of ground anchors for retaining structures can be found in (Fang, 1995).

In this thesis, only propped walls (both in one or multiple levels) are used, conveniently alternating the props between active anchors, struts, or the structure slabs as required.

1.3.1.1. Calculation methods

Earth retaining structures are designed to withhold both the soil pressures and the external loads that may be applied to it, being able to retransmit them to the foundation soil, under controlled deformations, and avoiding the collapse both of the structure and the surrounding soil.

Accordingly, Eurocode 7 (EN, 2004a) specifies two kind of checks to design retaining structures: serviceability limit state, and ultimate limit state. For the first of them the code is focused in the control of the displacements of the walls and the ground adjacent to them, mainly in order to avoid damage to existing adjacent buildings. Regarding the ultimate limit state, the code states:

> "*The design of retaining structures shall be checked at the ultimate limit state for the design situations appropriate to that state*".

For embedded walls, there are mainly four groups of ultimate states modes that shall be checked: a) Overall stability, b) Rotational failure, c) Vertical failure, and d) Structural failure. They can be seen schematically represented in **Fig. 4**. Although the first three groups are checked in the cases used in this thesis, they are not presented, as the thesis is centred in the structural behaviour of the diaphragm walls. Furthermore, when possible, cases with a large security factor against these modes were used to avoid any possible interaction with the structural failure.

There are currently in use a variety of methods to check the previously mentioned ultimate states in order to design embedded walls. A State of the art about the different available calculation methods was performed by (Delattre, 2001), were the evolution and development of the different methods is described. According to (Delattre, 2001), the diversity of methods arises from the complexity of the geotechnical structure, which is both supported but also loaded by the soil. (Delattre, 2001) classified the methods in the following categories: (1) classical methods, (2) subgrade reaction method, (3) finite element method and (4) empirical methods. The different methods are able to tackle, with different precision, the different ultimate states that should be checked.

The classical design methods are based on the classical Coulomb and Rankine soil behaviour methods and their extensions. These methods are centred on the pressures exerted on the structures by the soil, not taking into account the deformations of the structures and the adjacent soil.

The subgrade reaction method (based on the Winkler model) was later developed. It is able to take into account the soil and structure deformations considering the properties of both the soil and the retaining wall, and its interaction. However, like the classical methods, it is still not able to take into account the arching effect.
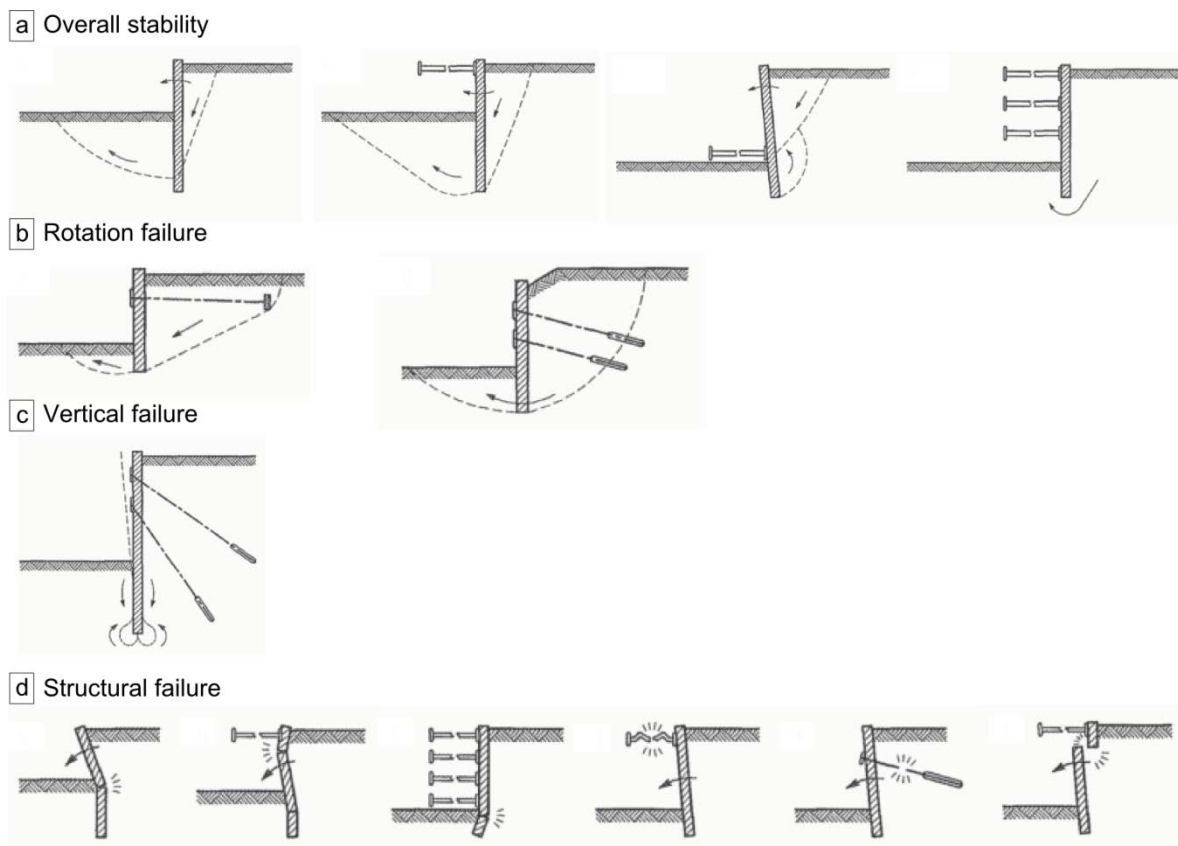
Fig. 4 - Typical ultimate states modes in embedded walls. [Fuente: Eurocode 7 (EN, 2004a)]

The empirical approach was mainly used in the English-speaking countries. It is based on comparing the characteristics of the project with monitored case histories results of resembling excavations.

Finally, from the 1970s, with the advance in the numerical methods and the generalization of computer calculations, the finite element method started to be used in geotechnical problems. The soil is considered as a continuum, which is discretized in several finite elements. Being both the structure and the soil modelled, it allows a more comprehensive representation which includes its interaction and the arch effect. Also, information of all the soil under study is obtained (Sanhueza Plaza & Oteo, 2007).

1.3.1.2. FEM in embedded walls problem

(Potts & Zdravković, 1999) and (Ou, 2006) can be named as example of books focused on geotechnical analysis through the FEM method.

A positive aspect of the method is that, in theory, as more factors are appropriately considered in the FEM models the accuracy of the results would be higher than the previous ones. On the other hand, the theories in which the method is based are wide more complex, as it is also its application, including pre and post processing. Furthermore, some of the theories and models are still under development (Ou, 2006) and, for every soil model, specific soil parameters need usually to be evaluated to have the required input data to acceptably model the soil behaviour.

Nowadays, the more widespread soil models used in FEM studies of diaphragm walls include: the well-known elastic-perfectly plastic "Mohr-Coulomb" ("MC"), the modified Cam Clay ("MCC" (Roscoe & Burland, 1968)), the Hyperbolic ("Hyp" (Duncan & Chang, 1970)), and the hardening soil ("HS" (Schanz, Vermeer, & Bonnier, 1999)) and, to a lesser extent, more advanced models such as the "MIT-E3" (Whittle, 1987).

As the accuracy of FEM-based models depends to a large extent on the selection of appropriate parameters to represent the constitutive behaviour of soils (Khoiri & Ou, 2013), many researchers focused their attention on direct or inverse ways to determine those parameters. For example, (Khoiri & Ou, 2013) used the MC and HS models to predict deformations based on measured data at the first excavation stage, also measuring the soil Young's modulus aiming to correlate it with the previous prediction; (Ou & Lai, 1994) analysed layered sandy and clayey soil using both the Hyp and the MCC models and establishing a procedure to determine the soil parameters; and (Calvello & Finno, 2004) (Hashash, Levasseur, Osouli, Finno, & Malecot, 2010) calibrated the soil parameters through back analysis.

There are many recent examples of studies, based on these methods, related to the design of diaphragm walls. For example, improvements of the empirical methods were performed by (G. T. C. Kung, Juang, Hsiao, & Hashash, 2007) and (Bryson & Zapata-Medina, 2012), who proposed new semi-empirical methods based on FEM parametrical analysis; the construction sequences were analysed and compared by (G. T.-C. Kung, 2009); different soil models (MCC, two variations of HS, MC and "undrained soft clay model") were analysed and compared by (Lim, Ou, & Hsieh, 2010) under undrained conditions, who concluded that all models could predict, with a correct parameter selection, the wall deflections, but only the last one was able to predict surface settlements correctly; finally, it can be mentioned the (Ou, Chiou, & Wu, 1996) study on the influence of the spatial effects in the wall behaviour.

It can be concluded that, in the last years, the FEM method (using the abovementioned soil models) has been frequently and increasingly being used to address wide different aspects of the diaphragm wall technique. In

the majority of studies, the focus is put both in the displacements of the wall and of the adjacent soil, mainly due to the importance they have to avoid damage to existing buildings.

Despite the difficulty to calibrate soil parameters, the FEM method seems to give good results regarding wall deflections with all the above mentioned soil models, therefore, it was chosen for the design of the cases analysed in this thesis. Among the soil models, the HS soil model was chosen mainly for two practical reasons: Firstly, it has been previously used in other diaphragm wall studies, were sand had to be modelled. Therefore, there are good quality documented cases, with soil parameters. Secondly, it was developed associated with PLAXIS, the FEM program available to carry out the calculations.

1.3.2. Waterproof concrete

Concrete is a porous material. It is possible to water to penetrate both through its porous and for its microcracks due to capillary absorption or due to hydrostatic pressure. Despite low water/cement ratio concrete properly produced has generally good durability and low permeability, no concrete can be considered absolutely waterproof (ACI Committee 212, 2010). However, it may be possible to reduce the permeability of the concrete of the second layer of the proposed solution to be considered sufficiently waterproof for the desired application. In this sense, there are a range of products called permeability-reducing admixtures (PRAs), with variances in performance, capable of reducing the concrete permeability. (ACI Committee 212, 2010; Chan, Ho, & Chan, 1999; Ramachandran, 1995) can be named as general references covering this subject, which main aspects are included hereafter.

The PRAs have to be used in well-proportioned concrete mixtures, and a w/c ratio below 0.45 is recommended for a waterproof concrete. The PRAs are usually divided in two subcategories, depending on whether the concrete is intended to resist non-hydrostatic conditions (called: PRAN, according to ACI; or "*damproofing*", according to (Ramachandran, 1995)), or if it will be exposed to hydrostatic conditions (called: PRAH, or "*waterproofing*", respectively).

As the range of PRAs is so wide, it is difficult to comprehensively classify these products. Moreover, these products usually improve other characteristics of the concrete (e.g. drying shrinkage, chloride ion penetration, freezing-and-thawing resistance, and autogenous sealing) and, at the same time, there are many admixtures designed for other porpoises that are also able to reduce the permeability of the concrete. ACI divides the PRAs in the following main families: a) Hydrophobic or water-repellent chemicals, b) Finely divided solids, and c) Crystalline materials.

(Ramachandran, 1995) presents an extended classification differentiating the finely divided solids into reactive and inert, and adding the conventional admixtures that are able to reduce permeability. Accordingly, ACI indicated that some authors included the supplementary cementing materials (CSM) among the finely divided soils. Within the CSM, the Condensed Silica Fume (CSF, also known as Silica Fume or Microsilica) shows particularly high performance reducing permeability and improving the durability of the concrete (Chan et al., 1999). The complete classification and a list of examples can be seen in **Table 1**. An alternative classification can be seen in (Chan et al., 1999).

The hydrophobic materials work causing a reversed angle on the water-solid interface, forcing the water out of the pores. This may be enough protection only if there is no hydrostatic pressure and if the concrete has no significant cracks. Finely-divided solids significantly reduce permeability increasing the concrete density or

by voids filling. Accordingly, both previous products are usually categorized as PRANs. Crystalline admixtures have active ingredients that react with the free water and cement particles in the concrete forming calcium silicate hydrates (needle-like crystals) that block capillaries and microcracks, even generated over the life of concrete (according to crystalline admixtures manufacturer, crystalline treated concrete is able to self-seal cracks up to 0.5 mm). As the generated protection is able to resist hydrostatic pressure (up to 120 m of head are registered) it can be categorized as a PRAH.

Table 1 - Classification and examples of permeability-reducing admixtures

Group		Example
Water repelling materials		-Soaps -Fatty acids -Wax emulsions
Finely divided solids	Inert (pore filling materials)	-Fullers earth -Talc -Bentonite -Other siliceous powders
	Chemically reactive or SCM	-Silicates -Finely ground blast furnace slag -Pozzolans
Crystalline materials		-Proprietary products
Conventional admixtures and miscellaneous		-Water reducing -Air entraining -Accelerator -Methyl siliconates -Polymer

The effects of the admixtures on the permeability of concrete can be evaluated both by direct and indirect (measuring conductivity of chloride penetration) methods. A review of these methods, even under loaded and cracked specimens, was performed by (Hoseini, Bindiganavile, & Banthia, 2009). As the measured permeability is strongly dependant on the test method used, authors seem to agree that there is a need to standardize the test procedures in order to be able to systematize the comparisons. (Hoseini et al., 2009; Ramachandran, 1995)

Finally, it can be said that the required waterproofness of the walls, considering the service conditions expected, can be reached if an appropriate PRA is selected and if cracking of the second layer is controlled.

1.3.3. Fibre reinforced concrete

Fibre reinforced concrete (FRC) is defined by (ACI Committee 116, 2000) as "*concrete containing dispersed randomly oriented fibers*". Its modern development started around the 1960s after the works of Romualdi, Batson, and Mandel (Zollo, 1997), gradually increasing afterwards its research and use in engineering applications.

The technique has been addressed in different books, for example: (Bentur & Mindess, 2007; Newman & Choo, 2003). There are also several manuals in this topic, such as (Aguado, Blanco, de la FUENTE, & Pujadas, 2012; Gallovich Sarzalejo, Rossi, Perri, Winterberg, & Perri Aristeguieta, 2005). It is also worth

mentioning as reference the ACI state-of-the-art report (ACI Committee 544, 2002), which also includes an exhaustive list of standards, books, and other references.

Reinforcement is required in cementitious materials, which are brittle materials with low tensile strengths. The traditional reinforcement used has been reinforcing bars, appropriately located to withstand tensile stresses. When fibres are used, as they are discontinuous and usually randomly distributed, they are not as efficient in withstanding the tensile stresses. On the other hand, as they are more closely spaced, they have a better performance at controlling cracking. This implies improvements in several properties of the SFRC, like toughness (ability to absorb energy after cracking), impact resistance, and flexural fatigue endurance. (ACI Committee 544, 2002)

Following the aforementioned differences, it can be named some nowadays extensively used applications where the use of fibres has advantages over conventional bars. (Bentur & Mindess, 2007) classify the applications in three groups:

1. Thin sheet elements. As conventional reinforcement cannot be used, the fibres are used as the primary reinforcement.
2. Elements subjected to heavy locally applied loads or deformations, e.g. tunnel linings, blast resistant structures, or precast piles.
3. Elements where cracking due to humidity or temperature variations must be controlled, e.g. slabs and pavements. In this case, fibres are often referred to as secondary reinforcement.

As an extra advantage, the placing of the mesh or reinforcing bars is eliminated in application where FRC is used. It is also worth mentioning that in these applications, the fibre reinforcement is not essential for the structural safety (Zollo, 1997).

A more recently important milestone for the FRC as a structural material in Europe happened with the publication of design codes and recommendations, which provided a scientifically founded, consistent and coherent framework for the design of FRC elements (di Prisco, Plizzari, & Vandewalle, 2009). In this sense, it is worthwhile mentioning, in order of time of publication, the German guidelines (DBV, 2001), the RILEM TC 162-TDF recommendations (RILEM TC 162-TDF, 2003), the Italian guidelines CNR-DT 204 (CNR, 2006), the Spanish code EHE-08 (CPH, 2008) and the Model Code 2010 (FIB, 2010). An exhaustive analysis and comparison of the mentioned codes was performed by (Blanco, Pujadas, de la Fuente, Cavalaro, & Aguado, 2013).

Besides these applications, there are some relatively new ones where the FRC can be partially or totally used in substitution of the conventional reinforcement. It is also worth mentioning that several studies, now also included in the codes, demonstrated the possibility of partial or total substitution of the shear reinforcement in beams, or the transversal reinforcement in thin-web elements (Martinola, Meda, Plizzari, & Rinaldi, 2010).

1.3.4. Sprayed concrete

Sprayed concrete is a special concrete that can be defined as: "*Mortar or concrete pneumatically projected at high velocity onto a surface*" (ACI Committee 116, 2000). Although the technique was originally patented as

"*Gunite*", it is usually called "*Sprayed concrete*" in the European influenced countries and "*Shotcrete*" in the area of influence of USA. (Simon Austin & Robins, 1995; Newman & Choo, 2003) can be named as book addressing this technique. It is also worth mentioning as reference the following state-of-the-art reports and recommendations (AFTES, 1996; Franzén, 1992; ITA, 1993). A brief summary of some of the salient aspects on the subject are presented hereafter.

The system involves spraying (projecting) the mix, which usually has small-sized aggregates, at a hard surface. Impelled by compressed air, the material is rapidly placed and compacted, even on vertical surfaces and, within certain limits, on an overhead position. If it is properly dosed and applied, the sprayed concrete is a structurally sound and durable material that generally shows a good bond to the usual base materials (e.g. concrete, rock or steel).

The basic constituent materials of the sprayed concrete are the same as in the conventional one, namely, cement, aggregates and water. Fibres, admixtures and additions are also usually incorporated into the concrete mix for spraying. Despite the physical properties of a correctly applied sprayed concrete are similar to those of a cast concrete with the same composition (Galobardes, 2013), some differences are registered, which have given place to recent studies focused on analysing and modelling these differences (e.g. (Galobardes, 2013; Goodier, 2000))

The concrete may be sprayed by two main systems: dry mix and wet mix processes, being the moment when the water is introduced to the concrete mix the main difference between them. Although the system started with the dry mix, since the 1990s a change towards the wet mix has been registered, being completely dominant nowadays in countries like Norway, which has a strong tunnelling activity (Franzén, 1992). The reason of this change is based principally in two reasons: better performance and environmental advantages. A comparison of both systems can be seen in (Galobardes, 2013).

One of the central advantages of spraying concrete is that two of the stages of the laying of the concrete (pouring and compacting) are merged. It is particularly convenient in cases where formwork is difficult to place, in areas of difficult access, and where thin or with variable thickness layers and extended surfaces are needed.

There are several applications where sprayed concrete is commonly used. Rock support is one of the main applications where sprayed concrete is used nowadays, being the technique mainly developed for its use in tunnelling. The advances in the technique allowed a change of role of the sprayed concrete, going from being used as a provisional lining in the early days, to a current use as a definitive structural lining. Other relevant uses of this technique include slope stabilization, structural repairs or reinforcements, and metallic structures protection.

Regarding the last developments in the sprayed concrete technique, a good insight can be seen in (S Austin, 2002), which presents the "proceedings of the ACI/SCA International Conference on Sprayed Concrete/Shotcrete". The conference, that took place in Edinburg in 1996, was the first conference that both organizations held jointly. According to Austin, the research in that period was focused on specifications, test methods, admixtures, fibre reinforcement, materials, the spraying process and performance. Moreover, after the conference it was clearly noticed the need of efforts towards the definition of test methods, and the research and development of design methods to assist engineers in the design of elements using this technique.

The increase in those efforts can be confirmed observing the amount of congresses that took place and journal papers published in the subsequent years. An idea of the direction of those efforts can be seen in (Celestino & Ishida, 2009), where the work done by the "ITA working group on sprayed concrete use" was presented. It includes a report that compile information provided from different "ITA National Groups", where it can be highlighted the trends followed in the last years (i.e. towards the wet-mix system, the progress in the use of alkali free accelerators, the use of sprayed concrete for permanent linings, and the substitution of wire mesh by fibres.). The report also compares the codes, standards and guidelines adopted in different countries. It remarks that different concepts were adopted in different countries for the design with sprayed concrete.

Therefore, despite the efforts and progress made, the sprayed concrete technique is still not mentioned in some of the more important concrete design codes at European level (e.g. Model Code 2010 (FIB, 2010), Eurocode 2 (EN, 2004b)), which may be one of the reasons for sprayed concrete not being extendedly used as a structural material. However, several standards and recommendations address different aspects of this technique. They can be grouped as they are mainly related to two technical committees: the American Concrete Institute (ACI) and the European Federation of Producers and Applicators of Specialist Products for Structures (EFNARC). A summary of standards related to both groups can be found in (Galobardes, 2013). The works related to sprayed concrete performed for this thesis were carried out mainly following the EFNARC guidelines.

1.3.5. Bond between concretes

Bond strength is a key parameter in the performance of structures composed by concrete placed in different times. Good bond strength is needed in order to allow the structure to behave monolithically and to effectively mobilize the strength of the different components.

A brief literature review about bond between concretes, written with a special focus on its application on the bi--layer diaphragm walls can be found in (Segura-Castillo & Aguado de Cea, 2012a) (Included in section 5.1 of this thesis).

1.4. GENERAL METHODOLOGY

The general work methodology is based on a combination of experimental works (laboratory and field) and numerical tools, where different data obtained in the experimental campaigns is used as an input for the models and to validate them. All along the thesis a special emphasis was placed on the SFRC layer contribution. The general methodology can be broken down into a series of tasks as follows:

M1. An on-site full scale experimental campaign, where the bi-layer walls were constructed, was performed during the construction of a building located in Barcelona. The campaign was focused on three aspects: (a) assess viability of the general solution (b) structural behaviour of the walls, and (c) bond between layers.

For the structural experimentation, displacements were measured by means of inclinometers and invar tape, strain gauges were placed in the reinforcement bars, and load cells at the anchorage points of two instrumented panels. Despite the different type of structural measurements, due to different problems

related to the on-site experimentation (load cell broken, need to change the reference point of the invar tape measurement, strain gages measures missed), the analysis was finally exclusively based on the inclinometers results, which had complete and reliable data.

For the bond between layers experimentation, cores from the bi-layers walls were extracted at different ages and taken to the lab to perform shear tests.

M2.   A direct shear test feasible to be used on extracted cores was adopted. Some adaptations were performed to adjust the test, originally designed for bituminous materials, to be used with concrete cores.

M3.   Using the developed test, an experimental campaign evaluating the evolution at early ages of the bond strength was performed.

M4.   A structural model for the walls behaviour was developed.

Two types of soil-structure interaction models where used. In a first instance, a Winkler model was used with two purposes, firstly to design the experimental campaign, and secondly to perform a preliminary parametric study in order to identify the main parameters. Afterwards, a FEM based model was developed to model the walls and the soil. A comparison between models was performed, after which it was decided to use the FEM model to perform the subsequent analysis.

M5.   The structural experimental results were analysed and the FEM model was contrasted and adjusted with them.

M6.   A sectional model, capable of modelling the different materials present in the compound cross-section (including the SFRC) was adopted. The AES model was chosen because it met the mentioned requirements.

M7.   Both structural and sectional models were integrated to establish an overall design method.

M8.   The profitability of the bi-layer walls was assessed using the overall design method.

The evaluation was performed comparing bi-layer diaphragm walls with equivalent alternatives of mono-layer walls. Both levels of analysis (structural and complete design) were used in the comparisons.

M9.   The overall design method was then used to perform a parametric analysis.

The effectiveness of different construction sequence, walls configuration and spraying sequence alternatives was studied in the parametric analysis. It focused on the first layer steel reinforcement and the displacements reduction.

M10. High level refereed journals as well as relevant conferences were selected for publishing papers and to disseminate the results.

The objectives and methods are summarized in **Table 2**. It can be seen that the detailed methodology is related to the objectives established.

1.5. THESIS STRUCTURE

In order to maximize the dissemination of results a thesis by publication was chosen. **Table 3** presents the list of papers that conforms the main body of thesis. The following information can be seen in the table: number of paper; Journal, indicating Impact Factor (I.F. 2012, according to ©Thomson Reuters Journal Citation Reports) and quartile in its category (included in the footnote); complete title of paper; and authors.

Table 2 - Summary of objectives and methods

Objective	Methodology
Corroborate the viability of the proposed solution (O1).	Full scale experimental campaign (M1)
Assess the bond strength reached between the concrete layers (O2).	Adapt a direct shear test feasible to be used in extracted cores (M2) and use it to evaluate the evolution at early ages of the bond strength (M3).
Assess the structural behaviour of the bi-layer diaphragm walls (O3).	Develop (M4) and validate (M5) a FEM structural model.
Develop an overall flexural design model (structural and sectional level) (O4).	Adopt a sectional model (M6) and integration with the structural model (M7) into an overall design method.
Quantify the efficiency of the method when compared with equivalent mono-layer wall alternatives (O5).	Evaluation of the profitability through therorethical comparisons of different bi-layer and mono-layer walls (M8).
Study the influence of the different constructions processes related to this type of walls (O6).	Parametric study based on the using the overall design method (M9).
Disseminate the results (O7).	Publish in high level refereed journal papers and present papers at relevant conferences (M10).

It can be seen that the thesis consists of: four journal papers (two of them already published (P. 1 and P. 4)), one accepted for publication (P. 2), and the last one already submitted and currently under the 2nd review after the Journal having asked for some changes (P. 3), all of them in renowned international journals; and one conference papers (already published (C.P. 1)).
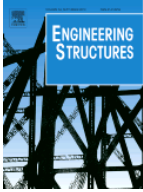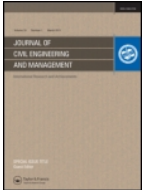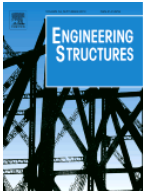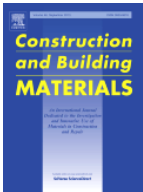
The PhD candidate was the first author of all the papers. The papers planning, state of the art, methodology, analysis, and conclusions were performed entirely by the PhD candidate with the recommendations of his advisors. The writing of almost the totality of the four papers was also done by the candidate. Furthermore, all the papers were written during the doctoral studies period.

The thesis is structured around the presented papers. Each of the journal papers conform a self-contained chapter of the main body of the thesis, as is schematically shown in **Fig. 5**. In the figure, the common part of the title of all papers, which describe the element under study (i.e. "Bi-layer diaphragm wall") was removed for the sake of clarity. The conference paper (Conference Paper 1) is included as an appendix, which complements the forth paper.

Besides the abovementioned journal and conference papers, two chapters complete the thesis: an introductory chapter and a final conclusions chapter. In the first one, the motivations to study the topic, the objectives, the general methodology, and the general thesis scheme are presented. In the final chapter, firstly, conclusions are established from the jointly consideration of the results of the different chapters, and then, a

brief summary of the main conclusions arisen in every chapter is presented. Also, further work lines (both theoretical and experimental) are outlined indicating future steps still needed in order to incorporate the proposed solution as a regular option.

Table 3 - List of papers and conference papers related to the thesis.

Paper	Journal / Congress		Title	Authors
Paper 1		Engineering Structures, 56, pp. 154-164 I.F.: 1.713 (Q1,CE*)	Bi-layer diaphragm walls: Experimental and numerical structural analysis	Segura-Castillo, Luis Aguado, Antonio Josa, Alejandro
Paper 2		Journal of Civil Engineering and Management (Accepted) I.F.: 2.016 (Q1,CE*)	Bi-layer diaphragm walls: Structural and sectional analysis	Segura-Castillo, Luis Aguado, Antonio de la Fuente, Albert Josa, Alejandro
Paper 3		Engineering Structures (2nd review) I.F.: 1.713 (Q1,CE*)	Bi-layer diaphragm walls: Parametric study of construction processes	Segura-Castillo, Luis Josa, Alejandro Aguado, Antonio
Paper 4		Construction and Building Materials, 31, pp. 29-37 I.F.: 2.293 (Q1,CB+)	Bi-layer diaphragm walls: Evolution of concrete-to-concrete bond strength at early ages	Segura-Castillo, Luis Aguado, Antonio
Conference Paper 1		XXXV Jornadas Sudamericanas de Ingeniería Estructural (Published)	Bi-layer diaphragm walls: Early ages concrete-to-concrete bond strength assessed through shear and pull-off tests	Segura-Castillo, Luis Aguado, Antonio

*CE: ENGINEERING, CIVIL
+CB: CONSTRUCTION & BUILDING TECHNOLOGY

The research work was originally structured into four main areas: (a) Structural level analysis; (b) Sectional level analysis; (c) General design and optimization; and (d) Bonding between layers. During the developing of the thesis, progress was made in parallel in the four areas, achieving different degree of results in each one of them. As soon as enough rigorous and coherent results were obtained, a paper was written and submitted for evaluation. Therefore, the papers interconnect the different aspects studied, as it is summarized in **Table 4**.

It can be seen that, on the one hand, the sectional level is less developed than the rest of the levels, and, on the other hand, that the bond level is less connected with the other levels (this can also be seen in **Fig. 5**). To justify this, it is worth mentioning two important aspects that were in the original thesis plan but could not be

included in the thesis. Firstly, the experimental analysis at sectional level, and secondly, the connection between the measured bond and a theoretical evaluation of the bond strength necessary for the correct behaviour of the walls. The first aspect was not included due to different errors during the experimental campaign, and the second, is currently under development but could not be included simply because of lack of time before submitting the thesis. Both aspects are included in the suggestions for future research at the end of the thesis.
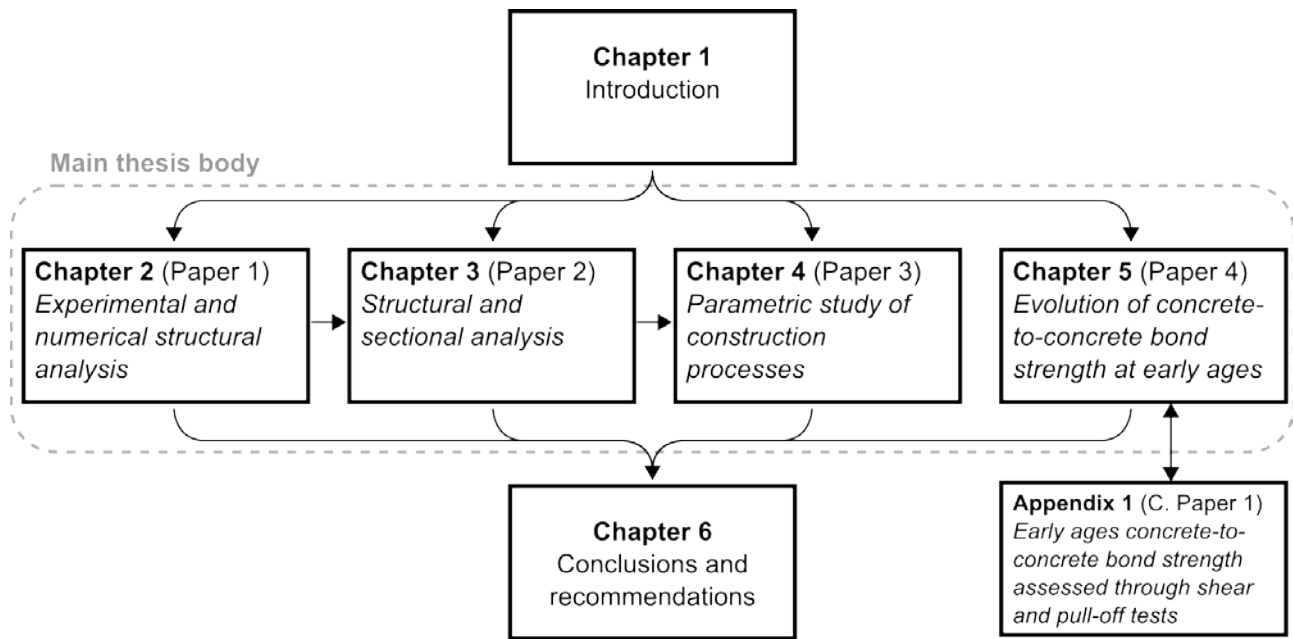
Fig. 5 - Outline of the thesis.

Table 4 - Connection between main areas, papers and methodology used.

Paper	Structural level analysis	Sectional level analysis	General design and optimization	Bond Strength
Paper 1	M1 – M4 – M5		M8	
Paper 2	M4	M6	M7 – M8	
Paper 3			M9	
Paper 4 & C. Paper 1				M1 – M2 – M3

1.5.1. Chapters outlook

A brief outlook of every chapter is outlined below, highlighting the connection between the different papers, and the methodology (M#) previously described. In each paper, the methodology used is further detailed.

Chapter 2 (Paper 1): Experimental and numerical structural analysis

The structural part of the experimental campaign (M1) is reported in this chapter, together with the structural model (M4) and its contrast and adjust (M5). A first evaluation of the advantage of the walls is performed

then with the developed model (M8). In this case, the profitability is evaluated just until the structural level, comparing the bending moments developed both in mono-layer and bi-layer walls.

Chapter 3 (Paper 2): Structural and sectional analysis

In this chapter, the structural model developed in the previous chapter (M4) is extended, changing the soil model to be able to use it in a larger excavation. A sectional model is adopted (M6) and integrated with the structural model (M7) to obtain the overall design method. With the overall design method, a study based on the comparison of various hypothetical cases of bi-layer diaphragm is performed to evaluate again the profitability of the new wall type (M8). This time, the comparison is based on the final design, comparing the use of both structural materials, and materials needed to complete different waterproofing systems.

Chapter 4 (Paper 3): Parametric study of construction processes

The overall model described in the previous chapter is used to analyze and quantify the influence of different construction process in the efficiency of the bi-layer diaphragm wall technique (M9). Thirty numeric simulations are used to study the parameters, that are grouped in two categories: (a) specific bi-layer diaphragm walls characteristics (i.e. number of stages of spraying, depth of spraying); and (b) general diaphragm walls and construction characteristics (i.e. wall thickness, construction sequence, final structure geometry).

Chapter 5 (Paper 4): Evolution of concrete-to-concrete bond strength at early ages

The part of the experimental campaign corresponding to the bond between layers is reported in this chapter (M1). To perform it, it was necessary to adapt a shear test to cores extracted from the walls (M2). With the adapted test, the evolution of bond strength between the two concretes at early ages was studied (M3). Three preparation techniques were used: milled surfaces, milled and epoxy-bonded surfaces, and saturated milled surfaces.

Appendix 1 (Conference Paper 1): Early ages concrete-to-concrete bond strength assessed through shear and pull-off tests.

Besides the shear test, pull-off test were also performed to evaluate the bond strength (M3). The objective was to establish a simpler test to be used as a routine bond test in this type of walls. The results of the paper 4 are summarized in this conference paper, and correlated with the pull-off results. As it was not possible to extract conclusive results from this correlation, it was decided to present this paper as an appendix separated of the thesis main body.

1.6. RESERCH FRAMEWORK

Since the incorporation to the research group headed by professor Antonio Aguado the candidate has participated in different research projects. The two main ones are directly related to the topic developed in this thesis. In the first place, the candidate is part of the research team working in the Spanish Ministry of Science and Innovation (MICINN) project CONSFIB (reference: BIA 1010-17478): Construction processes

by means of fibre reinforced concretes. Secondly, the candidate participated in the PERMASTOP project (CTT-8062). This was an enterprise-university project which aim was to develop the bi-layer diaphragm walls.

"Lo que hagamos debe tener algo que podríamos
llamar economía cósmica, estar de acuerdo con el orden
profundo del mundo, y sólo entonces podrá tener esa autoridad
que tanto nos sorprende frente a las grandes obras del pasado"
— Eladio Dieste

CHAPTER 2.   Experimental and numerical structural analysis[1]

ABSTRACT: The bi-layer diaphragm wall, a new type of wall, consists of two concrete layers, the first of which is poured and the second sprayed, in different construction stages. A major aim of the research conducted is to maximize the functional attributes of the second layer, enhancing both structural performance and watertightness. The central objective of this study is to corroborate the structural behaviour of these walls in experimental and numerical terms. It follows a three-step methodology: a full-scale experimental campaign; development of a Finite Element Model (FEM) capable of predicting the structural behaviour of the wall; and, assessment of the second layer contribution. The experimental campaign confirmed the viability of the constructive solution and the FEM model accurately reflected the experimental data. A comparison between the bi-layer wall and other single-layer walls showed that the contribution of the second layer permitted reductions in first-layer reinforcement, adding to its various other functional advantages.

2.1. INTRODUCTION

Large cities are encouraged to make efficient use of space, especially below ground level (Bobylev, 2006). Expanding fleets of vehicles require the adaptation of their transport systems for circulation and parking. Urban metro systems and road tunnels help to reduce traffic congestion and to minimize contamination. The excavation works that these structures require should not adversely affect existing infrastructure and should minimize any interruption to the daily life of the city. In this scenario, the *conventional diaphragm wall* technique frequently represents a viable solution.

Economies in a diaphragm wall project may be achieved at the beginning of the design process, when selecting the method, the construction sequence, and the type of wall, and in the optimization of the temporal and permanent use of the retaining structure (Gaba et al., 2003). Accordingly, material consumption, the final dimensions of the wall, maintenance requirements, and construction complexity should all be evaluated before the adoption of any one solution (Gaba et al., 2003).

A widespread problem associated with this construction technique is leakage whenever the walls are erected in water-bearing ground. As there are no existing techniques to make diaphragm walls fully watertight, a variety of alternatives have been developed to cope with the leakage problem (Puller, 1994).

A common technique is repairing locally with a waterproof mortar render over areas where leakage is detected. However, leakage usually only appears over long time periods, at different times, and in different areas of a wall, causing problems for both owners and contractors. A less widely applied solution consists of casting a second layer of waterproof mortar (or concrete) over the inner face of the walls. Since the whole surface is covered, this is an effective albeit expensive solution (Wong, 1997). Finally, another common practice, already standardized in British construction codes (BS 8102, 1990, 2009), is to construct an inner wall separated by a cavity (Puller, 1994), at the bottom of which the water is left to accumulate before it is pumped out. Although dry inner walls are still constructed, this solution presents some drawbacks: the inner wall loses significant volume in view of the cavity and construction tolerances and it may, at worst, conceal dangerous leakages and even structural problems.

The major aim of this research project is to maximize the functional attributes of the second layer of concrete, based on the second lining solution described above, by allowing it to play a structural role, in addition to its initial intended purpose (waterproofing). In accordance with the structural role of the second layer, the thickness and reinforcement of the first layer may therefore be reduced. The dimensions of this bi-layer diaphragm wall and its improved watertightness suggest that it could be a feasible structural solution.

Thus, the *bi-layer diaphragm wall* represents a new type of slurry wall made of two bonded concrete layers poured and then sprayed, in separate stages. The first is a conventional reinforced concrete (RC) diaphragm wall. Once this wall attains the necessary strength, soil within the perimeter is excavated and removed, and the second layer, this time of sprayed concrete with steel fibres (SFRC) and a waterproof admixture, is applied.

This research work has been structured into four main areas: a) Structural level analysis; b) Sectional level analysis; c) Bonding between layers; and d) General design and optimization. The main objective of this paper is to corroborate the structural level behaviour of the bi-layer diaphragm walls both experimentally and

numerically (i.e., the first of the aforementioned areas). To do so, a methodology with three components was followed: a) demonstrate the viability of the proposed solution, by reporting on the experimental campaign to assess the structural behaviour of the bi-layer walls; b) develop a Finite Element Model (FEM) capable of predicting the structural behaviour of the bi-layer diaphragm walls; and, c) assess the structural contribution of the second layer with the cast RC wall through a theoretical example of use.

2.2. EXPERIMENTAL PROGRAM

2.2.1. General Information

The structural behaviour of various bi-layer walls at a building site in Barcelona (Spain) was analysed in a full-scale experimental campaign. Before construction began, a geotechnical study analysed the characteristics of the soil. Inclinometer tubes were placed inside the walls to analyze the structural behaviour of the composite element, and test specimens with poured concrete were used for material characterization, as described below. The bond between layers, transversal displacements and anchorage loads were also measured and have been reported previously elsewhere (Segura-Castillo & Aguado, 2011; Segura-Castillo & Aguado de Cea, 2012a, 2012b).

Fig. 6a shows the layout of the building site. Standard construction methods were used to build the diaphragm walls that enclose the building site around its perimeter. The figure also shows the location of the two experimental walls, both running parallel to the street. Within the walls, the two instrumented panels are labelled Wall W35 and Wall W45. The number indicates the width of the first layer of cast concrete (e.g. 35cm). Cross-sections views of these panels are shown in **Fig. 6b** including the finished frameworks up to street level (level: 0.00 m), the temporary anchors, and the phreatic level. The cross-section detail of a finished bi-layer wall is schematically represented in **Fig. 6c**.
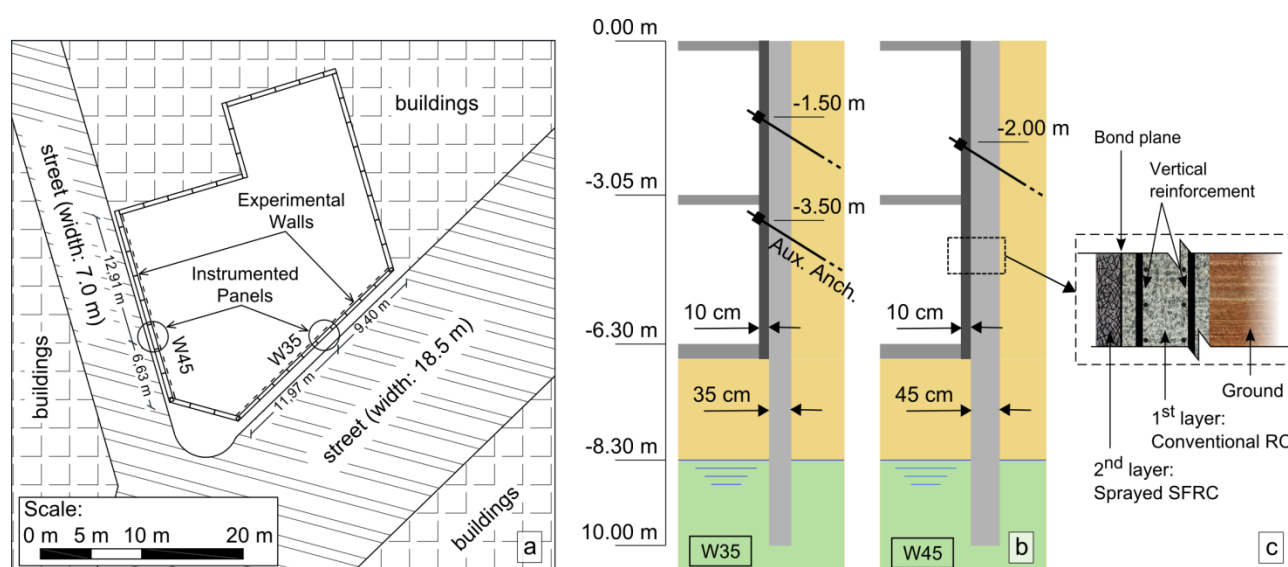
Fig. 6 - Experimental building: (a) site plan; (b) general cross-section; (c) detail of bi-layer cross-section.

The design of the experimental campaign was based on an uncoupled structure-section analysis. The structural analysis was performed using the Cypecad (CYPE Ingenieros, 2011) module for diaphragm walls:

a FEM-based program which considers soil-structure interaction, modelling the walls with FEM beam elements and the soil with a Winkler model. The numerical simulation of the mechanical behavior of the composite sections of the Wall was performed with the model "Analysis of Evolutionary Sections" (AES) (de la Fuente, Aguado de Cea, & Molins, 2008; de la Fuente, Aguado de Cea, Molins, & Armengou, 2012). This model allows simulation of the non-linear response of sections built with different materials (concrete and steel) and the structural contribution of the SFRC under tensile stress.

The Auxiliary Anchorage in Wall W35 was deliberately placed to cause flexural moments in the wall once the bi-layer section had been constructed, facilitating the analysis of the structural collaboration. When the Auxiliary Anchorage was eliminated, a bending increase in the wall occurred to redistribute the forces to the remaining anchorages and to the footing of the wall, placing the bi-layer cross-sections under greater bending moments.

2.2.2. Construction of experimental bi-layer walls

Details of the bottom-up construction sequence of the experimental bi-layer walls are summarized in **Table 5**. The following information is given for each stage: a brief description; number of days from panel casting to completion of the stage; a reference name used to identify the inclinometer reading; and the structural scheme of the model. A schematic diagram of the different construction sequence can be seen in **Fig. 7**. Details of the materials used and of the construction sequence are given below.
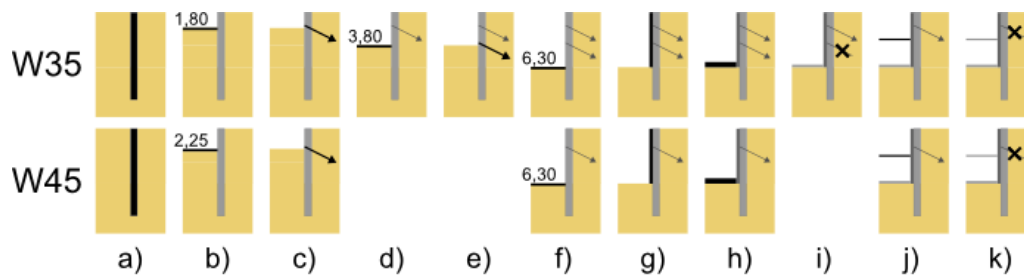
Fig. 7 - Wall construction sequence

A conventional reinforced-concrete diaphragm wall constituted the first layer of the bi-layer walls, with a theoretical compressive strength at 28 days of $f_c = 30$ MPa (UNE-EN 12390-3, 2003).

The excavation process began immediately after the cap beam had been placed in position over each complete line of panels. The main characteristics of the anchorages are given in **Table 6**. The rods were positioned when the excavation reached the required depth. Panels with anchorages alternated alongside panels with no anchorages. Struts instead of anchorages were fixed to the corner panels. A single line of anchorages was used around the entire perimeter, except in the experimental panel of Wall W35, where two anchorages were used.

Following completion of the excavation, surface preparation and roughening took place to improve the bond. Wall W45 was prepared by milling and Wall W35 by milling plus the addition of an epoxy bond product before spraying.

The second concrete layer was sprayed with a wet-mix process, thereby completing the structural element. Part of the spraying process can be seen in **Fig. 8**. There is general agreement in the literature that a bond

material with a modulus of elasticity that is similar to the modulus of the adjacent concrete is desirable in the application of concrete repairs, to ensure reliable performance (Saucier, Bastien, Pigeon, & Fafard, 1991; Wall & Shrive, 1988). The concrete manufacturers were therefore asked to prepare dosages with the same characteristic strength at 28 days. 30 kg/m^3 of DRAMIX RC-65/35-BN steel fibres were mixed into the concrete to be sprayed in the second layer.

Table 5 - Sequential stages of wall construction

Description of the stage*	Day		Reference name		Scheme
	W35	W45	W35	W45	
Casting the panel	0	0	**Cast**	**Cast**	**Fig. 7a**
Excavation before anchorage activation	40	33	**Exc180**	**Exc225**	**Fig. 7b**
Anchorage activation	40	33	**Anc150**	**Anc200**	**Fig. 7c**
(W45) Excavation progress-0	---	50	**---**	**ExcInt-0**	---
(W35) Excavation (3.80m)	57	---	**Exc380**	**---**	**Fig. 7d**
(W35) Aux. anchorage (3.50m) installation	57	---	**Anc350**	**---**	**Fig. 7e**
Excavation progress-1	68	61	**ExcInt-1**	**ExcInt-1**	---
End of excavation (6.30m)	78	71	**Exc630**	**Exc630**	**Fig. 7f**
Spraying of second layer	85	78	Spray	Spray	**Fig. 7g**
Construction of base slab	91	84	Base	Base	**Fig. 7h**
(W45) Control measurement-1	---	90	**---**	**Control-0**	**Fig. 7h**
(W35) Before aux. anch. elimination	97	---	**PreElim350**	**---**	**Fig. 7h**
(W35) Aux. anchorage (3.50m) Elimination-1	97	---	**Elim350-1**	**---**	**Fig. 7i**
(W35) Aux. anchorage (3.50m) Elimination-2	97	---	**Elim350-2**	**---**	**Fig. 7i**
Construction of lower slab	100	93	Slab	Slab	**Fig. 7j**
Before anchorage Elimination	109	102	**PreElim150**	**PreElim150**	**Fig. 7j**
Anch. Elimination-1	109	102	**Elim150-1**	**Elim200-1**	**Fig. 7k**
Anch. Elimination-2	109	102	**Elim150-2**	**Elim200-2**	**Fig. 7k**
Anch. Elimination-3	109	102	**Elim150-3**	**Elim200-3**	**Fig. 7k**
Control Measurement-2	110	103	**Control-1**	**Control-1**	**Fig. 7k**
Control Measurement-3	112	105	**Control-2**	**Control-2**	**Fig. 7k**

Bold letters indicate stages where inclinometer readings were performed
Underlined letters indicate stages selected for the comparison
*W45/W35 specified only where necessary, if stage differs in each wall

Table 6 - Anchorage properties

Anchor	Initial tensile load (kN)	Depth (m)	Total length (m)	Bulb length (m)	Cross-section area (mm^2)	Elastic modulus (KN/mm^2)	angle (°)
W35	500	1.5	20.0	14.0	563.92	198.46	30
W35 (Auxiliary)	300	3.5	13.5	8.5	281.96	198.46	30
W45	500	2.0	20.0	14.0	563.92	198.46	30

The required thickness of the second layer was 10 cm, however, layer thicknesses ranging from 9 cm to 17 cm were detected in subsequent core extraction tests, due to the intrinsic irregularity of the spraying system (Segura-Castillo & Aguado de Cea, 2012b). After spraying, the surface was kept wet for a whole day.

Fig. 8 - Bi-layer walls: (a) Spraying of second layer; (b) finished sprayed surface

Details of the mixture compositions and surface preparation used for constructing the walls can be found elsewhere (Segura-Castillo & Aguado de Cea, 2012a). Once the bi-layer wall had been completed, the base slab (70 cm thick) and the intermediate slabs (22 cm thick) were constructed.

2.2.3. Tests and Instrumentation

Samples were taken when concreting the walls to characterize the first concrete layer and to determine its compressive strength (UNE-EN 12390-3 (UNE-EN 12390-3, 2003)). During the spraying of the second layer, two moulds were filled with the same concrete and the procedure outlined in UNE-EN 14488-1 (UNE-EN 14488-1, 2006) was followed; cylindrical cores were extracted from the moulds to determine the compressive strength of the second layer (UNE-EN 12390-3 (UNE-EN 12390-3, 2003)).

An aluminium inclinometer casing was attached to the steel bar reinforcement cage of each experimental panel. The cages were then placed in the excavated area for casting the first concrete layer of the panel.

Inclinometer measurements were taken according to standard practice (Dunnicliff, 1993) at different depths (i), from 9.5m depth to ground level, separated 0.5 m each, at every critical structural stage (t). These stages are shown in **Table 5** in bold. Extra measurements were also performed: at an approximate depth of 5 m in the excavation (as it was not uniform, it had different depths in the different areas of the construction site); and in the anchorage release (the auxiliary anchorage in Wall W35 was released in two stages, both of which were measured, as the two cables that formed the anchorage were cut, one by one). Three measurements were taken for the main anchorage release, in order to assess the effect of any possible drag on the side panels. (i.e., one measurement was taken when the anchorage of the instrumented panel was released, and one for each of the side-anchored panels). Two extra control readings were performed at one and at three days after the main anchorage releases, to monitor the effects of possible time-dependent behaviour of the soil.

At each depth (i) and stage (t) two readings were taken: one in the main direction, and then another, repeated at the same point with 180 degree rotation the probe. The standard measurements of "Check Sum" (ChS_i^t), "Incremental Displacement" (I_i^t), and "Cumulative Displacement" (A_i^t) were then calculated (Dunnicliff, 1993).

2.3. NUMERICAL MODEL

The numerical model was calculated on the commercial geotechnical finite element software package PLAXIS (Brinkgreve, 2002). Experimentally determined parameters (or those calculated from them) were inputted into the model. Then, a final adjustment of the Young's modulus of the soil and the thicknesses of each layer were performed through a trial and error procedure.

These two parameters were chosen because of the well-known difficulties in determining the soil elastic modulus (Hsiung, 2009) and, because of uncertainties over wall thicknesses: the thickness of the grabbing tool gave a minimum value for the cast layer; and information from the extracted cores gave a range of values for the second layer (Segura-Castillo & Aguado de Cea, 2012b).

A 2D Finite Element Model (FEM) was used to represent a cross-section of wall and soil. The modelled panels were placed in the centre of the wall, 9.40 m away from the nearest corner for Wall W35, and 6.63 m, for Wall W45. Considering that this distance is in the same order as the excavation and, additionally, that the vertical joints between panels reduce horizontal stiffness, it is reasonable to assume that the constraints caused by the boundary effects at the corners of the walls were negligible.

The domain used in the analyses for Wall W35 is shown in **Fig. 9**. Horizontal fixity was assumed for the vertical boundaries and horizontal and vertical fixities were assumed for the bottom boundary, as shown in the same figure. A *fine* global coarseness was taken for the general mesh (automatically defined by the program), and refined in the vicinity of the bottom of the plate representing the diaphragm wall. A similar domain was used for Wall W45, differentiated mainly by the anchorage distribution.

The Mohr-Coulomb elastoplastic model assessed all four kinds of soils. It is considered sufficient for the analysis, as the study focuses more on the structural behaviour of the bi-layer walls than on soil behaviour and in view of the practical uncertainties involved in the definition of advanced model parameters for soil behaviour. The selected elements were 15-node triangular finite elements under plane strain.
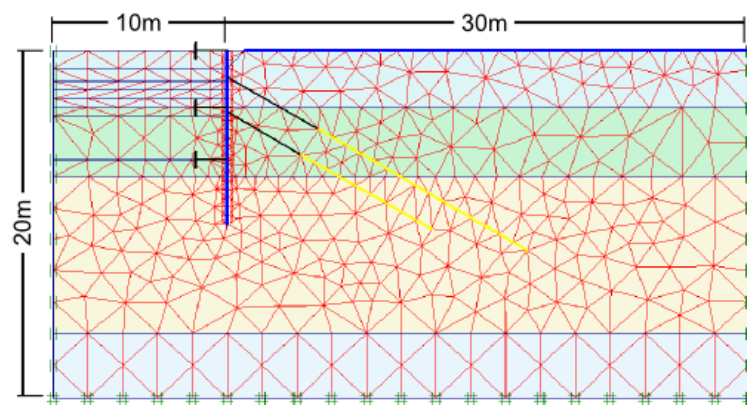
Fig. 9 - Finite Element mesh of W35 wall

The soil parameters determined by the geotechnical study and used in the model are shown in **Table 7**: total unit weight (γ); cohesion (c); friction angle (ϕ); coefficient of lateral earth pressure at rest (K_0), estimated by the expression of Jaky (Terzaghi, Peck, & Mesri, 1996); initial depth of the level (z_{ini}); strength reduction factor for soil-structure interface (R_{inter}); Poisson coefficient (ν); the Young's modulus approximated from

geotechnical parameters (E_0), and the one determined in back-analysis (E_{final}). As the phreatic level is below the maximum excavation, no water flows are considered in the analysis. The increase in the E value after adjustment of the model is in accordance with results published elsewhere (Ou & Hsieh, 2011), which point to high soil stiffness at small deformations.

Plate structural elements were used to model the diaphragm walls. A specific weight of 24 kN/m^3 was considered for the concrete. Its modulus of elasticity was calculated from the compressive strength ($f_{cm,28}$) according to standard EHE-08 (CPH, 2008), where: $E_{cm,28}$ = 27756 MPa. The elastic modulus time-evolution was ignored, as its difference was below 4% (see section 4.1). The same elastic modulus was also considered for both concrete layers as their values are relatively similar for both concretes (see section 4.1), and the change in the bi-layer stiffness is largely due to the increase in cross-sectional thickness, rather than any change in the elastic modulus.

The initial thicknesses considered in the analysis for both layers were their theoretical design values (i.e. 35 and 10 cm for the first and second layers of Wall W35; and 45 and 10 cm for Wall W45 respectively). The final values obtained after the back analysis are shown in **Table 8**. These values are reasonable considering, for the first layer, that an increase in the dig hole may be produced by the digging process and, for the second layer, the margin of thickness observed in the extracted cores.

Table 7 - Geotechnical parameters used in the PLAXIS model

Level	Type of soil	γ	c	ϕ	Ko	z_{ini}	R_{inter}	ν	E_0	E_{final}
		(kN/m^3)	(KN/m^2)	(°)		(m)			(KN/m^2)	(KN/m^2)
0	Heterogeneous fill	17.75	5.00	25.00	0.577	0.00	0.67	0.4	8000	50000
A	Brown silty clay	18.50	10.00	27.50	0.538	-3.25	0.67	0.4	40000	70000
B	Debris package of brown sand	18.75	0.01	31.50	0.478	-7.25	0.67	0.3	90000	70000
C	Brown, ochre and grey marly clay	18.60	13.50	28.00	0.531	-16.25	0.67	0.2	90000	80000

The stiffness values in the model are shown in **Table 8**. It can be seen that the flexural stiffness of the bi-layer wall is almost double that of the simple layer wall. Noting the PLAXIS recommendation: "*it is very important that the ratio of EI / EA is not changed, since this will introduce an out-of-balance force*" (PLAXIS 2D, 2010a), our interest centres on the bending moments that develop and the deflections that they cause. The calculated EI values for the bi-layer section were used, and the EA values of the bi-layer were calculated to maintain a constant EI/EA ratio. In the PLAXIS model, the wall stiffnesses were changed from the simple section to the bi-layer section after the spraying stage.

Table 8 - Thickness and flexural and normal stiffness of the walls used in the PLAXIS model.

	t_{final} (m)		EI (MN*m^2)		EA (MN)	
	1st layer	2nd layer	Simp.	Bi-layer	Simp.	Bi-layer*
W35	0.450	0.115	210.7	417.1	12.490	24.721
W45	0.550	0.140	384.8	759.8	15.265	30.142

* Value calculated to keep the EI/EA ratio unchanged

Geogrid structural elements and, *node-to-node anchor* elements were used to model the body and the free length, respectively, of the ground anchors. Their properties are shown in **Table 6**.

Two external loads were considered in the model: 3.0 kN/m^2 was placed over the pavement to represent its extra weight, and 50.0 kN/m^2 on the opposite side of the street, to represent the building weight. The street width is shown in **Fig. 6**.

2.4. EXPERIMENTAL RESULTS

2.4.1. Material characterization

Table 9 shows the material characterization for both layers of the wall and provides the mean compressive strength of the concrete and the elastic modulus of each layer. The concrete strengths of the first layer, which were already reported in (Segura-Castillo & Aguado de Cea, 2012a), corresponds to Wall W35. Other age strengths and Wall W45 values are also reported in (Segura-Castillo & Aguado de Cea, 2012a).

Table 9 - Compressive strength of concrete in both phases

Age of concrete, days		f_{cm}, N/mm2		E_{cm}, N/mm2		
1st layer	2nd layer	1st layer	2nd layer	1st layer (Eq. 1&2)	2nd layer (Eq. 1&2)	2nd layer (Eq. 3&4)
28	-	34.82	-	27756	-	-
87	2	38.94*	30.99	28703	27033	22047
91	6	39.05*	39.22	28728	29012	24826
120	35	39.97*	45.40	28929	30314	26726

* Values calculated according to the concrete maturity equations (Neville & Brooks, 2010).

The modulus of elasticity was calculated from the characteristic strength by two means. First, according to the EHE-08 (CPH, 2008) formulas:

$$E_{cm}=8500 \cdot \sqrt[3]{f_{cm}} \tag{1}$$

$$E_{cm,j} = (f_{cm,j} / f_{cm})^{0.30} \cdot E_{cm} \tag{2}$$

Where, E_m and f_{cm} are the modulus of elasticity and the mean compressive strength at 28 days, respectively, and $E_{m,j}$ and $f_{cm,j}$ are the modulus of elasticity and the mean compressive strength at time j, respectively.

Considering that for the same characteristic strength, the sprayed concrete seems to have a lower elastic modulus than the cast concrete (Galobardes, 2013; Malmgren, 2007), an estimation of the elastic modulus for the second layer concrete was also done by equations 3 and 4 (Galobardes, 2013), which adjust the coefficients of the EHE-08 formulas for sprayed concrete:

$$E_{cm}=7480 \cdot \sqrt[3]{f_{cm}} \tag{3}$$

$$E_{cm,j} = (f_{cm,j} / f_{cm})^{0.504} \cdot E_{cm} \qquad (4)$$

It can be seen that the differences in the strength and the elastic modulus of the concretes from both layers are relatively small, particularly for at least two ages that are shown, when the wall is placed under load. For example, the second layer elastic modulus, at 35 days, is 5% above (according to Eq. 1 and 2), or 7% below (according to Eq. 3 and 4) the first layer modulus. This validates the hypothesis of similar modules of elasticity in both layers.

2.4.2. Reliability of inclinometers

The inclinometer readings presented some systematic and individual measurement errors. Data pre-processing will be described using the results for Wall W35. The same process was followed for Wall W45, although its description is omitted here.

The values of the incremental displacements (I_i^t) are shown in **Fig. 10a**. Individual errors are abnormal values recorded at a specific stage and at a specific depth; for example, the four measures that are circled in **Fig. 10a** that are clearly beyond the normal range of displacements of the wall. Moreover, these points lie outside the normal range of recorded values for the offset. These disproportionate displacements may be produced by local deformations induced by the anchors, as they occurred at stages when the anchors were activated, and at points near the positions of the anchors.

Systematic error can be of two types: abnormal values repeatedly registered at various depths throughout the same stage, or at different stages at the same depth.

Two depths (6.5 m & 9.5 m) are circled in **Fig. 10a**. The readings at a depth of 9.5 m were taken from the bottom of the inclinometer tube. As it was the first measurement in each series, this reading could have been taken while the inclinometer sensor was still not properly stabilized. The inconsistencies registered at depth 6.5 m, might be due to an imperfection in the inclinometer tube. At this depth, there is a coupling between two sections of the inclinometer casing. A slight break could be seen in the connection in a photo taken during the casting of the wall. Furthermore, the break can be seen if the "absolute position" of the measures is plotted.
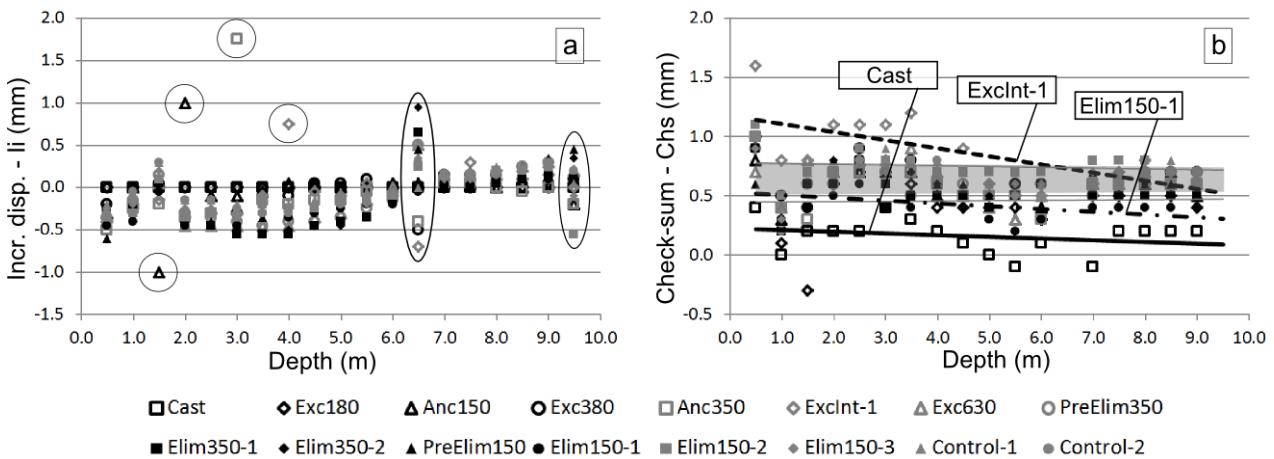
Fig. 10 - Inclinometer results of W35 wall: a- Incremental displacements; b- Check-sum values

The plot of the Check-sum values is shown in **Fig. 10b**. Linear trend lines of the values of the offset for every stage are also shown in **Fig. 10b**. Systematic errors at these stages can be identified by observing these trend lines. "*The check-sum is usually equal to twice the zero offset (bias) of the transducer (…) and ideally should remain constant for all depth intervals in a given data set.*" "*Check-sum may vary randomly about a mean value. Small variations do not usually indicate a problem*" (Dunnicliff, 1993). The area where 13 out of 16 trend lines are concentrated is shadowed in grey, and the three trend lines clearly out of this area are individually plotted. Small variations are due to the experimental error. However, the lines further away from the general trend indicate a systematic error in the measured stage.

Both systematic and individual measurement error will be omitted from any future analysis, in order to strengthen confidence in the measurements for this analysis. Accordingly, the natural reference stage (i.e. the "cast" stage) is omitted, so the selected reference stage is specified in each analysis.

2.4.3. Selection of representative stages

Fig. 11 shows the incremental displacements of different readings that correspond to the same structural stage; in this case, the elimination of the anchor of Wall W35 at a depth of 1.5 m. The instant readings (stages "Elim150" numbers 2 & 3) were taken immediately after releasing each of the anchors of the instrumented panel and the adjacent panels. New readings were taken (stages "Control" number 1 & 2), at one day and at three days after release.

The soil shows time-dependent behaviour. As this study focuses on the structural behaviour of the diaphragm wall rather than soil behaviour, the most representative reading of each structural stage is taken to perform the structural analysis. As a rule, the final reading is selected from each stage to record the largest possible deformations caused by behaviour over time.
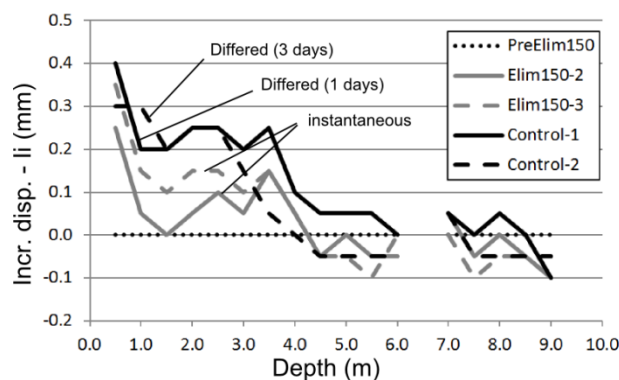
Fig. 11 - Incremental displacements at the same structural stage and at different times for W35 (Reference stage: PreElim150)

Two readings were taken on the day the anchorages were installed: one before the installation and one immediately after it. The soil could only develop instant deformations between these stages. As the excavation resumed after installation of the anchors, the effects of any subsequent soil deformation were combined with the excavation effects. A clear reading of the situation after anchorage installation could not therefore be taken, so the readings taken just after these stages could not be used in the structural analysis.

Only very slight incremental displacements were observed at some stages, particularly in Wall W45, that have greater flexural stiffness. Therefore, the results were qualitatively evaluated in the stages with small displacements (i.e. Wall W45), while the stages with large displacements (i.e. Wall W35) were used for the quantitative adjustment of the model parameters.

The most representative stages on which to perform the structural analysis, underlined in **Table 5**, were selected on the basis of the above-mentioned criteria (i.e.: Elimination of individual and systematic measurement errors; selecting the last reading when several readings were taken over one structural stage and; discarding the readings taken just after anchorage installations).

2.5. MODEL VS. EXPERIMENTAL COMPARISON

2.5.1. Model adjustment

The experimental incremental displacements are plotted with error bars in **Fig. 12** through the representative stages of Wall W35. The error bars indicate the standard deviation of the Check Sum of each inclinometer. The corresponding values obtained by the model are plotted with a continuous line in the same figure.

Worse adjustment was registered for Wall W35 at stage Exc380, at depths of below 3.0 m. The auxiliary anchorage was positioned at a depth of 3.5 m on this panel after partial excavation in the area surrounding the panel, and not when the general site excavation had reached the necessary depth. A dragging effect from the neighbouring panels might have been the cause of these differences between the model and the experimental data, as soil still surrounding the side panels might have resisted any lateral displacement towards the excavated area caused by the partial excavation in the experimental panel.
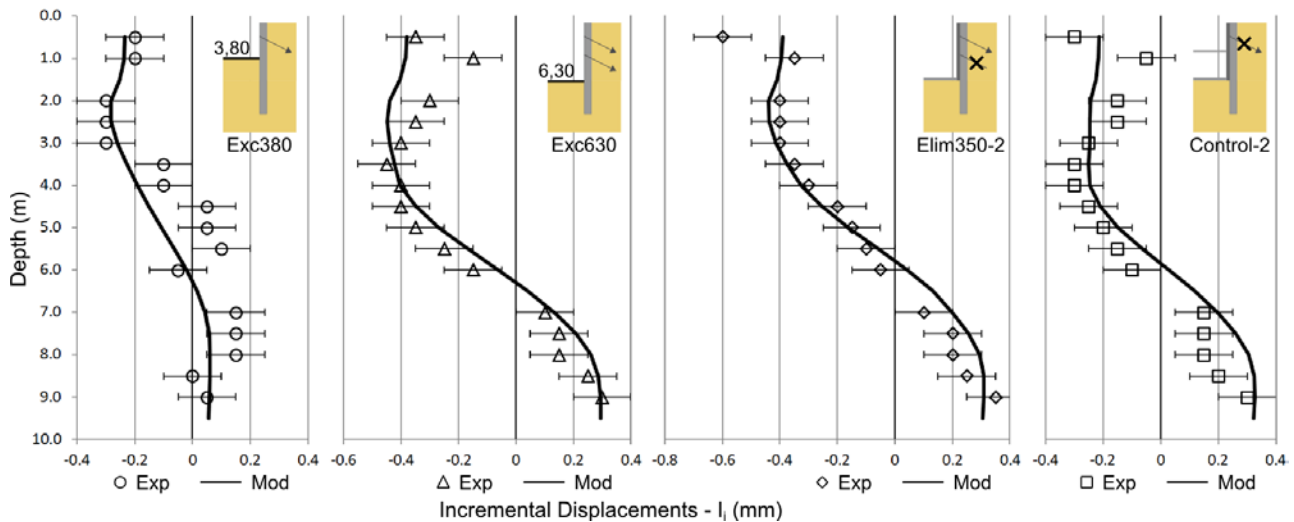
Fig. 12 - Comparison of incremental displacement values calculated by the PLAXIS model and experimental values for the representative stages of Wall W35. (Reference stage: Exc180)

The series of plots in **Fig. 12** show two that correspond to displacements when the bi-layer was still not activated (stages "Exc380" and "Exc630"), and two that correspond to displacements after the "Spraying" stage (stages "Elim350-2" and "Control-2"), upon completion of the bi-layer wall. Similar levels of adjustment were therefore achieved in both the pre and post-spraying stages.

The corresponding displacements for Wall W45 are plotted in **Fig. 13**. It can be seen that notably different levels of adjustments were reached in the different stages.
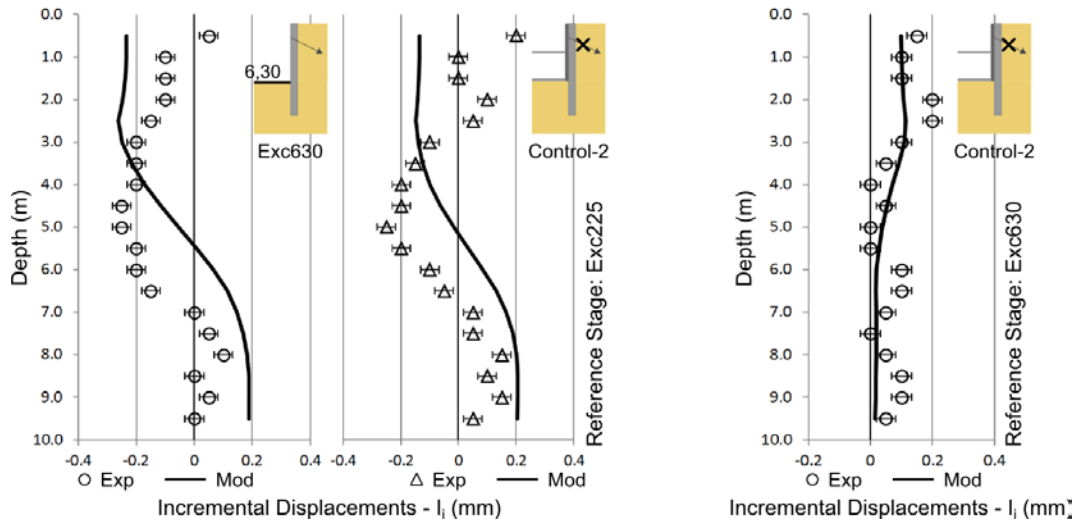
Fig. 13 - Comparison of incremental displacements calculated with the PLAXIS model and experimentally obtained for the representative stages of Wall W45

Larger qualitative differences between experimental and model data were recorded in this wall, although the displacement magnitudes remained within the same range. In this case, the differences might be due to lower precision of the experimental data at the selected reference stage, evident from the trend of the offset that lay slightly outside the general trend of the data set at that stage, equivalent to those included in section 4.2. for Wall W35. In confirmation of this hypothesis, **Fig. 13** also shows the relative incremental displacement of the "Control-2" stage using the "Exc630" stage as a reference stage. The adjustment is evidently better, although the displacement is smaller.

Notwithstanding the uncertainties in the experimental data and the simplifications in the model, good adjustment may generally be seen between both in the two walls.

2.5.2. Wall behaviour

Horizontal displacements and bending moments of the adjusted PLAXIS model for Wall W35 are shown in **Fig. 14**. The expected qualitative behaviour can be observed in general throughout the different stages. One result that may attract attention is the small deflection after the first excavation, when the walls behave in cantilever mode, which could be explained by a number of reasons. A preliminary excavation of 1.0 m in depth was completed in the area prior to the construction of the walls, which was also included in the model. Moreover, the high superficial loads (50 kN/m^2) on the other side of the street, introduced to account for the nearby buildings, increase the pressures, and hence the displacements, in the lower parts of the walls. Finally, the finite element model and the Mohr-Coulomb elasticity model overestimated soil decompression during the excavation, reducing horizontal pressures in the interior soils, thereby causing large-scale horizontal displacements at the bottom of the walls towards the interior.

The reason for placing the auxiliary anchorage in Wall W35 is now evident. The change in bending moments, from stage "exc630" to "elim350", is indicated by a hatched area in **Fig. 14**. This increment,

which was activated in a controlled manner through the anchorage release, was resisted by the compound section.
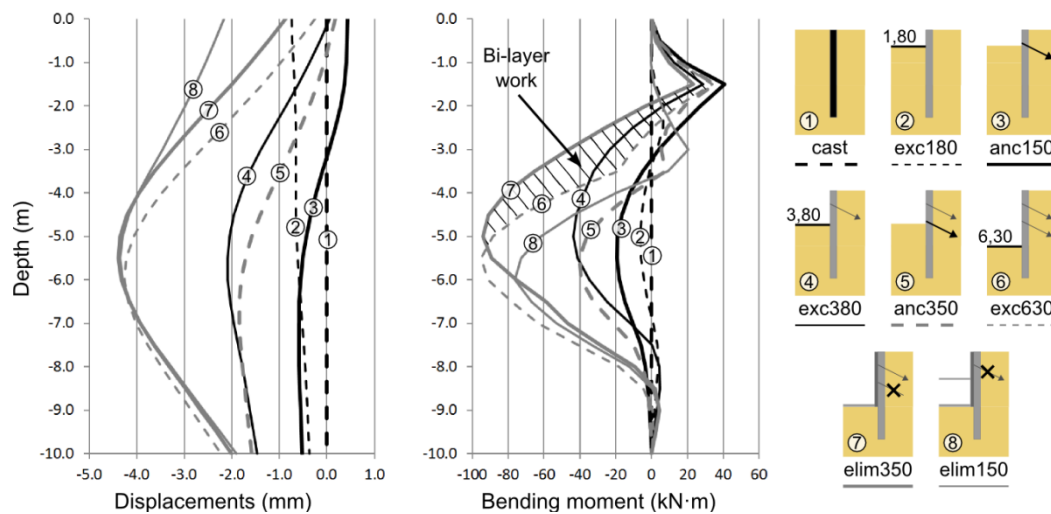
Fig. 14 - Horizontal displacements and bending moments obtained by the adjusted PLAXIS model for Wall W35

The corresponding Horizontal displacements and Bending moments of Wall W45 are shown in **Fig. 15**. A comparison of these plots with those for Wall W35 reveals the difference in stiffness of both walls. While the displacement of Wall W45 differs by almost 2 mm from the top to the centre, Wall W35 has differences of more than 3 mm.
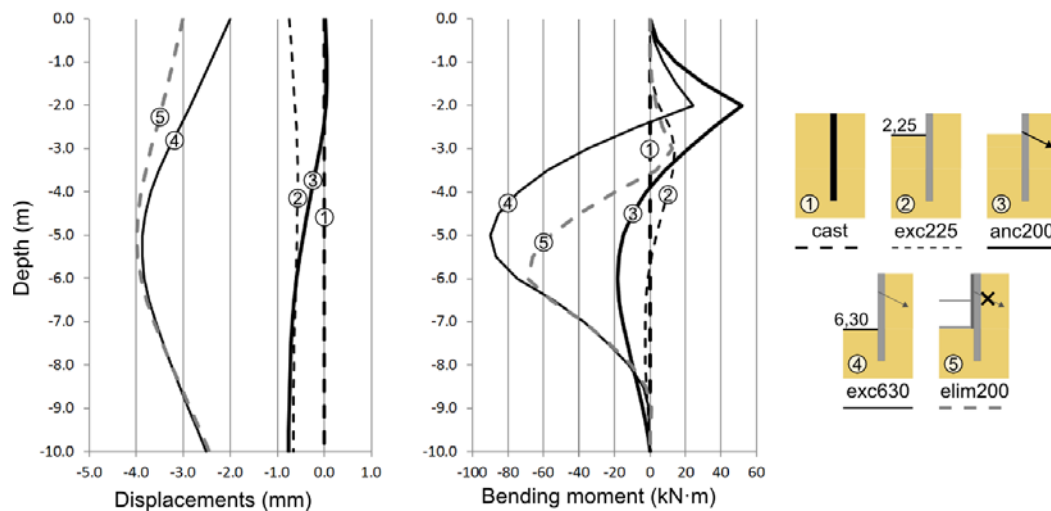
Fig. 15 - Horizontal displacements and bending moments obtained by the adjusted PLAXIS model for Wall W45

2.6. DISCUSSION – DESIGN PROCESS AND COMPARISON

A bi-layer wall case study (namely Wall T.BLW35, with a cast layer of 35 cm and a sprayed layer of 10 cm) is discussed in this section. Its design method takes advantage of the compound section. A comparison with two conventional single-layer walls quantified differences with regard to the performance of bi-layer walls. The first wall (T.W35) had the initial thickness of the bi-layer wall (35 cm), and the second (T.W45) had the final thickness (45 cm). All cases were implemented with the previously described model. The analyses

presented below cover the structural level, leaving the sectional analysis for a further paper, which will apply a similar strategy to that presented in (de la Fuente, Aguado de Cea, et al., 2012).

2.6.1. Description of case studies

All the general characteristics of the model of Wall W45 described in section 2.3 are used in these models, except for the modifications specifically described below.

The construction stages are indicated in **Table 10**. The characteristics of the anchorage are identical to those described for the experimental case of Wall W35.

Table 10 - Sequence of construction stages of theoretical walls

	Reference name		
Description of the stage*	T.W35	T.BLW45	T.W45
Casting of panels	Cast	Cast	Cast
Excavation before anchorage activation	Exc175	Exc175	Exc175
After anchorage activation	Anc150	Anc150	Anc150
(T.BLW45) Intermediate excavation	---	Exc525	---
(T.BLW45) Spraying of second layer	---	Spraying	---
End of excavation	Exc630	Exc630	Exc630
Construction of base & slabs	Base&Slab	Base&Slab	Base&Slab
Anchorage elimination	Elim150	Elim150	Elim150

*T.BLW45 specified when stage differs in other cases

Central to the bi-layer wall design is its capability to withstand the moments that develop during the final stage of the excavation. The application of a sprayed layer during the construction stages gave the compound section greater strength to resist these forces as they developed. This situation is no longer the same as in the previously described experimental cases, in which the compound section was tested through the addition of an auxiliary anchorage.

2.6.2. Results for theoretical cases

This analysis centres on two usually crucial factors in the design of the walls: on the one hand, the deformations, and, on the other hand, the bending moments that develop in the walls.

2.6.2.1. Displacements

The displacements that the model generated in the case of Wall T.BLW45 are plotted in **Fig. 16**. The maximum deformations at the top and at the centre of the wall are observed in the last constructive stage (elim150). This stage will be used to perform the comparison, as in the other two theoretical cases.

The maximum displacements in the three theoretical cases are plotted in **Fig. 17**. Similar displacements were calculated for the two cases with the same thickness of cast layer (T.W35 and T.BLW45), while a smaller deep inward displacement, and a larger surface displacement was calculated for the thicker wall (T.W45).
The influence of the second layer on any final displacements was not very large and may in future be calculated in accordance with the thickness of the first layer.
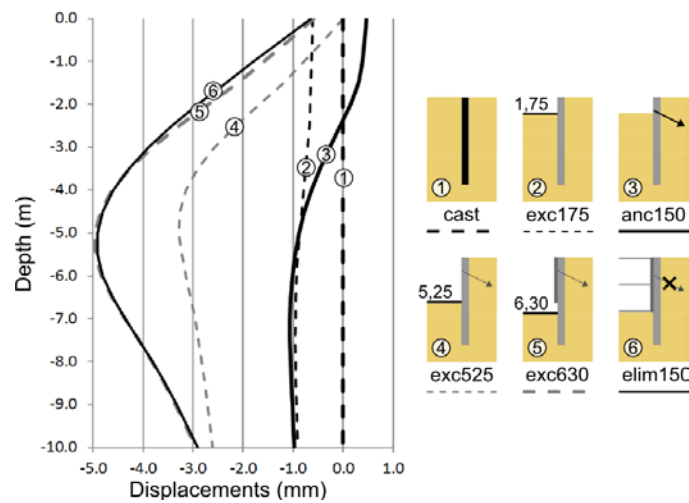
Fig. 16 - Horizontal displacements obtained by the PLAXIS model for the T.BLW45 design
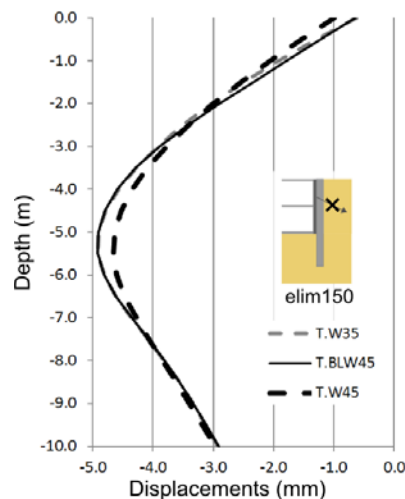
Fig. 17 - Maximum displacements for the three comparative cases

2.6.2.2. Bending moments

Calculation of the reinforcement is not discussed here for the sake of brevity. Instead, in a simplified approach, the comparison will be performed directly with the bending moment diagram.

The bending moments in the case of Wall T.BLW45 are plotted in **Fig. 18**. From the first stage up until stage exc525, the wall only consists of the cast section. After this stage, the second layer is sprayed, from the top of the wall to a depth of -5.0 m. Therefore, the contribution of the compound section can be considered in that area, in the stages after exc525. A slight increment in bending moments at depths of between -3.0 m and -5.0 m can be seen in **Fig. 18** when moving from stage exc525 to stage exc625. Subsequently, when the anchorage is released, the positive bending moments around the anchorage point, turn negative, when it is eliminated, creating a new area of bending moments from the top of the wall to a depth of -3.0 m.

After spraying the second layer, the compound section is able to resist the bending moments that are generated, which allows us to consider the collaboration of the second layer of sprayed steel fibre concrete in the aforementioned stages.
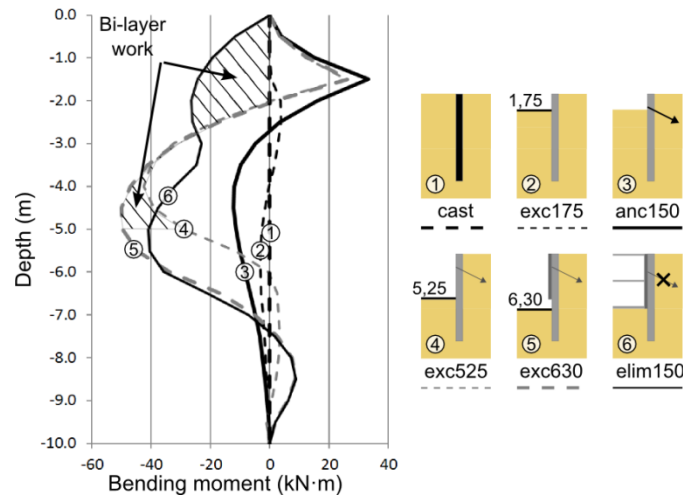
Fig. 18 - Bending moments obtained by the PLAXIS model for the T.BLW45 design example

The bending moment envelopes for all three cases are compared in **Fig. 19**. Clearly, the more flexible the wall, the smaller its bending moments, which is due to soil behaviour. When the soil structure adapts to the structure, this leads to changes in soil pressure, tending towards values of smaller magnitude that reflect active pressure, which explains the larger differences between Wall T.W45 and the other two cases.

There are also differences between the two cast-section walls with a width of 35 cm. These arise after the spraying stage due to the increased stiffness of Wall T.BLW34. The maximum bending moments in these two cases are: -48.3 kN·m for Wall T.W.35 and -50.0 kN·m for Wall T.BLW35.

2.6.2.3. Optimum design

Two zones may be differentiated in the case of Wall T.BLW35 in **Fig. 19**: the bending moment envelope of the stages where only the simple cross section of the cast layer is operational (continuous line); and the envelope of stages after spraying of the second layer, where the compound cross section is working (dashed line, patterned fill). Obviously, the first layer envelope applies to both single-layer walls.

Maximum performance could be reached, if it were possible to design the reinforcements of both layers, in order to resist those bending moments that they are precisely intended to withstand. In other words, a first layer section (amount of reinforcement bars) capable of resisting the continuous line envelope of moments, and a second layer (amount of steel fibres), so that the compound section resists the corresponding dashed line envelope of moments. Although this ideal situation is difficult to reach, as the steel fibres (with a lower tensile strength than the traditional reinforcement) strengthen the second layer, it is still possible to give the second layer considerable load bearing capacity in the ultimate capacity of the compound section.
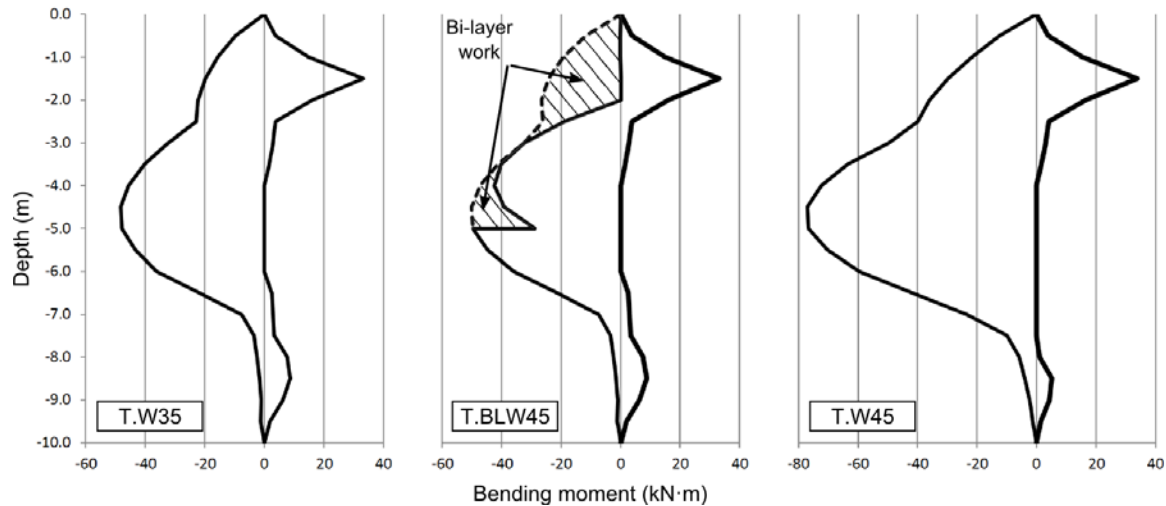
Fig. 19 - Bending moment envelopes for the three comparative cases

2.6.3. Comparison

The main characteristics and the principal results of the theoretical cases are summarized in **Table 11**. The following information is given for each case: area of the bending moments envelope from **Fig. 19**, discriminated by type of cross section working, and total of both areas; maximum horizontal displacements, on the top of wall, and in the central region; theoretical thickness of the wall; and, finally, whether it is a watertight design.

Table 11 - Main results of theoretical comparison performed with PLAXIS model

		T.W35	T.BLW45	T.W45
Bending moments	Simple section	266.3	220.1	393.5
envelope area	Compound section	---	57.9	---
(kN·m·m)	Total	266.3	278.0	393.5
Horizontal displacement	Top	0.63	0.64	0.99
(mm)	Centre	4.99	4.97	4.70
Theoretical thickness (cm)		35	45	45
Waterproof wall		NO	YES	NO

Regarding the displacements of Wall T.W35, the results are even practically comparable to the bi-layer solution, with differences of below 2%. In return, a reduction in the reinforcement needed for the simple cross section can be achieved. In the case of Wall T.35, the simple section must withstand 266.3 kN·m·m, whereas in the T.BLW35, the value to be withstood is reduced to 220.1 kN·m·m (which implies a reduction of 17%). Although it is impossible to take full advantage of this moment reduction, reductions in the reinforcement of up to 10% have been obtained in preliminary calculations. It should not be forgotten that the main advantage of the bi-layer wall is its watertight design.

The single-layer Wall T.W45 was considered to compare two solutions with the same final thickness. Besides the previously mentioned considerations regarding the addition of the second layer, the slender solution is advisable for all comparative parameters listed in **Table 11**, except for deformation in the centre of the wall. Thus, the thickness of the cast layer may be reduced insofar as is permitted in accordance with

the maximum displacement. Then, the advisability of using the bi-layer solution may be analysed according to the guidelines outlined in the previous section.

The main drawback of the bi-layer solution, compared to a single-layer one, may be the increase in cost implied by the placement of the second layer, which not only includes the material cost, but also other factors such as placement logistics and design. The additional drawback of an increased final thickness of the wall in the bi-layer solution (i.e. less available space inside) should also be considered. Nevertheless, the final thickness of the single-layer wall will ultimately be as thick as, or thicker than, the bi-layer wall, following the selection and the application of one of the common methods to improve watertightness.

In contrast, the following functional advantages may be outlined for a bi-layer solution: 1- a wall that has improved watertightness built into its design, avoiding future uncertainty over repair work due to leakage; 2- even surface finish provided by the second layer; 3- economical use of space, especially compared with the construction of inner wall solutions; and 4- improved efficiency in the use of materials, through the multiple functionalities of the second layer. The solution also appears particularly suitable if used on large construction sites, where the switch between excavation, temporary support, and spraying tasks is not a significant problem.

2.7. CONCLUSIONS

A new structural type of slurry wall, referred to as a bi-layer diaphragm wall, and its associated structural and functional improvements have been described in this paper. Structural sections are usually designed as a conventional diaphragm wall to which a second waterproofing layer may be added afterwards. However, in this proposed solution, the second layer is sprayed and bonded to the first one during construction, so that it fulfils a structural role. Hence, this procedure leads to an optimized section with improved watertightness.

An experimental and theoretical study applied to a full-scale case has been performed which examined two bi-layer walls of different cross-sections. The experimental results of readings from inclinometers embedded in the walls were reproduced with a numerical model running on the PLAXIS FEM program. This model was subsequently used to quantify the structural contribution of the second layer with the cast RC wall.

The following conclusions have been drawn:

1. An experimental campaign involving bi-layer walls was successfully conducted. The results support the viability of this solution and demonstrate the monolithic behaviour of the combined layers. The results, however, only apply to this particular case study and care must be taken directly extrapolating to other examples without further research.

2. A comparison of the results from the calibrated model and from the experimental campaign demonstrated a very good correlation, which validated the model. It considered cross-sectional changes in the stages after spraying the second layer and reproduced both the qualitative and the quantitative displacements of the instrumented walls with a high degree of accuracy.

3. The model compared a theoretical bi-layer wall (35+10 cm thick) with two referenced single-layer walls (35 cm and 45 cm), in order to identify possible structural improvements. The structural behaviour of both the bi-layer wall and the single-layer wall with the same first layer thickness was

similar in relation to their bending moments and deformation. The second layer however, allowed a reduction in the reinforcement required in the first layer. In the theoretical case, a 17% reduction in bending moments was achieved for the first layer, which would result in a partial reduction in reinforcement.

2.8. ACKNOWLEDGEMENTS

"All in all it's just another brick in the wall.
All in all you're just another brick in the wall."
— Pink Floyd – The Wall

CHAPTER 3.   Structural and sectional analysis[2]

ABSTRACT: The bi-layer diaphragm wall, a new slurry wall type designed to cope with the problem of watertightness is studied in this paper. These walls consist of two bonded concrete layers, the first, a conventional Reinforced Concrete (RC) diaphragm wall, and the second, a Sprayed Steel Fibre Reinforced Concrete (SFRC). The main objective of this paper is to analyze the structural and sectional behaviour of these walls. A study in the form of an uncoupled structural- section analysis based on various hypothetical cases of bi-layer diaphragm walls was performed to fulfil the objective. It is concluded that there exists a potential of reduction in the reinforcement of the RC layer through the structural use of the SFRC layer. However, when the reduction is quantified, even though a reduction of between 3.2% and 1.7% in the RC reinforcement is confirmed, it appears insufficient to offer a cost-effective solution. Nonetheless, the system becomes a promising solution when particular conditions are taken into account, such as basement space limitations.

Keywords: waterproof, diaphragm walls, fibre concrete, sprayed concrete, numerical analysis, FEM, PLAXIS.

3.1. INTRODUCTION

A widespread problem associated with diaphragm wall construction is the occurrence of leakage whenever erected in water-bearing ground. There are no techniques to make diaphragm walls fully watertight, so a variety of alternatives, all of which with different drawbacks, have been developed to cope with the leakage problem (Puller, 1994). The waterproof system in these solutions is added to the wall after their construction is complete, so it is not an integral part of the structure of the walls.

Considering the aforementioned points, one conceivable solution would be a waterproof layer that also assumes a structural function. The *bi-layer diaphragm wall*, a new slurry wall type, designed to cope with the problem of watertightness in these types of walls has previously been presented by Segura-Castillo *et al.* (2013)(Segura-Castillo, Aguado, & Josa, 2013). These walls consist of two bonded concrete layers poured and then sprayed, in separate stages. The first is a conventional Reinforced Concrete (RC) diaphragm wall. Once this wall attains the necessary strength, soil within the perimeter is excavated and removed, and the second layer, this time of Sprayed Steel Fibre Reinforced Concrete (SFRC) and a waterproof additive, is applied.

This paper is part of an experimental and theoretical study on bi-layer diaphragm walls, which has been structured into four main areas: a) Structural level analysis; b) Sectional level analysis; c) Bonding between layers; and d) General design and optimization. Of these, the structural level behaviour was partially reported in (Segura-Castillo, Aguado, & Josa, 2013), and the bond analysis in (Segura-Castillo & Aguado de Cea, 2012a).

The main **objective** of this paper is to analyze the structural and sectional behaviour of the bi-layer diaphragm walls. The overall design method is presented. With it, the contribution of each layer is quantified, placing special emphasis on the SFRC layer contribution.

3.2. METHODOLOGY

A study in the form of an uncoupled structural-section analysis based on the hypothetical case of various bi-layer diaphragm walls was performed to fulfil our objectives.

A 2D Finite Element Model (FEM) was selected to analyze the <u>*structural behaviour*</u>. A numerical rather than a simplified model is necessary, as the constructive sequence is considered (Carrubba & Colonna, 2000), which includes the cross-section changes that take place when the SFRC is sprayed, together with general wall and soil properties. The literature contains many studies that utilize these models to analyze ground movements caused by deep excavations, due to their importance in the prediction of possible damage to adjacent buildings during excavation process (e.g. (Hsiung, 2009; Khoiri & Ou, 2013; G. T. C. Kung et al., 2007; G. T.-C. Kung, 2009)). On the other hand, fewer studies (e.g. (Carrubba & Colonna, 2000; Costa, Borges, & Fernandes, 2007; Ou & Lai, 1994)) have evaluated the forces and stresses produced on the walls.

It should be mentioned that use of the elastic-perfectly plastic "Mohr-Coulomb" model means that the soil has to be discretized into several horizontal layers and its elastic properties have to be changed as the depth increases, before the model responds to any increase in the soil modulus of elasticity, due to increased

vertical pressure (Khoiri & Ou, 2013). The hardening soil model (HS) (Schanz et al., 1999) was therefore chosen, as it models the entire ground in the study with only one set of parameters.

The numerical simulation of the mechanical behaviour of the *composite sections* of the wall was performed with the model "Analysis of Evolutionary Sections" (AES) (de la Fuente, Aguado de Cea, et al., 2012). This model simulates the non-linear response of sections built with different materials (concrete and steel) and the structural contribution of the SFRC, when subjected to tension. In the AES model, the concrete sections are discretized in layers of constant thickness (see **Fig. 20a**), whereas steel rebars are simulated as concentrated-area elements.

In this study, the procedure to design the reinforcement of the concrete wall followed the basic design principles for traditional reinforced concrete presented in (EN, 2004b). According to these hypotheses, the ultimate bending moment (M_U) is calculated and compared with the maximum design bending moment (M_d), calculated by the structural analysis, for the most unfavourable construction stage and for each kind of section.

The compressive behaviour of the concrete (see **Fig. 20b**) was simulated, on the one hand, by considering the constitutive law proposed in EC-2 (EN, 2004b). On the other hand, the tensile response of the SFRC was simulated through constitutive law σ_c-ε_c, as suggested in (RILEM TC 162-TDF, 2003). Finally, the mechanical performance of the steel bars was simulated with the bilinear diagram presented in **Fig. 20c**.
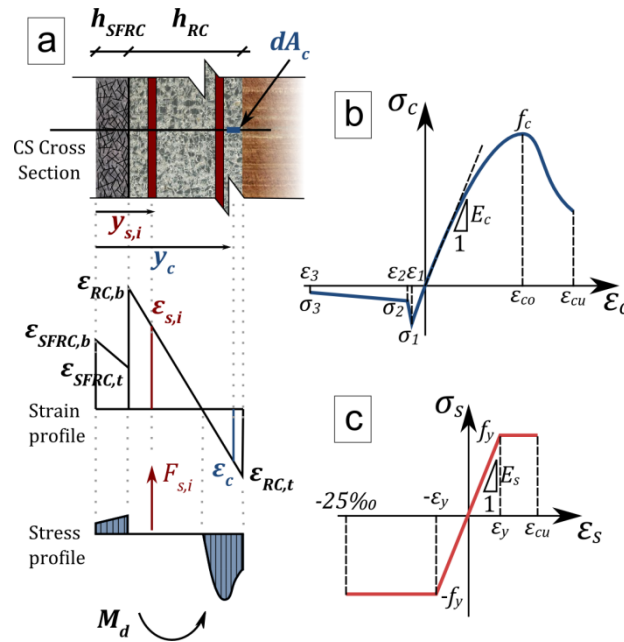
Fig. 20 - (a) Sectional discretization; (b) SFRC and (c) steel bar constitutive equations.

In addition to the internal equilibrium conditions, the following hypotheses are also considered: (1) the sections remain plane before the application of the external forces or after imposing fixed strains; (2) failure of the composite section is achieved when there is either excessive compressive strain in the upper concrete layer ($\varepsilon_{RC,t}$ = -3.5‰) and/or excessive elongational strain in the tensioned steel bars ($\varepsilon_{s,i}$ = 10.0‰); and, (3) a perfect bond between the concrete and the rebars, as well as between the RC and the SFRC layers. Regarding

the latter, it has to be mentioned that the suitability of this assumption has previously been studied in (Segura, Aguado 2012).

3.3. CHARACTERISTICS OF THE WALLS

3.3.1. Geometry and construction sequence

This study is based on the hypothetical case of the construction of walls designed for use in a four level basement. The comparison considers one conventional diaphragm wall, referred as the mono-layer wall (ML) for the sake of clarity, and two bi-layer walls (BL), differentiated only by their thicknesses (all other properties remaining constant):

- ML_{60}: Conventional RC diaphragm wall of 60 cm thickness.
- BL_{60+10}: Bi-layer RC wall with a thickness of 60 cm onto which a 10 cm thick SFRC layer is sprayed.
- BL_{55+10}: Bi-layer RC wall with a thickness of 55 cm onto which a 10 cm thick SFRC layer is sprayed.

The general characteristics of the walls used in this study are similar to those used by Carrubba & Colonna (2000), in order to contrast our results with others from the technical literature. Apart from some minor differences, a major difference is the increase in the penetration depth of the walls. This change is because the one in the reference is below the usual range for this depth of excavation (Long, 2001).

The selected diaphragm wall was 20.0 m high and required an excavation depth of 12.5 m (with a 7.5 m embedded footing), as illustrated in **Fig. 21a**. During the excavation process, the wall was supported by up to 4 rows of ground anchors vertically spaced at 3.0 m and horizontally spaced at 5.0 m in the two upper rows: Superior Anchorages (S.A.); and at 2.5 m in the two lower rows: Inferior Anchorages (I.A.).
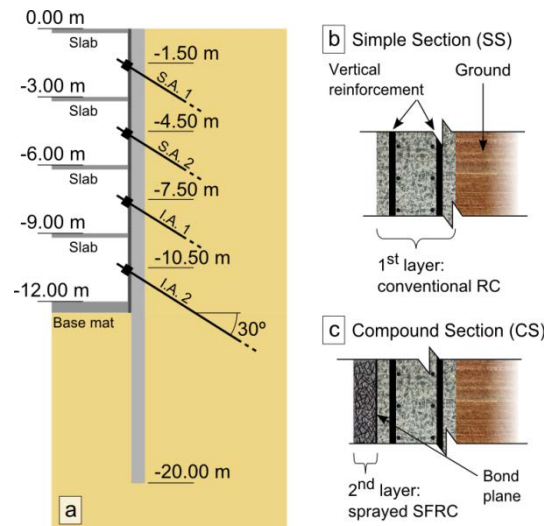
Fig. 21 - (a) Model geometry: Anchorages and slabs positions; (b) Simple Section; (c) Compound Section

The "bottom-up" construction sequence of the three alternatives is detailed in **Table 12**. The stages are divided in 5 groups, the first 4 of which correspond to the Excavation (Exc.) works required for each of the 4

Anchorage (Anc.) installations. In the fifth group, apart from a small final excavation, the slabs are built and the 4 anchorages removed (Anc.Out).

Table 12 - Construction stages sequence

Group	Depth* (m)	ML_{60}	BL_{60+10} and BL_{55+10}
	---	Wall constr.	Wall constr.
1	1.75	Exc.1	Exc.1
	1.50	Anc.1	Anc.1
	3.75	---	Exc.2a
	3.50	---	Spray.2a
2	4.75	Exc.2	Exc.2b
	4.50	---	Spray.2b
	4.50	Anc.2	Anc.2
	6.75	---	Exc.3a
	6.50	---	Spray.3a
3	7.75	Exc.3	Exc.3b
	7.50	---	Spray.3b
	7.50	Anc.3	Anc.3
	9.75	---	Exc.4a
	9.50	---	Spray.4a
4	10.75	Exc.4	Exc.4b
	10.50	---	Spray.4b
	10.50	Anc.4	Anc.4
	12.50	Exc.5	Exc.5
	12.25	---	Spray.5
5	---	slabs	slabs
	---	Anc.Out	Anc.Out

* Excavation base, Anchorage position, or Spraying base, according to the respective stage

The soil extraction process for the BL_{60+10} and BL_{55+10} bi-layers walls is sub-divided into shorter stages. In addition, after each partial excavation stage, the SFRC layer is Sprayed (Spray.), from the last sprayed level to the lower excavated level, changing the cross-section from the Simple Section (SS, see **Fig. 21b**) to the Compound Section (CS, see **Fig. 21c**) in the sprayed stretch.

3.3.2. Material and model characteristics

The numerical model was calculated on the commercial geotechnical finite-element software package PLAXIS (Brinkgreve, 2002). The FEM mesh used is shown in **Fig. 22**. Horizontal fixity was imposed for the vertical boundaries as well as both horizontal and vertical fixities for the bottom boundary, as shown in the same figure. A *fine* global coarseness was taken for the general mesh (automatically defined by the program), and refined in the vicinity of the wall. A model with a more refined mesh verified that the element size had no significant effects on the analytical results. Besides, no external loads were considered in the model.

Plate structural elements (linear elastic) were used to model the diaphragm walls, which were considered *wished in place* (Bryson & Zapata-Medina, 2012). A compressive strength f_{ck} = 30 MPa, a Poisson ratio υ =

0.2, and a specific weight of 24 kN/m^3 were considered for the concrete of both layers. Its modulus of elasticity, according to EC-2 (EN, 2004b), was $E_{cm,28} = 33000$ MPa.
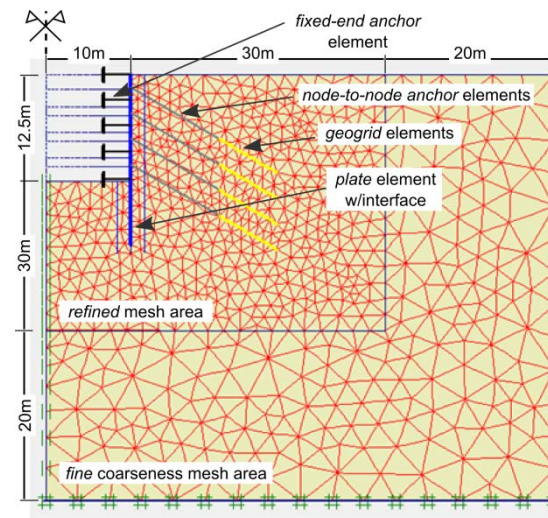
Fig. 22 - Finite element model mesh and main elements

The flexural (*EI*) and normal (*EA*) stiffness values calculated for the SS and the CS cross-sections, are shown in **Table 13**. All stiffnesses have been reduced by 20% from the nominal value (uncracked cross-section) to consider the existence of cracks in the wall (Khoiri & Ou, 2013). In the FEM model, the self-weight and stiffnesses were updated from the SS to the CS values for the corresponding beam lengths that had been sprayed after each of the spraying stages. As *"it is very important that the ratio of EI / EA is not changed"* to avoid numerical inconsistencies (PLAXIS 2D, 2010a) and our main interest centres on the bending moments, the EA values of the bi-layer were calculated to maintain a constant EI/EA ratio. It can be seen that the flexural stiffness of the CS for both bi-layer alternatives increased by about 60% in comparison with that of the SS.

Table 13 - Flexural and normal stiffness of the different walls

		ML_{60}	BL_{60+10}	BL_{55+10}
EI	SS	475.2	475.2	366.0
(MN·m^2)	SC	---	754.6	604.2
EA	SS	15840	15,840	14,520
(MN)	SC$^+$	---	25,153	23,967

+ Value calculated to keep the EI/EA ratio unchanged.

The soil elements were 15-node triangular finite elements under plane strain. A sandy soil was chosen for this analysis, as water filtration problems are more likely in a permeable soil.

The soil parameters and the values used for the selected model correspond to the "*Lake sand layer*", taken from an experimental case reported in the literature (Hashash et al., 2010). The coefficient of lateral earth pressure at rest (K_0) was automatically estimated by the program using the expression of Jaky (Terzaghi et al., 1996). A total unit weight of $\gamma = 20.0$ kN/m^3 was selected for the soil. Interface elements were set out for the soil in contact with the plate elements (with a strength reduction factor for soil-structure interface of $R_{inter} = 0.66$ (Khoiri & Ou, 2013)) and continued 1.0 m below the bottom end of the walls, as suggested by

PLAXIS (PLAXIS 2D, 2010b). A *Drained* analysis was used, even though the phreatic level was below the model boundaries and therefore no water flow was considered.

The permanent wall supports were modelled with *fixed-end anchors*. A normal stiffness of $EA = 7.26 \cdot 10^6$ kN/m (equivalent to a 22 cm thick massive slab) with an equivalent support length of 10 m (the length from the walls to the axis of symmetry of the model) was used for the upper slabs. A stiffness of $EA = 1.65 \cdot 10^7$ kN/m (equivalent to a 50 cm thick massive slab), also with an equivalent support length of 10 m was used for the bottom slab.

Geogrid structural elements and *node-to-node anchor* elements were used to model the body and the free length, respectively, of the ground anchors. The following properties were used. Initial tensile load: 50 kN/m for "S.A. 1 and 2" and 100 kN/m for "I.A. 1 and 2"; Horizontal distance: 5.0 m for "S.A. 1 and 2" and 2.5 m for "I.A. 1 and 2". The rest of the properties are equal for both types of anchorages. Total length: 20 m; Bulb length: 14 m; Cross-section area: 450 mm^2; Elastic modulus: 200 KN/mm^2; and Angle: 30º.

A fibre content of 25 kg/m^3 was used in the SFRC. The post-cracking behaviour of the SFRC may be defined by the expressions given in (de la Fuente, Escariz, de Figueiredo, Molins, & Aguado de Cea, 2012). The nominal cover used for the RC bars was 70 mm.

3.4. STRUCTURAL RESULTS

The *displacement* plot of the three wall types corresponding to the final stage ("*Anc.Out*") are shown in **Fig. 23**. The upper part of the plot is enlarged for clarity. In general terms, the displacement of each wall type is similar, with differences in the maximum displacement value of less than 0.8 mm (4.6%), and within the order of magnitude of displacements of the reference case (Carrubba & Colonna, 2000).
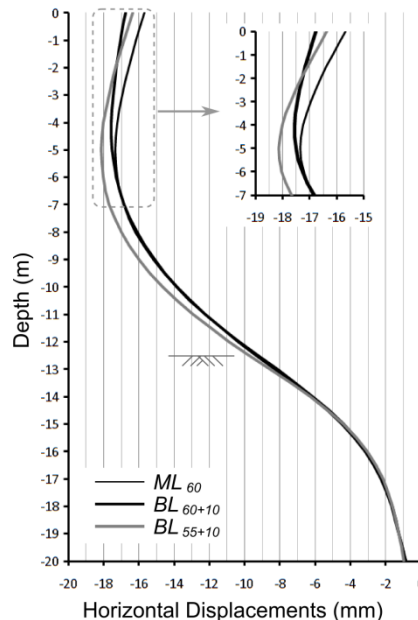
Fig. 23 - Wall displacements: "Anc.Out" stage for the three walls

Displacements at depths of between -5m to -20m of the walls with a RC width of 60 cm ("ML_{60}" and "BL_{60+10}") are practically identical. The reduced influence of the second layer is, on the one hand, due to the

stiffness of the two types of walls, which are the same at depths of between -12.5m and -20.0m. On the other hand, increased stiffness at depths of between -6.0m and -12.5m following spraying of the SFRC layer is noted during the final excavation stages, after most of the soil pressure had been already mobilized.

The displacements of the "BL55+10" wall type are slightly higher than the previous ones. This behaviour, which coincides with data reported in (Segura-Castillo, Aguado, & Josa, 2013), is due to the fact that the stiffness of the RC layer determines the overall displacement behaviour.

Larger displacements than in "ML_{60}" wall at depths of between 0.0 m and -5.0 m can be seen in the "BL_{60+10}" wall. Although it might appear contradictory, this is reasonable because the flexural stiffness of the bi-layer wall increases after spraying of the SFRC layer. Therefore, the curvature increase of the bi-layer wall is smaller than in the mono-layer alternative as the bending moment increases. In this instant, as the wall is more restrained in the lower part (at depths of below -5.0 m) owing to the embedded end of the wall and the stiffer lower anchors, the upper free end of the wall is dragged outwards at greater extent.

The envelope of *flexural design moments* (M_d) obtained for all three wall types, for both the SS and for the CS sections, are shown in **Fig. 24a**. A partial factor of $\gamma = 1.5$ was applied to the actions of the ground on the wall. The positive moments of the envelope are the same for both kinds of sections. In turn, while there is a single envelope for the negative moments of the mono-layer wall, the envelope is broken down into two envelopes for the bi-layer walls. The envelopes of maximum moment, until the CS was completed (i.e. until the SFRC was sprayed) are shown by a continuous line (M_d^{SS}) and the envelopes where the CS was completed by a dashed line (M_d^{CS}). The way these envelopes were generated is explained below in greater detail. In general terms, the envelopes are qualitatively similar and within the order of magnitude of the reference case (Carrubba & Colonna, 2000).
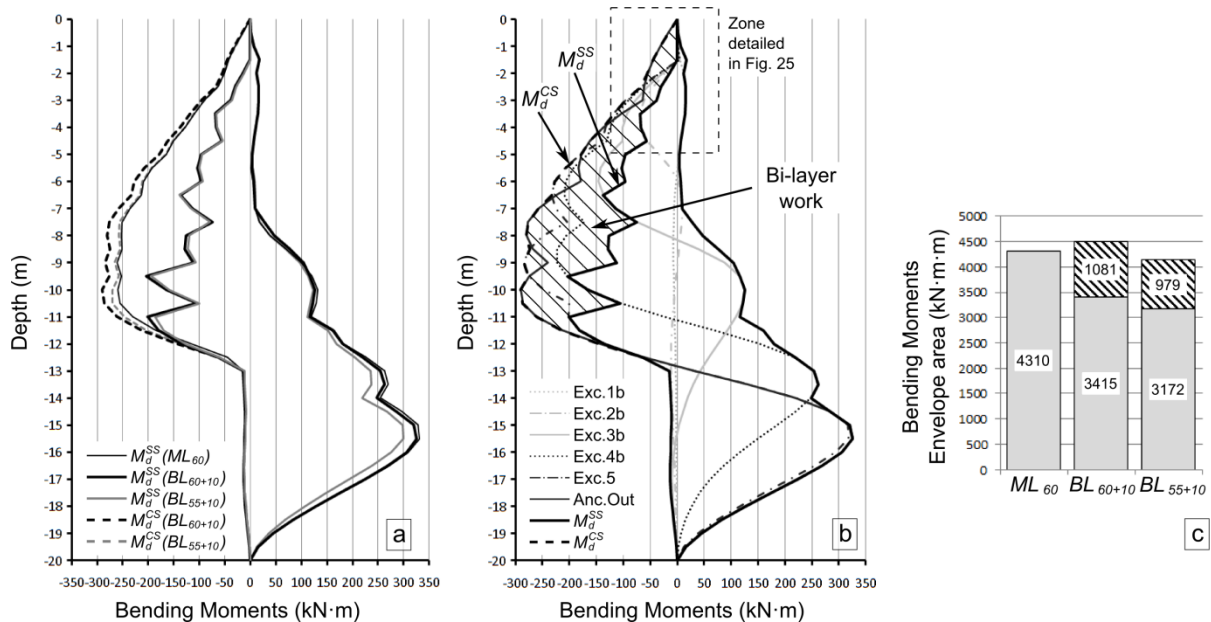
Fig. 24 - Bending moments: (a) Envelopes for the three wall types; (b) Representative stages and envelopes for the "BL60+10" wall type; (c) envelope areas for all three wall types.

Comparing the bi-layer walls, it can be seen that the "BL_{60+10}" shows larger moments than the "BL_{55+10}" along the whole length of the wall. This is a consequence of the greater stiffness of the RC layer and, therefore, greater stiffness both in the SS and in the CS cross-section.

The "ML_{60}" and "BL_{60+10}" wall types show practically identical envelopes in the embedded section of the wall (between depths -12.5m and -20.0m). In this section, both walls have the same cross-section (i.e., the RC layer) for all the stages. The biggest differences between these wall types was registered in the centre of the walls, between depths -5.0m and -12.0m, in which the "BL_{60+10}" envelope was larger. As the SFRC layer is sprayed, the upper stretches become stiffer, diminishing any relative collaboration of the embedded part of the wall.

The bending moments of the "BL_{60+10}" wall type are detailed in **Fig. 24b**, in which light-grey lines indicate the moment of the representative stages of each excavation stage. The interval between the envelopes previously introduced in **Fig. 24a** (M_d^{SS} and M_d^{CS}) is highlighted with slanting lines. This area represents the increase in the moments after spraying the SFRC layer (i.e., where the CS cross-section is working).

As stated in (Segura-Castillo, Aguado, & Josa, 2013), the highlighted area represents the potential use of the bi-layer wall, since it is possible to cover these moments with the resistance of the CS section. It can be seen that for the depths where the CS section is present, a significant portion of the bending moments are developed after the SFRC layer has been sprayed. These increases range from 30% to 269% at depths of between -2.5m and -11.0m, with an average increase of 123% in the design moment of those depths after the SFRC layer is sprayed.

The value of the area within the SS cross section envelope is represented with a solid bar graph to compare the three wall types, in **Fig. 24c**. The value of the area of the CS cross section (as shown in **Fig. 24b**) is also plotted (slanting lines). It may be noted that the potential of use of the SFRC layer covers approximately 25% of the area of moments.

The bending moments plots of the "BL_{60+10}" wall type at depths of between 0.0 m and -5.0 m, for the stages from "*Exc.2a*" to "*Spray.2b*" are shown in **Fig. 25**. For each plot, dark lines indicate the moments of the stage and light-grey lines indicate the moments of the previous stages. The *envelopes of moments* already shown in **Fig. 24** are obtained when the following process explained below is applied to all the stages.
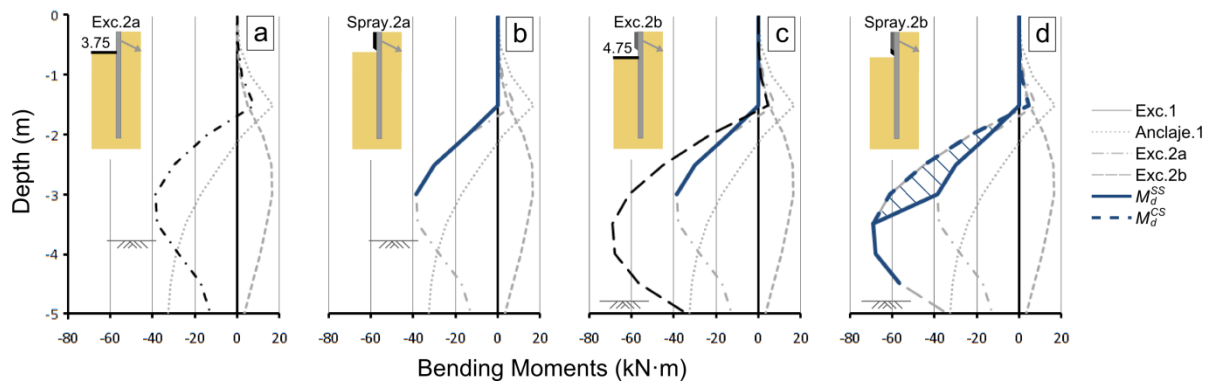
Fig. 25 - Diagrams of moments at stages prior to the second anchor installation

It can be seen that the bending moments of the excavation stage (**Fig. 25a**) are identical to those of the stage where the SFRC is sprayed (**Fig. 25b**). This is because, immediately after spraying, all the SFRC layer adds is its own-weight, which is considered in the model by updating the weight of the beam element. This implies a small change in the normal stresses of the element and an insignificant change in the bending moments. The external loads on the wall remain constant until a new excavation stage takes place.

The differential time-dependent strains between RC and SFRC layers are left out of the model, bearing in mind that the RC layer, as a slurry wall, has a high confined water content (before excavation) and that the sprayed SFRC layer, with a waterproofing additive, has a greater capability of withholding moisture.
After the spraying stage, the wall has the CS cross-section at depths of between 0.0m and -3.0m. Therefore, until this stage is complete, the bending moments are resisted exclusively by the SS cross-section. The envelope of these moments is represented with an unbroken bold line.

The changes in bending moments of stage "*Exc.2b*" are shown in **Fig. 25c**. The increase in bending moments at depths of between 0.0m to -3.0m can now be withheld by the CS cross-section. The maximum moments that develop once the CS cross-section is completed are referred to as M_d^{CS}, and its envelope is represented with a bold dashed line, as shown in **Fig. 25d**. This figure represents the situation after spraying the second stretch (Spray.2b), in which the two kinds of envelopes may be seen.

3.5. SECTIONAL RESULTS

The <u>*design criteria*</u> set the ultimate moment resistance as equal or greater than the design moment of each cross-section ($M_U \geq M_d$). This particular criterion is used for the dimensioning of the main vertical reinforcement, which accounts for the differences introduced by the various wall types analysed in this study. Therefore, secondary reinforcements (e.g., for transversal stresses or time-dependant effects) are neglected in this study as they are considered the same for all three wall types. The shear force, and its reinforcement, is also neglected as it is not usually a determinant in the design of the walls.

Reinforcement of the RC layer involves: a) a symmetric reinforcement on both sides of the wall with the minimum mechanical reinforcement "$A_{S,min}$" (according to the EHE-08 code (CPH, 2008)); and b) one extra reinforcement per side of the Wall, one for the positive moments "$A_{s,+}$", and another one for the negative ones "$A_{s,-}$", to cover the extra moment that the minimum reinforcement does not cover. The addition of both areas "A_T" was used in the calculations for cross-sections in which both reinforcements were present. Only tensioned bars were used in the calculation.

Two ultimate moment resistances, whether or not we consider the SFRC layer, were obtained for the bi-layer wall types, one for the SS ("M_U^{SS}") and another for the CS cross-section ("M_U^{CS}"). In this way, the design condition for the bi-layer walls can be differentiated according to the type of section that is active at each instant, establishing that every cross-section must at every instant simultaneously satisfy both relationships given by the following inequalities:

$$M_U^{SS} \geq M_d^{SS}$$

(5)

$$M_U^{CS} \geq M_d^{CS}$$

(6)

The *values of the reinforcements* obtained for the three wall types are shown in **Table 14**. The following information is given for each alternative: bar diameter "*d*" and bar spacing "*s*" expressed in the form "*$\phi d/s$*"; the position of the reinforcements "z^{inf}" and "z^{sup}" (see **Fig. 26**) and the ultimate moment resistance of the SS and the CS cross-sections.

Table 14 - Reinforcements and M$_U$ of the different wall types

Wall Type	Reinforcement		Position [a]		M_U	
			z^{inf}	z^{sup}	M_U^{SS}	M_U^{CS}
	[mm]/[cm]		[m]	[m]	[kN·m]	[kN·m]
	$A_{S,min}$:	Φ16/24	-20.0	0.0	186	---
ML$_{60}$	$A_{S,+}$:	Φ12/16	-17.5	-12.0	337	---
	$A_{S,-}$:	Φ10/22	-11.5	-5.0	263	---
	$A_{S,min}$:	Φ16/24	-20.0	0.0	186	223
BL$_{60+10}$	$A_{S,+}$:	Φ10/12	-17.5	-12.0	326	---
	$A_{S,-}$:	Φ10/24	-11.5	-5.5	257	294
	$A_{S,min}$:	Φ16/25	-20.0	0.0	161	195
BL$_{55+10}$	$A_{S,+}$:	Φ16/28	-17.5	-11.5	300	---
	$A_{S,-}$:	Φ12/28	-11.5	-5.5	240	275

[a] Anchorage length not included.

The ultimate resistance of the CS cross-section where the positive moment reinforcements were placed was not calculated, since this reinforcement is placed at depths lower than 12.5m, where there is no second layer. The ultimate moments obtained with the aforementioned reinforcements cover the design moments in the whole wall (Ec. 1 and 2).

The increase in the ultimate moment resistance, given by the contribution of the SFRC layer, ranges from 14.5% ("$A_{S,-}$" of the *BL$_{55+10}$* wall type) to 21.0% ("$A_{S,min}$" of the *BL$_{55+10}$* wall type) in relation to the resistance of the SS cross-section.

In the wall types with a 60 cm thick RC layer, the above percentages are barely superior to the moment increase following the application of the second layer, i.e. the increase in the cross-section resistance, when the SFRC layer is added, is barely higher than the increase in the design moments when the second layer is considered in the structural calculation. In turn, the reduction of the maximum positive moments in the bi-layer wall type also implies a small reduction in the given reinforcements.

As the *BL$_{55+10}$* wall type has a thinner cross-section, it requires, on the one hand, a smaller minimum reinforcement but, in the other hand, stronger local reinforcements to carry the design moments, even though these are smaller than in the *BL$_{60+10}$* alternative.

As an example of design, the ultimate moment resistance for the "*BL$_{60+10}$*" wall type is shown in **Fig. 26**. The previously introduced design moments ("*M$_d$*") are also shown in the same plot. It can be seen that inequalities of Eqs. 5 and 6 are satisfied in every instance.

It can be seen that at depths of between 0.0m and -5.5m the wall contains the SFRC layer although it is not strictly necessary, as the resistance of the SS cross-section itself is sufficient to cover the design moments. It

would be possible to optimize the use of the fibres, placing them only in the stretches where they are needed for the ultimate resistance of the cross-section. This is, to place the SFRC layer at depths of between -5.5m and -12.5m, and to place just sprayed concrete with the waterproofing additive at depths of between 0.0m and -5.5m (for waterproofing purposes and to even the surface).
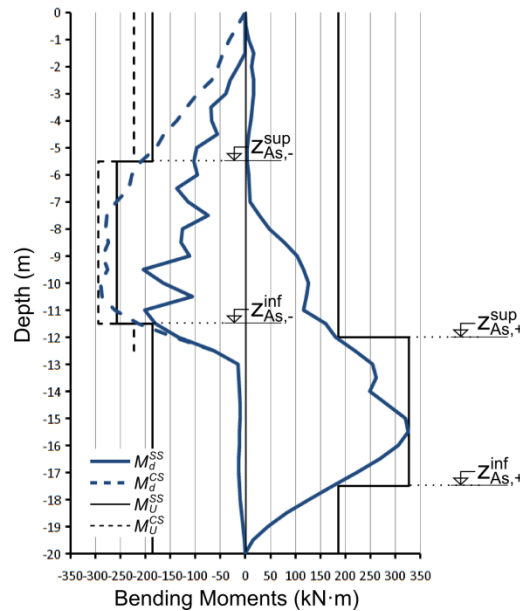
Fig. 26 - Ultimate and design moments for the "BL60+10" wall

3.6. DISCUSSION

Besides the structural solutions that have been presented, different systems to deal with leakages on diaphragm walls are compared in this section.

Two standard systems aiming to ensure a dry inner wall after building a conventional mono-layer wall are: a) *Drained cavity* ("*DC*"): a second inner wall separated from the diaphragm wall. The cavity between them is drained and the water accumulated at the bottom is later pumped out. b) *Waterproof mortar layer* ("*WML*"): consists of casting a second layer of waterproof mortar over the inner face of the diaphragm wall. This layer is usually about 5 cm width, and is cast after the diaphragm wall has been finished, without structural function.

Additionally, an optional modification is added to each of the bi-layer wall types. The *Optimized fibres* ("*Opt.*") system utilizes the idea introduced at the end of section 5, where the fibres are only placed where strictly necessary (i.e. at depths of between -5.5m and -12.5m, using a sprayed concrete without fibres for the rest of the spraying layer). The system where fibres are uniformly placed all along the second layer are called "*Unif.*" to differentiate it from the preceding option.

The main differences between these systems are summarised in **Table 15**. It includes the basic material required for the construction of the complete systems; the maximum displacement registered; the final thickness of the system; and its waterproofing if any.

Table 15 - Comparison of different waterproofing systems

			Mono-layer			Bi-layer			
			ML_{60}	ML_{60} $+ DC^{\spadesuit}$	ML_{60} $+ WML$	BL_{60+10} *"Unif."*	BL_{55+10} *"Unif."*	BL_{60+10} *"Opt."*	BL_{55+10} *"Opt."*
Concrete volume	Cast layer	(m^3/m)	12.00	12.00	12.00	12.00	11.00	12.00	11.00
	Sprayed layer*	(m^3/m)	---	---	0.63	1.25	1.25	1.25	1.25
	Total	(m^3/m)	12.00	12.00	12.63	13.25	12.25	13.25	12.25
Steel weight	Cast layer	(kg/m)	391	391	391	382	381	382	381
	Sprayed layer	(kg/m)	---	---	---	31	31	18	18
	Total	(kg/m)	391	391	391	414	412	400	399
Maximum displacement		(mm)	-17.3	-17.3	-17.3	-17.6	-18.1	-17.6	-18.1
Final thickness^{+}		(cm)	60	85	65	70	65	70	65
Waterproof system			NO	YES	YES	YES	YES	YES	YES

* corresponds to the volume of the mortar layer in the "$ML_{60} + WML$" system.

$^{+}$ the theoretical thickness is considered, without taking accidental deviations into account.

$^{\spadesuit}$ the consumption of extra materials of a different class is not considered in this system.

The different materials are grouped below in accordance with their class. Thus, the volume of the two types of concrete (RC and SFRC) and the mortar used in the "*WML*" system are grouped under the heading "*concrete*" and the conventional steel bars used in the RC layer and the steel fibres used in the SFRC layer under "*steel*". In both cases (*concrete* and *steel*), cast and sprayed materials were differentiated. The consumption of extra materials of the "*DC*" system, as it is of a different class, is not considered in the table. Although the dosages, placing procedures and cost are not the same for the different types of materials, this simplification allows a simple first approach to compare the different systems.

With regard to material consumption, the ML_{60} wall type is the one with minor outlay in every material category. Considering that maximum displacements are similar for all systems and that this one, in particular, has the smallest ones, and finally, that this system has the smaller thickness, this system is undoubtedly the most appropriate whenever waterproofness is not required.

The bi-layer wall types achieve a reduction in the RC layer steel reinforcement. The percentage of reduction in this layer compared with the ML_{60} alternative is, 2.1% for the BL_{60+10} wall type and 2.5% for the BL_{55+10} wall type. However, the steel increment in the SFRC layer exceeds the reduction reached in the RC layer. The percentage increment compared with the ML_{60} wall type is 8.0% for the "*Unif.*" system, and 4.5% for the "*Opt.*" bi-layer system. As the material and labour costs per cubic meter of sprayed SFRC are higher than the cost of RC, the structural system of the bi-layer solutions is not favourable in this case.

Comparing the complete systems, including both the structural and the waterproof system, the "*Opt.*" systems are more efficient than the "*Unif.*" systems and will therefore be used in all subsequent comparisons. The $ML_{60} + DC$ system is nowadays one of the more commonly used for waterproofing the wall surface. The material required for the drained cavity (leaf wall and extraction pump) is assumed to be relatively low. The main drawbacks of this system are: a- Reduced interior space (crucial in the basements of buildings designed for underground parking and other economic activities); b-Need to activate a pump as excess water accumulates; and c- It hides the source and the extent of the leakages, or any other possible structural problem that the walls may have (Puller, 1994).

If the use of materials of the ML_{60} + WML system is compared with the BL_{60+10} ("*Opt.*"), the latter registers an increase of 5.0% in concrete use and 2.3% in steel. Considering that the thickness of the BL system is also larger, the BL alternative is not favourable in this case.

If the ML_{60} + WML system is compared with the BL_{55+10} ("*Opt.*"), it should first of all be noted that both have the same final thickness and are also the slenderest of all the waterproof systems under study. Regarding the materials, it can be seen that a reduction of 3.0% in the amount of concrete (the only material-related value favourable to the bi-layer systems). Finally, an increase in the total amount of steel (2.0%) is still registered.

3.7. CONCLUSIONS

A design method for the bi-layer diaphragm walls, a new type of slurry wall, has been presented. It allows two levels of comparison, the first of which is based on the structural analysis and the second on the final design, where the comparison includes final material use. The structural behaviour of a conventional ML wall (60 cm width RC layer) has been compared with two BL alternatives (60 cm and 55 cm width RC layer plus 10 cm width SFRC layer). Furthermore, starting with these wall types, several systems to deal with leakages have been added to the comparison. The main conclusions are summarized in the following points. There exists a potential of reduction in the reinforcement of the RC layer of the diaphragm walls through the structural use of the SFRC layer. This potential is measured by the area of moments envelope covered by the simple section (M_d^{SS}). This area is reduced 21% and 26% in both BL alternatives, compared with the ML wall.

However, it is not possible to take advantage of all this potential in the design process for two reasons that are explained as follows. The increase from the M_d^{SS} to the M_d^{CS} is, on average, 123% of the M_d^{CS} (at depths of between -2.5m and -11.0m). Besides, the increase from the M_U^{SS} to the M_U^{CS} are, in this case, between 15% and 20% of the M_U^{CS}. This means that, if the SS section is designed to cover only the SS design moments, the second layer does not provide the additional bending strength to the CS cross-section to cover the moments developed after the second layer is sprayed. Therefore, the SS sections should be designed to cover the M_d^{SS} and part of the M_d^{CS} moments. The second reason, is that the minimum M_U^{SS}, given by the minimum reinforcement, already covers a part of the M_d^{CS} design moments.

Even though a reduction in the RC reinforcement is confirmed for both wall types (2.1% and 2.5%), it appears insufficient to compensate for the extra technologies and consumption of materials to build the bi-layer solutions. Nonetheless, the complete waterproof system becomes an interesting solution when particular conditions are taken into account, such as basement space limitations or if continuous maintenance wants to be avoided.

Future work should include a parametric study to evaluate, by means of the two level comparison presented in this study, the influence of the general condition and wall design on the profitability of the bi-layer wall type.

3.8. ACKNOWLEDGEMENTS

CHAPTER 4.   Parametric study of construction processes[3]

ABSTRACT: The bi-layer diaphragm wall is a new type of slurry wall, designed to improve watertightness and to counter leakage problems. These walls consist of two bonded concrete layers: the first, a conventional Reinforced Concrete (RC) diaphragm wall and the second, a sprayed Steel Fibre Reinforced Concrete (SFRC) layer with a waterproof additive. Here, we analyse and quantify the influence of different construction process parameters on the effectiveness of the bi-layer diaphragm wall technique. Thirty numeric simulations were conducted with an uncoupled structure-section analysis, placing special emphasis on the SFRC layer contribution. The results show that, in all cases, the main flexural strength is provided by the RC layer, with a secondary flexural contribution (between 8% and 15%) by the sprayed SFRC layer. Using satisfactory spraying sequences (detailed herein), a reduction in the steel reinforcement of the RC layer can be obtained in every structural configuration and construction sequence, reaching a maximum percentage reduction of 7.0% of the total bending reinforcement. The displacements are almost completely governed by the thickness of the first layer, and a minor reduction (less than 7.3%) is obtained, when the second layer is included.

Keywords: fiber concrete, sprayed concrete, numerical analysis, FEM, PLAXIS, watertightness.

4.1. INTRODUCTION

Diaphragm walls are hardly ever fully watertight, as there is generally a degree of permeability between their panel joints (Brown & Bruggemann, 2002). Hence, some techniques have been developed to deal with the leakage problem in diaphragm walls built in water-bearing ground (Puller, 1994). The bi-layer diaphragm wall (Segura-Castillo, Aguado, & Josa, 2013) is a new type of slurry wall, mainly designed to counter leakage. The waterproofing system, added in the course of internal site excavations, assumes a structural function as an integral part of the wall structure.

A generic solution and part of the construction of the first experimental walls of this type (Segura-Castillo et al. (Segura-Castillo, Aguado, & Josa, 2013)) can be seen in **Fig. 27**. These walls consist of two bonded concrete layers poured and then sprayed, in separate stages. The first is a conventional Reinforced Concrete (RC) diaphragm wall (which forms the simple cross-section, see **Fig. 27c**). Once this wall attains the necessary strength, subsoil in contact with the wall within the perimeter is excavated and removed, and the second layer, this time of sprayed Steel Fibre Reinforced Concrete (SFRC) and a waterproof additive, is applied (both layers form the compound cross-section, see **Fig. 27b**).
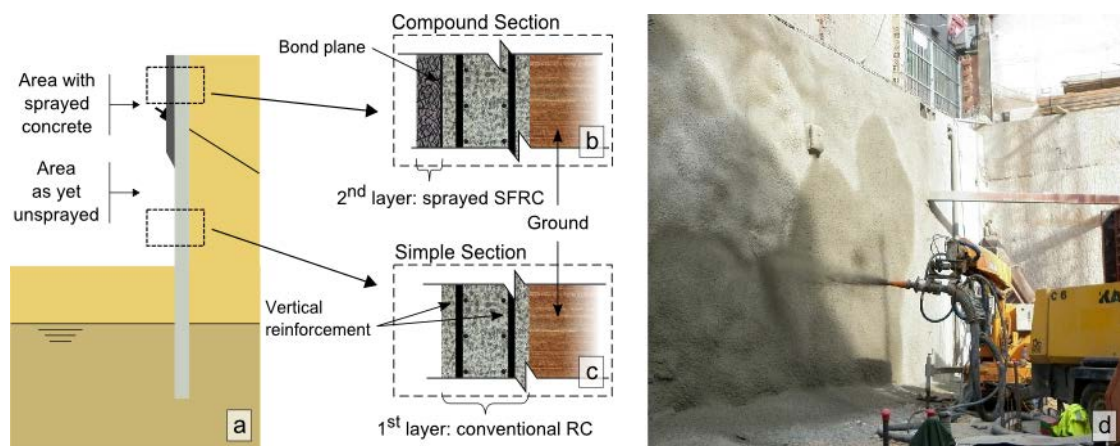
Fig. 27 - Bi-layer diaphragm walls. a) general scheme; b) compound cross-section; c) simple cross-section; and d) spraying of an experimental wall.

The main **objective** of this paper is to analyze and quantify the influence of different construction process parameters in the efficiency of the bi-layer diaphragm wall technique, measured in terms of reduction in the reinforcement and in displacement. This paper is part of an experimental and theoretical study of bi-layer diaphragm walls, structured into four main areas: a) Structural level analysis (Segura-Castillo, Aguado, de la Fuente, & Josa, 2013; Segura-Castillo, Aguado, & Josa, 2013); b) Sectional level analysis (Segura-Castillo, Aguado, de la Fuente, et al., 2013); c) Bonding between layers (Segura-Castillo & Aguado de Cea, 2012a); and d) General design and optimization. This paper sets out the basis for the fourth of these aforementioned areas.

The parameters under study are grouped into two categories: (a) specific bi-layer diaphragm walls characteristics (i.e. number of spraying stages, depth of sprayed concrete layer); and (b) general diaphragm walls and construction characteristics (i.e. wall thickness, construction sequence, final structural geometry).

Many studies have reported on the parametric analysis of deep excavations, studying the parameters of the second of the aforementioned categories. The studies mainly involve two approaches: analysis of a comprehensive case history database (e.g. (Clough & O'Rourke., 1990; Long, 2001; Moormann, 2004; Wang, Xu, & Wang, 2010)), and numerical analysis based on models calibrated against well documented case studies (e.g. (Bose & Som, 1998; Bryson & Zapata-Medina, 2012; G. T. C. Kung et al., 2007; G. T.-C. Kung, 2009)). The main focus of these studies is on wall and ground movements, due to their importance in the prediction of damage to adjacent buildings.

Thirty numeric simulations of diaphragm walls, with varied parameters, were run with an uncoupled structure-section analysis to fulfil the objective. Besides the displacements, the structural response was also analysed, focusing on the bending moments, with special emphasis on the SFRC layer contribution.

4.2. METHODOLOGY

4.2.1. Model description

A 2D Finite Element Model (FEM) developed in PLAXIS was used in the structural study. The soil was modelled with the Hardening Soil model (HS) (Schanz et al., 1999) and the wall and supports with linear elastic elements. In the FEM model, the stiffnesses were updated from the simple cross-section to the compound cross-section in the corresponding wall sections that had been sprayed after each of the spraying stages. No movements were considered during struts and slabs installation, and the walls were considered "*wished in place*", i.e. the stress changes or displacement of the wall installation in the soil are not considered in the model (Bryson & Zapata-Medina, 2012).

In all cases, diaphragm walls of 20 m in height were built for subsequent excavation work to a depth of 12.5 m, and with embedded footings of 7.5 m in depth. No adjacent buildings were considered (i.e. no external loads were introduced in the models). A sandy soil ("*Lake sand layer*") and its parameters were taken from a case presented elsewhere (Hashash et al., 2010). This is a good quality, only slightly deformable soil. The type and characteristics of the finite elements, the mesh discretization and its boundary conditions, as well as properties taken for the wall, anchorages, and slabs, are the same as those in (Segura-Castillo, Aguado, de la Fuente, et al., 2013). The struts were modelled with *fixed-end anchors*. A normal stiffness of $EA = 2.00 \cdot 10^4$ kN/m/m for the superior strut and of $EA = 4.00 \cdot 10^4$ kN/m/m for the inferior one was selected, both with an equivalent support length of 10 m (with stiffnesses in the range of the Kung (G. T.-C. Kung, 2009) parametric analysis).

The "Analysis of Evolutionary Sections" (AES) model was used to perform the numerical simulation of the mechanical behaviour of the composite cross-sections of the wall (de la Fuente, Aguado de Cea, et al., 2012; de la Fuente et al., 2008). It simulates the non-linear response of cross-sections built with different materials (concrete and steel) and, most especially, the structural contribution of the SFRC under tension. The characteristics of the aforementioned structural and sectional models are fully described in (Segura-Castillo, Aguado, de la Fuente, et al., 2013), likewise, the properties of the materials were also taken from the aforementioned paper.

The design of the reinforcement followed the same criteria in all cases: (a) a symmetric reinforcement at each face of the wall with the minimum reinforcement area ($A_{s,min}$) (CPH, 2008); and (b) extra

reinforcements ($A_{s,ext}$) in each point where the design bending moment (M_d) exceeded the ultimate bending moments (M_u) given by the reinforcement of (a). Only tensioned bars were taken into account in the calculation.

For the sake of simplicity, the reinforcement was defined indicating only the necessary steel area, without defining the type, diameter, and number of bars. On the other hand, although the criteria used in the analysis are not completely realistic (for example, in some cases, reinforcement is placed just to cover a small increase in the bending moments), they allow quantification and comparison of the quantity of reinforcement steel required in the different solutions.

4.2.2. Parameters under study

Table 16 presents the parameters and a brief description of the alternatives that are studied. As the combination of all alternatives would lead to a total of 120 cases, a selection of combinations (30 cases) is presented, in order to analyse the influence of: type of wall (mono-layer or bi-layer), construction sequence, number of underground levels in the final configuration, number of spraying stages and depth of sprayed concrete layer.

Given the large number of cases, the following labels are proposed for ease of identification:

> NL / W1-W2 / CS / NU / NS / DS

where:

NL   is the number of layers of the wall: conventional diaphragm walls, referred to as mono-layer walls (ML) for the sake of clarity, and bi-layer walls (BL).

W1   is the thickness, in cm, of the 1st layer (the conventional RC wall): 55 and 60.

W2   is the thickness, in cm, of the 2nd layer (the SFRC sprayed layer): 0 (ML wall) and 10.

CS   stands for the construction sequence, where three alternatives are considered: two Bottom-Up (BU) sequences, one with struts as temporary supports (BUs) and one with temporary anchorages (BUa); and the Top-Down sequence (TD), where the wall is directly supported by the finished slabs.

NU   is the number of underground levels of the finished structure configuration, where two alternatives are considered: 2 and 4 underground levels, represented by 2u and 4u (6.0 m and 3.0 m high), respectively.

NS   is the number of spraying stages performed to cover the whole external wall surface, where four alternatives are considered (0, 1, 2 and 4 spraying stages), represented by 0S (ML wall), 1S, 2S and 4S, respectively.

DS   stands for the depth of the excavation at the moment where the last spraying stage was carried out. Four alternatives are considered: (M) where there is no spraying (ML wall); (A) the depth of the final excavation (i.e. -12.5 m); (B) one meter before the final excavation depth (i.e. -11.5 m); and (C) two meters before the final excavation depth (i.e. -10.5 m).

As an example, a Wall labelled "*BL/55-10/BUs/4u/2S/A*" corresponds to a bi-layer wall with a RC layer thickness of 55 cm and a SFRC layer thickness of 10 cm, built with the Bottom-Up construction sequence

using struts, with a final structure of 4 underground levels, and a two-stage spraying process, the second of which is sprayed when an excavation depth of -12.5 m is reached.

Table 16 - Parameters and alternatives for each case.

Parameter	Alternatives	Description
Number of layers	ML	Mono-layer
(NL)	BL	Bi-layer
1st layer thickness (W1)	55	55 cm 1st layer
	60	60 cm 1st layer
2nd layer thickness (W2)	0	Mono-layer type
	10	10 cm 2nd layer
Construction sequence (CS)	BUs	Bottom-Up with struts
	BUa	Bottom-Up with anchorages
	TD	Top-Down
Final number of underground levels	2u	Infrastructures
(NU)	4u	Dwelling basements
Number of spraying stages (NS)	0S	Mono-layer type
	1S	1 stage spraying
	2S	2 stage spraying
	4S	4 stage spraying
Depth of sprayed concrete layer in the	M	Mono-layer type
last stage (DS)	A	Depth: -12.5 m
	B	Depth: -11.5 m
	C	Depth: -10.5 m

The two final configurations, both of which can be relatively common, are shown in **Fig. 28**. The first alternative (see **Fig. 28a**) is a structure with an intermediate slab, apart from the base slab and the ground level slab. It could, for example, be an underground station, where the upper enclosure would be for the station service area, and the lower one for the platforms, tracks and other railway equipment. The second alternative (see **Fig. 28b**) has three intermediate slabs, besides its top and bottom slabs, which might, for example, be an underground car park at four levels.
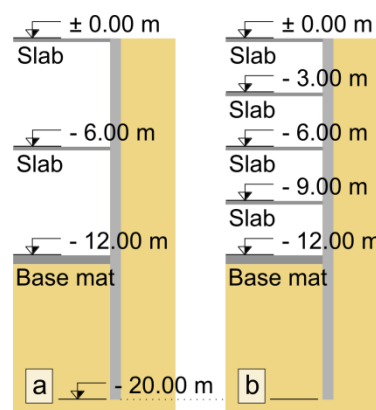
Fig. 28 - Final construction design: (a) 2 levels "2u"; (b) 4 levels "4u".

Fig. 29 shows examples of the construction sequence. A generic BU sequence for the 4u alternative is represented in **Fig. 29a**. The temporary supports are generically represented with a horizontal arrow in the

position where the supports are positioned. The BU construction sequences for the 2u case are equivalent to those shown here, with the difference that in the "slabs" stage, the slabs that correspond to the 2u final design are built (see **Fig. 28**a). The construction sequence TD for the 2u case is represented in **Fig. 29b**. Four additional stages must also be considered for the TD sequence of the 4u case: two intermediate excavations (1.75 m below the slabs: -4.75 m and -10.75 m deep) necessary for the additional intermediate slabs (at depths of -3.00 m and -9.00 m).
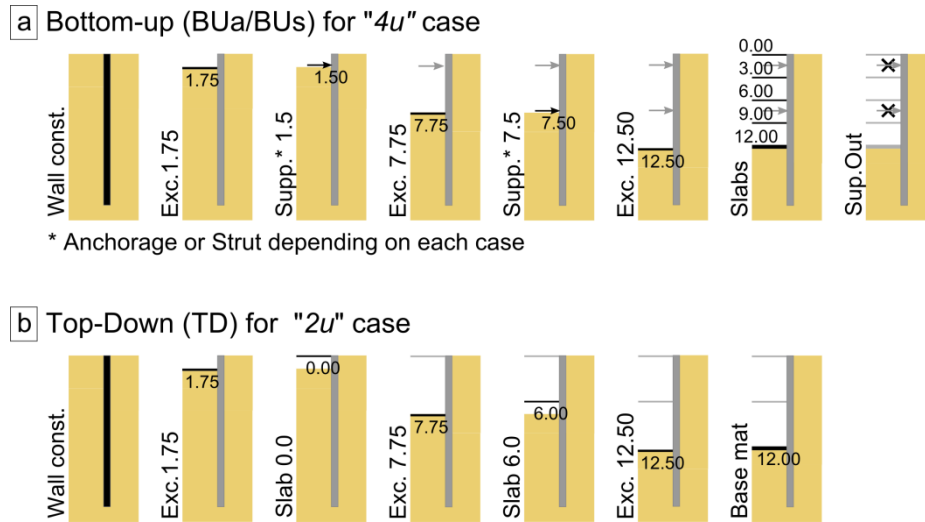
Fig. 29 - Construction sequences: (a) Bottom-Up "BU"; (b) Top-Down "TD".

Fig. 30 shows examples of the different depths of sprayed concrete layer. The temporal supports and slabs, which should be considered according to each case, are omitted from the figure. The SFRC is sprayed when the depth of the excavation is 25 cm below the depth indicated for each spraying section, in case of any possible excavation irregularities. The three alternatives for the DS parameter (indicated in **Fig. 30**) were only studied in cases that involved two spraying stages (2S). When the excavation reaches the final depth, the last section of the second layer is completed. As it is the last section, and its height is not over 2 m, this section may be completed with in-situ concrete instead of sprayed concrete. There are actually three spraying stages in the 2S/(B) and 2S/(C) alternatives, although in view of the short length of the third section they are left with the 2S cases.
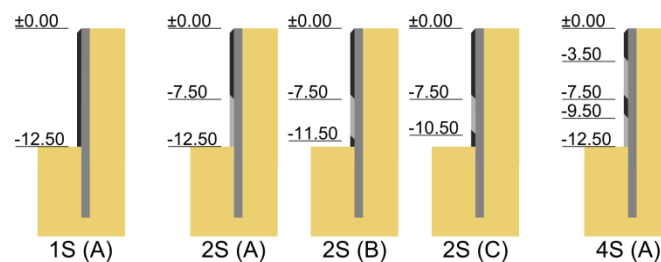
Fig. 30 - Spraying discretization considered.

4.3. STRUCTURAL AND SECTIONAL RESULTS

Table 17 summarizes the general results for all of the cases. The horizontal double line separates the cases with different final structural configurations (2u and 4u). The dark lines separate the different construction

sequences for the 2u configurations. In all cases, the light line separates groups of cases with different first layer thickness (55 cm and 60 cm). The first case in every group corresponds to a mono-layer alternative, with the remainder referring to different spraying alternatives for the bi-layer walls.

Table 17 - General results for all cases.

Case	EA(M_d^{SS}) (kN m m)	EA(M_d^{CS}) (kN m m)	M_U^{SS} (kN m)	M_U^{CS} (kN m)	W($A_{s,ext}$) (kg)	ΔW($A_{s,ext}$) (kg)	$\delta_{H(max)}$ (mm)	$\Delta\delta_{H(max)}$ (mm)
ML/60-0/BUs/4u/0S/M	4518	---	300.2	---	49.2	---	-9.73	---
BL/60-10/BUs/4u/1S/A	4323	213	298.6	336.3	48.7	-0.5	-9.74	0.00
BL/60-10/BUs/4u/2S/A	4180	355	298.6	336.3	46.4	-2.8	-9.74	-0.01
BL/60-10/BUs/4u/4S/A	4017	568	307.6	345.4	49.0	-0.3	-9.71	0.03
BL/60-10/BUs/4u/2S/B	4004	549	265.9	303.2	35.8	-13.5	-9.73	0.01
BL/60-10/BUs/4u/2S/C	4052	529	309.8	347.6	49.2	0.0	-9.70	0.03
ML/55-0/BUs/4u/0S/M	4089	---	267.6	---	55.7	---	-10.23	---
BL/55-10/BUs/4u/1S/A	3909	197	264.0	299.0	55.8	0.1	-10.22	0.01
BL/55-10/BUs/4u/2S/A	3797	294	267.8	302.8	54.0	-1.7	-10.24	0.00
BL/55-10/BUs/4u/4S/A	3643	475	270.2	305.3	55.8	0.1	-10.17	0.06
BL/55-10/BUs/4u/2S/B	3648	460	234.1	268.7	42.1	-13.6	-10.24	-0.01
BL/55-10/BUs/4u/2S/C	3695	413	268.7	303.8	55.3	-0.4	-10.21	0.02
ML/60-0/BUs/2u/0S/M	4874	---	345.1	---	66.5	---	-10.25	---
BL/60-10/BUs/2u/2S/A	4202	719	314.8	352.7	53.3	-13.1	-10.12	0.13
BL/60-10/BUs/2u/2S/B	4026	914	319.3	357.2	54.3	-12.1	-10.11	0.14
ML/55-0/BUs/2u/0S/M	4436	---	307.7	---	73.6	---	-10.88	---
BL/55-10/BUs/2u/2S/A	3815	657	279.1	314.3	62.2	-11.4	-10.69	0.19
BL/55-10/BUs/2u/2S/B	3667	824	283.0	318.2	63.3	-10.3	-10.69	0.19
ML/60-0/BUa/2u/0S/M	6564	---	488.0	---	188.1	---	-25.28	---
BL/60-10/BUa/2u/2S/A	5685	1033	468.8	508.4	174.5	-13.5	-25.29	-0.01
BL/60-10/BUa/2u/2S/B	5226	1566	479.4	519.1	176.8	-11.2	-25.26	0.02
ML/55-0/BUa/2u/0S/M	6104	---	454.9	---	211.6	---	-27.16	---
BL/55-10/BUa/2u/2S/A	5277	954	435.5	472.7	195.7	-15.9	-26.95	0.21
BL/55-10/BUa/2u/2S/B	4850	1458	447.6	484.9	204.3	-7.3	-26.73	0.43
ML/60-0/TD/2u/0S/M	4987	---	355.8	---	69.7	---	-7.29	---
BL/60-10/TD/2u/2S/A	4598	432	328.1	366.1	59.6	-10.2	-6.84	0.45
BL/60-10/TD/2u/2S/B	4451	623	298.5	336.2	48.1	-21.7	-6.84	0.45
ML/55-0/TD/2u/0S/M	4666	---	317.3	---	77.8	---	-8.10	---
BL/55-10/TD/2u/2S/A	4289	423	291.4	326.7	69.3	-8.5	-7.55	0.55
BL/55-10/TD/2u/2S/B	4160	598	273.3	308.4	61.0	-16.8	-7.56	0.55

Table 17 includes information on: bending moment envelope areas (as described below), for both the simple cross-section EA(M_d^{SS}) and the compound cross-section EA(M_d^{CS}); internal ultimate moment (M_U) for the negative extra-reinforced cross-section, broken down both for the simple cross-section (M_U^{SS}) and the compound cross-section (M_U^{CS}); weight of extra reinforcement steel (W($A_{s,ext}$)) used in each case (as defined in section 4.2.1); steel weight variation (ΔW($A_{s,ext}$)), comparing each case with the corresponding mono-layer alternative (i.e. the first case in each group); maximum displacement ($\delta_{H(max)}$); and maximum displacement variation ($\Delta\delta_{H(max)}$), once again in comparison with the corresponding mono-layer alternative. Although something different is specifically indicated, all the values in the paper correspond to a 1 m wide strip of wall.

Only the weight of the extra steel reinforcement is included in **Table 17**, as the weight of the minimum reinforcement is constant for each 1ˢᵗ layer thickness (i.e. 261.6 kg for W1 = 60 cm; and 251.8 kg for W1 = 55 cm) and the secondary reinforcement is considered to be similar in all cases. The weights shown correspond to a 1 m wide wall.

An example of bending moments obtained for a generic bi-layer case is shown in **Fig. 31**. The design bending moments (M_d) are represented with blue lines. The envelopes, both positive and negative, are broken down into two in the bi-layer cases. The maximum moments envelope of the simple cross-section (M_d^{SS}), until the stage where the compound cross-section is completed (i.e. when the SFRC is sprayed), are plotted with a continuous line. The bending envelopes developed when the compound cross-section had already been completed (M_d^{CS}) are plotted by a dashed line. The M_d that are shown include a partial security factor ($\gamma = 1.5$). The way these envelopes are generated is explained in (Segura-Castillo, Aguado, de la Fuente, et al., 2013) in more detail. The figure also shows the ultimate bending moments (M_U) (M_U^{SS} with a continuous black line; and M_U^{CS} with a dashed black line).
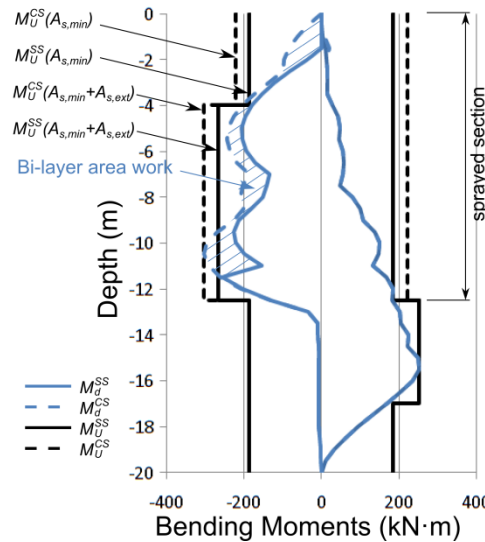
Fig. 31 - Example of bi-layer wall bending moment envelopes.

The design moments increase between M_d^{SS} and M_d^{CS} can be resisted by the ultimate moment of the cross-section when the SFRC layer is added (M_U^{CS}). Therefore, the area between the M_d^{SS} and the M_d^{CS} envelopes, indicated in the figure with a pattern fill, which will be called *bi-layer area work*, is a measure of the potential contribution of the second layer, which is included in **Table 17** as EA(M_d^{CS}). The area inside the M_d^{SS} envelopes (EA(M_d^{SS})) is also included in **Table 17**. It can be seen that EA(M_d^{SS}) is smaller in the bi-layer than in the mono-layer alternatives for all groups, which is consistent with the previous results (Segura-Castillo, Aguado, de la Fuente, et al., 2013; Segura-Castillo, Aguado, & Josa, 2013). The reduction ranges from 4% to 21% according to each particular case.

Envelope area is not directly related to the variation in steel reinforcement that can be obtained, even though it is a useful indicator. Different variations in steel reinforcements ($\Delta W(A_{s,ext})$) were obtained for the different cases in each group, ranging from a slight increase (0.1 kg in case "*BL/55-10/BUs/4u/4S/A*") to a

significant drop (-21.7 kg in case "*BL/60-10/TD/2u/2S/B*"), although the EA(M_d^{SS}) variation is similar within each group.

Two considerations should be noted to explain the aforementioned situation. Firstly, the steel reduction is limited by the contribution of the SFRC layer. As can be seen in **Table 17**, the M_U increase in the cross-section when the SFRC layer is added (from the M_U^{SS} to the M_U^{CS}) remains relatively constant (between 43.6 kN m and 39.7 kN m in all cases), and represents a percentage increase of between 8% and 15% of the M_U^{SS}. The main flexural strength is provided, in all cases, by the strength of the first layer (with conventional bars reinforcement), while the second layer (with SFRC) provides a secondary flexural contribution.

Secondly, it can be seen from **Table 17** that the spraying sequence is a relevant parameter in the design of bi-layer walls. Walls with different spraying sequences, but with the same final structural configuration and construction sequence lead to widely different steel variations. For example, only a significant steel reduction (13.5 kg) could be obtained for the case with SD=(B) in the first group. This behaviour is studied in further detail in the following sections.

It is worth mentioning that for all the final structural configurations and construction sequences under study, there is at least one bi-layer alternative where a steel reinforcement reduction greater than 10 kg is obtained. The largest reduction (-21.7 kg) is reached in the case of a TD construction sequence and 60 cm first layer thickness ("*BL/60-10/TD/2u/2S/B*"). It represents a percentage reduction of 7.0% of all the longitudinal steel reinforcement, and of 45.1% in terms of the extra steel reinforcement as defined at the end of section 4.2.1.

Finally, it can be seen that the maximum displacements are closely related to the construction sequence that is followed with only minor reductions (smaller than 0.6 mm) if the bi-layer type is used. At the same time, it may be seen that the reduction is generally greater in cases with a 55 cm first layer thickness. However, even though similar displacements are obtained for each final structure configuration and construction sequence, in all cases the incorporation of the second layer is not enough to compensate for the extra displacements that take place, if the cross-section of the first layer is reduced from 60 cm to 55 cm.

4.3.1. Influence of the number of spraying stages

There are construction reasons to analyze the number of spraying stages. On the one hand, spraying the concrete for the second layer in a single stage may require sophisticated equipment (e.g. a spraying robot) and might even be impossible in large-scale sections. On the other hand, spraying is easier, if divided into sections of a few meters, when sprayed from various levels as the excavation progresses, and it is even possible to do so with manually operated equipment. Likewise, spraying in several stages makes it easier to coordinate this task with the excavation and the installation of props, thereby reducing construction time. However, concrete joints between the different spraying stages, where the strength of the concrete may be weaker and its watertightness less effective, appear in this case in the SFRC layer. This parameter figures in the structural calculations, as indicated below, and influences the development of bending moments, which may influence the structural contribution of the SFRC layer.

Fig. 32 shows the bending moment envelopes for the cases with 1, 2 and 4 spraying stages. The negative local maximums and the moments developed in the intermediate stages where the second layer was sprayed

are also shown in the figure with black lines. A circle indicates the depth of the sprayed concrete layer at the corresponding stage.
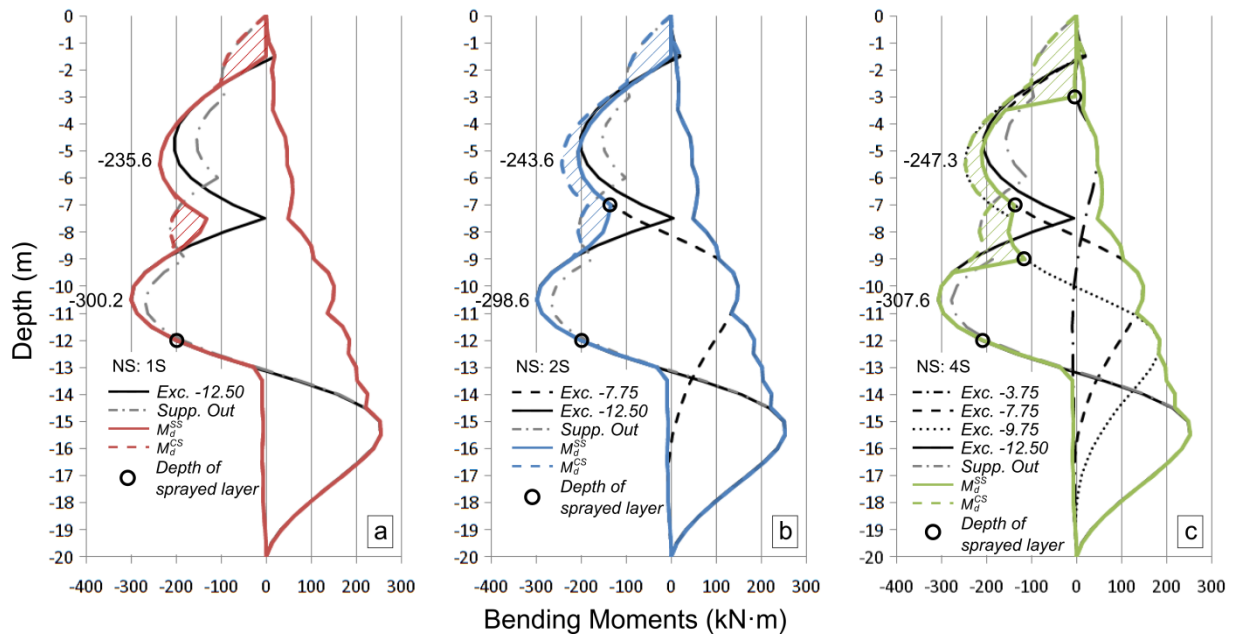
Fig. 32 - Bending moment envelope for different spraying discretizations: (a) 1 spraying stage; (b) 2 spraying stages; (c) 4 spraying stages.

It can be seen that in the case of a single spraying stage ("*BL/60-10/BUs/4u/1S/A*", see **Fig. 32a**) the area of bi-layer work is small, representing 5% of the total envelope area. This smaller area is because the SFRC is sprayed when the excavation is completed (depth -12.5 m), so all the moments provoked by the excavation have already developed. Therefore, the increase in bending moments after the compound cross-section is completed is exclusively due to redistribution of the internal forces that took place when the temporal supports were removed. The redistribution of forces is minor, as the final structural configuration (5 slabs) is stiffer than the temporal supports (2 struts).

In cases where the spraying was in 2 stages ("*BL/60-10/BUs/4u/2S/A*", see **Fig. 32b**), it can be seen that the area of bi-layer work was greater than in the previous case (8%). In this case, the increase in bending moments after the compound cross-section is completed also occurred in the excavation process, in addition to the aforementioned redistribution of forces. Nonetheless, note that the increase in bending moments in the sprayed section (at depths of between 0.0 m and -7.0 m) caused by the subsequent excavation is small, even more so if compared with the change in moments that took place at lower depths (between -7.0 m and -20.0m). For example, the maximum moments variation is 97.8 kN m in the upper section (depth -1.5 m), and 443.9 kN m in the lower section (depth -10.5 m). In other words, most of the moments will have already developed in the area onto which the second layer will be sprayed.

It can be seen that the case with 4 spraying stages ("*BL/60-10/BUs/4u/4S/A*", see **Fig. 32c**) follows the same pattern (the greater the spraying discretization, the more work done by the bi-layer area) and rises to 12%.

In contrast, it can be seen that, in general, the maximum negative moments are somehow larger (in absolute terms), in cases with greater discretization of the spraying stages. This behaviour is logical, considering that the moment increase, throughout the excavation, is greater in the sections already sprayed, due to the

increase in cross-sectional stiffness. Nonetheless, the maximum envelopes are quite similar in the three cases. The greatest difference between them is 9.8 kN m (depth -9.5 m, comparing the "4S" case with the "1S"), which represents a percentage difference of 3.7%

Fig. 33 shows the horizontal displacements for the corresponding cases shown in **Fig. 32**. The displacements of the corresponding mono-layer case ("*ML/60-0/BUs/4u/0S/M*") are also included.
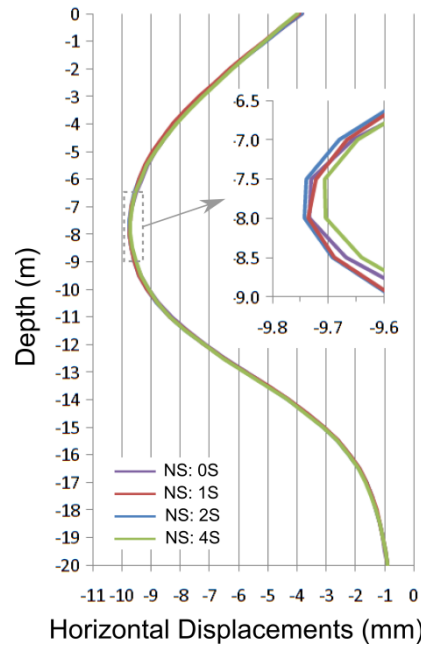
Fig. 33 - Displacements for different spraying discretizations.

The displacements are practically identical in all cases, with maximum differences of about 0.1 mm. This is because the stiffness increase given by the second layer is applied to the sections where the moments (and therefore the deformations) have already developed (as pointed out for the case in **Fig. 32b**). In other words, large deflections will have already taken place in the area that has just been excavated and that is therefore as yet unsprayed and with no compound cross-sections to assist with the displacement reduction.

4.3.2. Influence of the depth of the sprayed concrete layer

The depth of the excavation level when the spraying takes place and, therefore, the depth of the sprayed concrete layer, will also influence the contribution of the SFRC layer, as discussed below. **Fig. 34** shows the bending moment envelopes for the cases with a final SFRC layer sprayed at the following depths: (A) -12.5 m ("BL/60-10/BUs/4u/2S/A"); (B) -11.5 m ("BL/60-10/BUs/4u/2S/B") and (C) -10.5 m ("BL/60-10/BUs/4u/2S/C").

Once again, similarities emerge between the maximum envelopes for the three cases. Moreover, the M_d^{SS} envelopes between depth 0.0 m and -7.5 m are identical, as they are defined at the stages prior to the first spraying, which are the same in all three cases. The area where the main differences between the three cases are concentrated is detailed in **Fig. 34b**, which also includes the position of the maximum local "M_d^{SS}" moment before the second section was sprayed.

Firstly, the bending moments increased with the excavation depth, therefore the deeper the excavation when the second layer is sprayed, the larger the M_d^{SS} envelope. This includes the value of the local maximum moment (see arrow 1 in **Fig. 34b**). In the extreme case, when the SFRC is sprayed after the excavation is completed (depth -12.5 m), the value of the maximum M_d^{SS} coincides with the value of M_d^{CS}, meaning that there is no bi-layer area work at all.
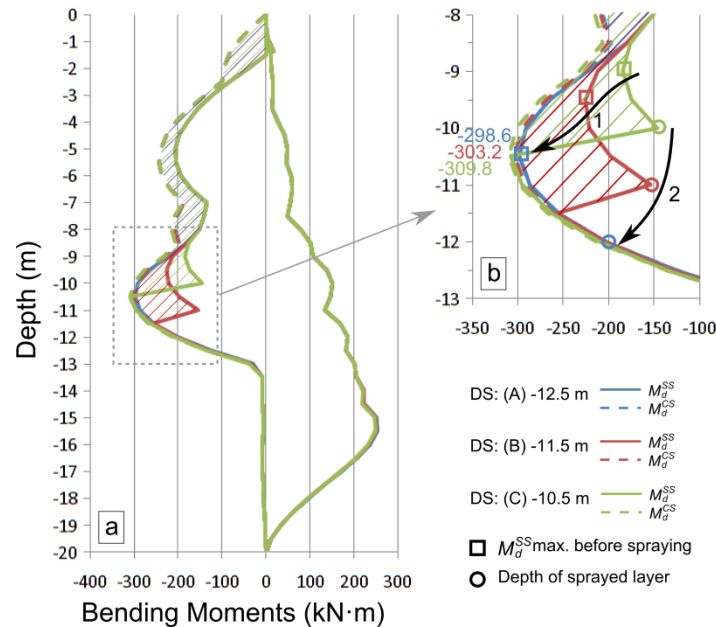
Fig. 34 - Bending moment envelope for cases with different depths of sprayed concrete layer: (a) general; (b) detail.

Secondly, there is a rise in the values of the M_d^{SS} envelope, located at one extreme of the intermediate sprayed section and produced after a subsequent increase in the bending moments. This rise is not desirable in the position where the maximum moment develops, as the simple cross-section should be designed to resist that moment, regardless of the extra strength provided by the second SFRC layer. So, it is convenient to spray the concrete at a lower excavation depth, so as to move the rise away from the position where the maximum moment develops (see arrow 2 in **Fig. 34b**).

Considering both aspects, the design of the bi-layer walls is, in these cases, sensitive to variations in the parameter under study. The strength increase provided by the SFRC layer can only be used in the intermediate situation (case (B), red envelope in **Fig. 34**), while it is of no use in the extreme situations (case (A), blue envelope, and case (C), green envelope, in **Fig. 34**). So, the possibility of taking full advantage of the bi-layer walls depends on a correct selection of the spraying sequence. This is a negative factor of the technique, complicating both the design and the construction of the wall, as it entails careful control over excavation depths and spraying sequences on the building site.

Thirdly, it can be seen that the value of the maximum moment differs in the three cases. As seen in the previous sections, the earlier the SFRC is sprayed, the larger the value of the bending moment, where a maximum difference of 11.2kN m is observed (3.8%, for case (C) as a percentage of case (A)).

Finally, it is worth mentioning that although the depth of the sprayed concrete layer was analysed towards the end of the excavation, the results can be extrapolated to an intermediate excavation situation, at the maximum local moment between depths of -4.0 m and -6.0 m. Besides, as described in section 4.3.1, in a similar way, the deformations associated with the three cases are practically identical.

4.3.3. Influence of the final structure configuration

The bi-layer diaphragm walls have a different structural response depending on the final structural configuration. This aspect is studied further by developing the analysis in the previous sections (all with NU=4u) for its application to a case with a different final structural configuration (NU=2u).

The bending moment envelopes for a case with 4 underground levels ("*BL/60-10/BUs/4u/2S/A*") and a case with 2 underground levels ("*BL/60-10/BUs/2u/2S/A*") are shown in **Fig. 35a** and **Fig. 35b**, respectively.
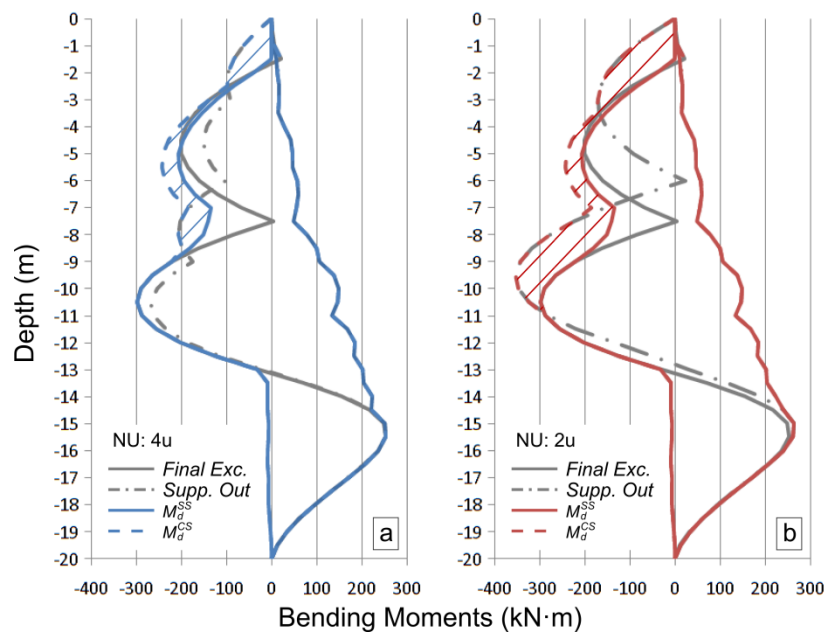
Fig. 35 - Bending moment envelope for two final structural set-ups: (a) 4 underground levels; (b) 2 underground levels.

As the excavation stages are identical for both cases, the envelopes differ at the stage when the temporal supports are removed and the walls are supported by the finished slabs. As seen in section 4.3.1, in the "4u" case (see **Fig. 35a**) the internal redistribution of forces is small and the values of the maximum bending moment (around depth -10.0 m) even decrease.

In contrast, the final configuration in the "2u" case (see **Fig. 35b**) is not as stiff (3 slabs) as in the "4u" configuration. Therefore, a larger redistribution of forces occurs and, particularly, an increase in the maximum bending moments after the final excavation (see **Fig. 35b**, between depths -7.0 m and -11.0 m). This increase can be resisted with the additional strength given by the SFRC layer, i.e. use the additional strength given by the second layer, even if it is sprayed after the excavation is finished.

Fig. 36 shows the horizontal displacements for the corresponding cases shown in **Fig. 35**. It also includes the displacements in the respective mono-layer cases ("*ML/60-0/BUs/4u/0S/M*" for the "4u" case; and "*ML/60-0/BUs/2u/0S/M*" for the "2u" case).

Fig. 36 - Displacements for different final structure configurations.

As is reasonable to assume, the maximum displacement in the "2u" case is larger (0.4 mm) than in the "4u" case, in accordance with the different stiffnesses of both final configurations. Once again, there are no appreciable differences between the mono-layer and bi-layer alternatives for the same structural configuration, the maximum differences being in an order of magnitude of 0.1 mm. Nonetheless, the displacements are barely smaller in the bi-layer cases due to the increased stiffness contributed by the second layer.

4.3.4. Influence of the construction sequence

The selection of the construction sequence in a deep excavation project depends on many factors, for example: adjacent excavations and constructions (and their foundations); construction timetable, equipment and budget; and the geometry and dimensions of the building (Ou, 2006). These factors influence the response of the bi-layer technique and are analysed below.

Fig. 37 shows the bending moment envelopes for the cases with construction sequence BUa ("*BL/60-10/BUa/2u/2S/A*"), BUs ("*BL/60-10/BUs/2u/2S/A*"), and TD ("*BL/60-10/TD/2u/2S/A*"). It also includes the bending moments of six representative intermediate stages (in grey and black lines), which are the stages that best define these envelopes.

The structural configuration, in both its temporary and its final stages, largely determines the magnitude of the bending moment values that develop in the walls. The cases that are shown here, although built with different construction sequences, show comparable results, as all three have 2 supports during the

construction (2 struts and 2 anchorages in the Bottom-Up cases, and 2 slabs in the Top-Down case. In the latter case, after the base slab is in place, no further bending moments are evident).
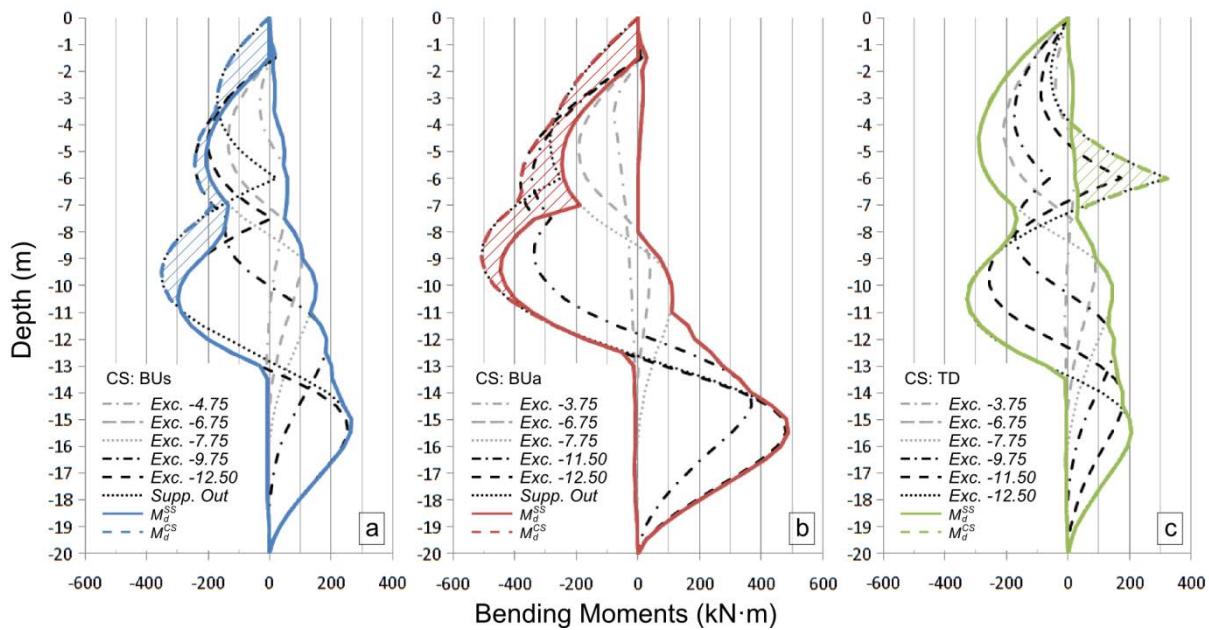
Fig. 37 - Bending moment envelope for different construction sequences: (a) Bottom-Up with struts; (b) Bottom-Up with anchorages; (c) Top-Down.

It can be seen that the "BUa" case (see **Fig. 37b**) shows a similar shape in the bending moment diagrams as the "BUs" case. However, the values are significantly higher, because the upper part of the wall has larger displacements, as the supports are more flexible (the anchorages have lower stiffness than the struts). The embedded section of the wall is therefore under greater strain, increasing the bending moments along the wall.

Behaviour quite unlike the previous two cases (resulting in a different diagram shape), can be seen in the case with the "TD" construction sequence (see **Fig. 37c**). As the slabs have a significantly higher stiffness than the temporal supports and are built during the excavation process, they apply greater reactive forces than the supports of the other construction sequences. Two consequences can be mentioned. Firstly, as with the "BUa" case, but in a contrary sense, in this case the supports are stiffer and, therefore, the displacements and bending moments are smaller. Secondly, that the local maximum moment produced by the intermediate slab (depth -6.0 m), reaches positive moment values.

There is an area of bi-layer work that can be seen around the positive maximum. The positive moments at this depth developed after the second layer had been sprayed. Therefore, the additional compound cross-section strength provided by the second layer can be harnessed, this time with the SFRC working in compression. However, note that there are high shear forces near the support together with the peak of moments. Therefore, the shear strength of the element and the debonding risk between layers should be evaluated with particular attention.

Note also that there is no internal redistribution of forces in the TD sequences, as in these cases the walls are directly supported by the finished slabs.

Fig. 38 shows the horizontal displacements for the corresponding cases shown in **Fig. 37**. It also includes the displacements of the respective mono-layer cases ("*ML/60-0/BUa/2u/0S/M*" for the "BUa" case; "*ML/60-0/BUs/2u/0S/M*" for the "BUs" case; and "*ML/60-0/TD/2u/0S/M*" for the "TD" case).
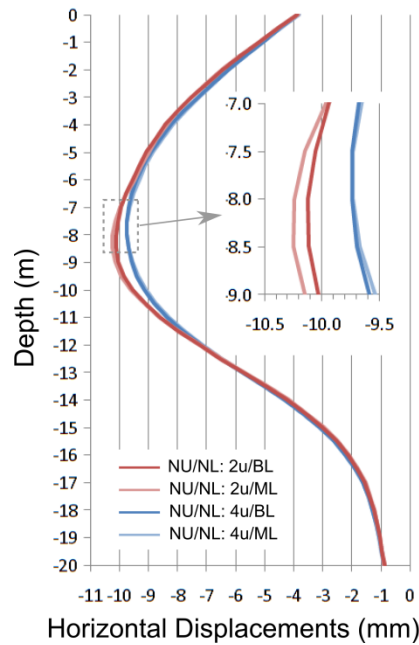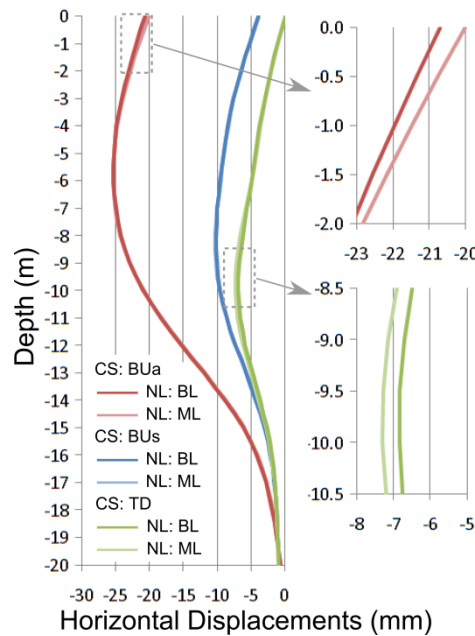

Fig. 38 - Displacements for different construction sequences.

Large differences can be seen in the displacements of the three construction sequences. The smallest displacements were registered for the TD case, followed by the BUs, and finally the BUa cases. This order reflects the support stiffness. Moreover, the anchorages have extra flexibility, provided by the deformability of the ground surrounding the bulb area, besides the flexibility of the element itself.

The displacements, although small, fall within the range of expected values in the Moormann database (Moormann, 2004). They reflect reasonable values, if we remember that a relatively stiff soil was used in this study, and that the supports were placed early in the excavation process, before appreciable displacements were recorded.

The figure shows that, once again, the influence of the bi-layer (dark lines) in the displacements is small compared with the differences in the construction sequence. Nonetheless, the differences between bi-layer and mono-layer in the TD and BUa are greater than in the BUs cases, already described in section **Error! Reference source not found.**. In the BUa case (see **Fig. 37b**), these large differences arise as larger moments are recorded after the first spraying, which subsequently causes a greater difference in the curvatures of the bi-layer and mono-layer walls (due to their different stiffnesses). The different deflections are recorded at the top of the wall, because it is a free end in the structural configuration. The maximum displacements difference in this case is 0.68 mm. However, the difference in the maximum displacements (depth -6.0 m) is minimal (0.02 mm in this case).

Meanwhile, large differences in the bending moments can be seen in the TD case, both above and below the excavation depth, after each excavation stage (see **Fig. 37c**). Regarding the displacements of this case, they can be observed mainly between depths -6.0 m and -12.0 m, as depths of between 0.0 m and -6.0 m are

strongly fixed by the upper slab (depth 0.0 m) and the intermediate slab (depth -6.0 m). Therefore, despite being a quite stiff structural configuration, a maximum displacement difference of the same order of magnitude (0.45 mm) may be seen.

4.3.5. Sectional results

As an example, reinforcement design of different walls is shown in **Fig. 39**. The same representation used for **Fig. 31** is followed here. It can be seen that the design inequalities ($M_U^{SS} \geq M_d^{SS}$ and $M_U^{CS} \geq M_d^{CS}$, see (Segura-Castillo, Aguado, de la Fuente, et al., 2013)) are satisfied in each instance.
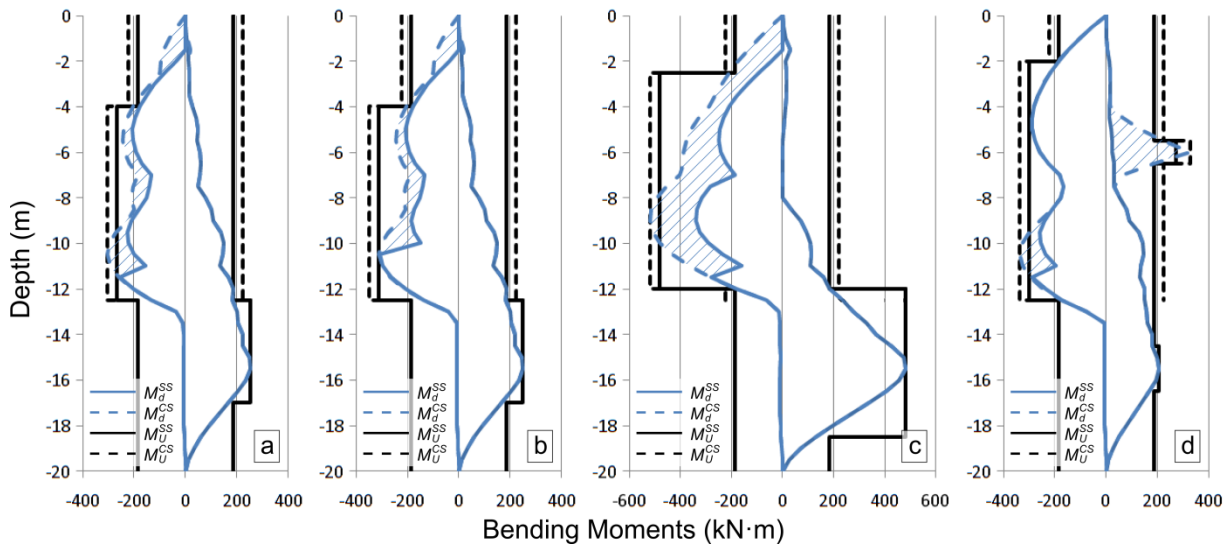
Fig. 39 - Design and ultimate bending moments envelope examples: (a) efficient design; (b) inefficient design; (c) large increase in bending moments after spraying; (d) Top-Down case.

Fig. 39a shows a case ("*BL/60-10/BUs/4u/2S/B*") where the maximum design moments are relatively similar to the ultimate moments for each type of cross-section (i.e. $M_U^{SS} \approx M_d^{SS}$; and $M_U^{CS} \approx M_d^{CS}$). The moments that are recorded, up until the second layer was sprayed, are resisted by the M_U^{SS} , and the subsequent moment increase is resisted by the M_U^{CS} . It can be considered an efficient design, in the sense that, in the ULS, the entire strength of the materials is needed to resist the design moments, both in the simple cross-section and in the compound cross-section.

In a case where the maximum M_d^{SS} is equal to the maximum M_d^{CS} (see case "*BL/60-10/BUs/4u/2S/C*", **Fig. 39b**), the M_U^{SS} resisted both design moments. In contrast to the previous one, this design may be considered inefficient, because even though the second layer increases the strength of the cross-section, this increase is not needed to cover the design moments. Therefore, it can be said that spraying the SFRC layer is a necessary but not a sufficient condition: the spraying sequence must also be taken into account to allow a reduction in the steel reinforcement.

Fig. 39c shows a case ("BL/60-10/BUa/2u/2S/B ") where there is a large increase in the values of bending moments after the SFRC layer has been sprayed. The values for M_d^{CS} are much higher than the values of the M_d^{SS} (for example, in the maximum: M_d^{CS} = 519.1 kN m and M_d^{SS} = 339.1 kN m).

This situation is not desirable as, on the one hand, the greater the increase in the forces after the spraying the larger the shear forces in the bond plane. On the other hand, higher bending moments in the compound cross-sections mean higher tensile stresses in the SFRC in the service state, which increases the risk of crack formation and, hence, water filtration. Finally, as was seen in sections **Error! Reference source not found.** and **Error! Reference source not found.**, the earlier the SFRC is sprayed, the larger the increase in the bending moments.

The Top-Down cases (see **Fig. 39d**) show two areas where reinforcements for the positive moments are needed, in the embedded area and at the depth where the intermediate slab is connected (-6.0 m). This moment is larger in the bi-layer alternatives, as the stiffness of the wall is higher after spraying the SFRC layer. In turn, the negative moments in the intermediate area of the wall (depths between -6.0 m and -15.5 m) are reduced. This change in the bending moments is also translated into a reduction in the extra reinforcement, as the negative reinforcement has to be placed across a larger section of the wall than the positive one.

4.4. ADDITIONAL CONSIDERATIONS

A diaphragm wall civil engineering project involves many parameters. The classification by Kung (G. T.-C. Kung, 2009) lists some of them: inherent parameters (e.g. stratigraphy, and site environment), design-related parameters (e.g. properties of retaining system, excavation geometry, and strut prestress), and construction-related parameters (e.g. construction methods, over-excavation, and prior construction).

Although the analysis developed here was limited to the study of 6 parameters, it provides the basis for the understanding of the behaviour of other parameters that are not included; for example, if a stratigraphy with an elevated ground water table is considered. In this case, a common construction technique consisting of lowering the water table during the excavation to avoid soil liquefaction may be used. Once the excavation and the substructure have been completed, the water table may be restored to the original value, increasing the loads on the wall. This increase can also be covered by the extra strength provided by the SFRC layer, as was done with the increase caused by the internal redistribution of forces described in section 4.3. In a similar way, the analysis can be extended to other type of soils.

To quantify this, four additional cases were simulated, comparing mono-layer and bi-layer alternatives. The first new case ("Water Ground") is similar to the "*BL/60-10/BUs/4u/2S/A*" case, but incorporates a water table at depth -5.0 m. The construction sequence was also modified, adding the lowering of the water level described above. The second new case ("Loose Sand") is similar to the "*BL/60-10/BUs/2u/2S/A*" case, but the properties of the soil were modified to reflect a looser sand (the elastic parameters E_{50}, E_{oed} and E_{ur} were reduced by 50%, and the φ by 5°). The corresponding mono-layer alternatives for each of the previous cases were also simulated. The main results are summarized in **Table 18**, where the same information as in the previous cases is provided.

In the "Water Ground" case, a steel reduction of 8.5 kg is obtained. Although the reduction is not large, it is a relevant improvement compared with the base case ("*BL/60-10/BUs/4u/2S/A*", where the reduction achieved was of only 2.8 kg), due to the contribution of the SFRC layer that withstands the moment increase caused by the water table level recuperation. The reduction may even be improved if an adequate spraying sequence is selected.

Table 18 - General results for the additional cases

Case	EA(M_d^{SS}) (kN m m)	EA(M_d^{CS}) (kN m m)	M_U^{SS} (kN m)	M_U^{CS} (kN m)	W(A$_{s,ext}$) (kg)	ΔW(A$_{s,ext}$) (kg)	δ$_{H(max)}$ (mm)	Δδ$_{H(max)}$ (mm)
(ML) Water Ground	3737	---	288.0	---	30.0	---	-8.85	---
(BL) Water Ground	3361	403	259.0	296.3	21.5	-8.5	-8.81	0.04
(ML) Loose Sand	6168	---	514.9	336.3	139.1	---	-16.70	---
(BL) Loose Sand	5413	722	477.9	517.5	122.7	-16.4	-16.47	0.23

In the "Loose Sand" case, it can be seen that both the bending moments and the displacements have increased considerably compared with the base case ("BL/60-10/BUs/2u/2S/A"), in agreement with the change made. However, a reduction of 16.4 kg in the amount of steel (within the range of the other cases) was still possible.

4.5. CONCLUSIONS

By means of a numerical study, a parametric analysis of six relevant bi-layer diaphragm wall parameters has been performed. Several construction impacts have been detailed through the paper, and the steel reinforcement and displacements reduction have been quantified. The main conclusions are:

- In all cases, the main flexural strength is provided by the strength of the first layer (with conventional bar reinforcements) and a secondary flexural contribution by the second layer (with SFRC). This contribution increases the ultimate strength of the simple cross-section by between 8% and 15%.

- Feasibly, all final structural configurations and construction sequences could reduce the steel reinforcement of the RC layer by taking full advantage of the strength added by the SFRC layer. Using the appropriate spraying sequence, a reduction in steel reinforcements of over 10 kg can be obtained in every configuration and sequence, reaching a maximum reduction of up to 21.7 kg. This represents a percentage reduction of 7.0% of the total bending reinforcement, and of 45.1% over the extra bending reinforcement.

- The spraying sequence is a relevant parameter in the design of the bi-layer walls. In general terms, in cases with no increase in moments following the excavation process, the SFRC should be sprayed during the excavation, if full advantage is to be taken of the strength increase given by the SFRC layer. Otherwise, spraying must be done after finishing the excavation process. In each case, the sooner the SFRC is sprayed, the larger the bending moments that are recorded.

- The displacements, which are governed by the thickness of the first layer, are practically identical for each combination of final structural configuration and construction sequence. Although a displacement reduction is registered when the second layer is included, it is minor compared with the total displacements. The maximum reduction obtained (0.6 mm) represented a percentage reduction of 7.3%.

4.6. ACKNOWLEDGEMENTS

"Crazy, but that's how it goes
Millions of people living as foes
Maybe it's not too late
To learn how to love
And forget how to hate"
— Ozzy Osbourne

CHAPTER 5.   Evolution of concrete-to-concrete bond strength at early ages[4]

ABSTRACT: An innovative structural element typology is proposed, referred to as a bi-layer diaphragm wall. Its two layers are poured and sprayed, respectively, in two phases; the first layer is a standard reinforced-concrete diaphragm wall, while the second consists of a layer of sprayed concrete with steel fibres, which performs a dual waterproofing and structural role. Through an experimental campaign, our research aims to study the evolution of bond strength between the two concretes at early ages. Three preparation techniques were studied: milled surfaces, milled and epoxy-bonded surfaces, and saturated milled surfaces. The results reveal that the shear strength of milled surfaces follows a typical maturity law, regardless of the milling direction. In contrast, a wide range of results is evident for in-situ epoxy-bonded surface preparations.

Keywords: shear test, fibre, sprayed concrete.

5.1. INTRODUCTION

Leakage represents a widespread problem in diaphragm walls built under certain conditions, such as enclosures in water-bearing ground. Ever since the first walls of this type were built, in the 1950s and 1960s, their potential waterproofness has been widely discussed and several techniques have emerged to prevent the emergence of leaks or repair them (Puller, 1994).

A standard technique for repairing leaky walls is to repair the affected areas, chipping away the damaged element and restoring it with a waterproof mortar. Leakage usually only becomes apparent over lengthy periods and it appears at different times in different areas of the walls, meaning that repair works may often extend over indefinite periods of time and require several sessions. A solution that is less widely used consists of casting a second layer of waterproof mortar (or concrete) over the inner face of these walls. Since the whole surface is covered, this is an effective albeit expensive solution (Wong, 1997). An example of this solution was used by Li in the study of tensile creep in concrete at early ages (Li et al., 2008).

Part of a larger research project, this study aims to maximize the functional attributes of the second layer of concrete by allowing it to play a structural role, in addition to its initial intended purpose (waterproofing). In view of the structural role of the second layer, the thickness of the first layer may be reduced. The dimensions of this bi-diaphragm wall and its watertightness make it a feasible structural solution.

In this way, the bi-layer diaphragm walls are made of two concrete layers poured and sprayed, respectively, in separate phases. The first, a diaphragm wall is built in the conventional manner. Once this wall attains the necessary strength and after excavating the soil within the perimeter, sprayed concrete with steel fibres forms the second layer. The solution is schematically represented in **Fig. 40**.
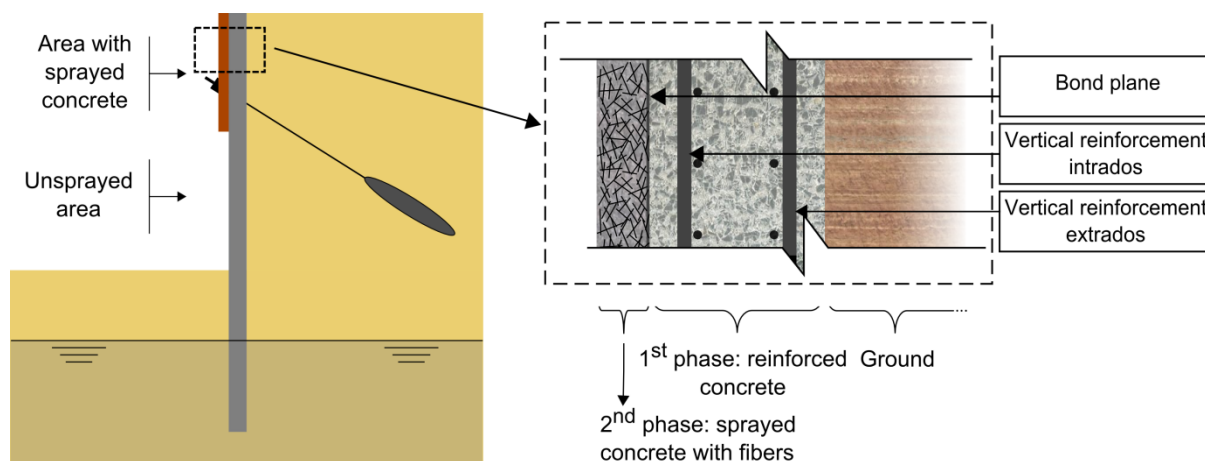
Fig. 40 - Sketch of bi-layer wall: general and sectional view.

The bond between both concretes plays an important role in the performance of the structure. If bond strength is sufficiently high, the structure behaves monolithically, effectively mobilizing all the strength of its different elements. This is very necessary for the repair and reinforcement of concrete structures. It is common practice, first of all, to increase the roughness of the base layer, by applying a bonding agent and/or steel connectors in some cases, followed by the reinforcement layer (Júlio, Branco, Silva, & Lourenco, 2006). Usual examples of this application include bridges built in several stages, techniques for pavement

reinforcement (Delatte Jr., Wade, & Fowler, 2000) and more complex techniques such as NSM (Near Surface Mounted), among others (Bonaldo, Barros, & Lourenco, 2005).

Bond strength depends mainly on interface adhesion, friction, aggregate interlock and time-dependent factors (Momayez, Ehsani, Ramezanianpour, & Rajaie, 2005). An essential requirement relates to the development of full bond strength over time between the reinforcement and the base layer. Talbot (Talbot, Pigeon, Beaupré, & Morgan, 1994), in reinforcement with sprayed concrete, and Delatte (Delatte, Williamson, & Fowler, 2000), in reinforcement for bridges, both studied bond durability and maturity at increasing ages.

The values obtained for the strength of the bond depend strongly on the chosen test method (Momayez et al., 2005). Several authors have performed different studies which, on the one hand, describe and classify the methods and, on the other hand, compare the results they obtain (Abu-Tair, Rigden, & Burley, 1996; Simon Austin, Robins, & Pan, 1999; Júlio, Branco, & Silva, 2004; Momayez et al., 2005). The slant shear test (Wall & Shrive, 1988) has become the most widely accepted test and has been adopted by several international regulations as the test for assessing the bond between resinous repair materials and the base concrete (Abu-Tair et al., 1996). However, there is no agreement among researchers with regard to the suitability of non-resinous materials (Momayez et al., 2005).

The lack of consensus over any one test or another may be due to their associated problems. In most cases, the bond surface in a direct shear test is, in fact, subjected to shear stress and to slight bending. In some tests, shear stress is combined with a normal, either tensile or compressive, stress. Saucier (Saucier et al., 1991) devised a test for assessing shear bond strength under different compression levels, and Austin (Simon Austin et al., 1999) considered bond failure as an envelope covering all possible normal/direct stress states. However, when stress was introduced into the shear plane by means of steel plates, it caused stress concentrations at the edge of the bond plane. Smaller stress concentrations reduced the scatter in the test results (Momayez et al., 2005).

The most widespread methods for the shear test are designed to test samples produced in a laboratory. The LCB test (Miró Recasens, Martínez, & Pérez Jiménez, 2005) and the Guillotine Direct Shear Test (Delatte et al., 2000) are worth mentioning as suitable tests for cores obtained in the field, .

The aim of this research is to study the evolution of bond strength at early ages (2, 6, and 35 days) that is obtained between sprayed concrete and a previously-milled base layer of concrete, which together make up the bi-layer diaphragm wall. The study also analyzes the influence of contact conditions, for which purpose several other alternatives have been added, such as priming with an epoxy resin coat and water saturation of the contact surface. Likewise, it examines the influence of the milling direction and the compressive strength of the constituent concretes on the actual bond strength.

The study was conducted at a real construction site. Some of the techniques that are commonly associated with the construction of diaphragm walls do not, according to the literature, always offer the best results. However, it was decided to maintain these techniques to simplify the implementation of the new structural typology. Thus, for example, milling was used instead of sand blasting (with better results according to (Júlio, Branco, & Silva, 2005)), and adhesive epoxy, instead of modified-cement (with better results according to (Momayez et al., 2005)).

This article represents an important step forward in the development of bi-layer diaphragms, contributing knowledge on the bond formed at early ages by concrete that is sprayed over an existing layer, especially over a milled concrete surface, one of the most usual practical methods of in situ preparation. It is useful for engineers that design bi-layer elements and structural repairs involving sprayed concrete reinforcements, in general.

5.2. EXPERIMENTAL PROGRAM

An experimental campaign was developed to test the proposed methods. The previously described bi-layer walls were constructed at a building site located in Barcelona (Spain). Inclinometers were placed on the walls (on both layers), as well as strain gauges and load cells (at the anchorage points); transverse displacements were measured by means of invar tape, in order to analyze the structural behaviour of the composite element. Likewise, for the purpose of this study, casts filled with the concrete were used for the characterization of the material and cores were extracted from the wall in order to study the bond between the two layers, as described below.

Fig. 41a, shows the layout of the building site. Standard construction methods were used to build the diaphragm walls that run around the entire perimeter of the building site. As may be seen, the building plant is not very large and is located in an urban environment with height restrictions laws. The figure also shows the location used for the analysis of bonding conditions, referred to as follows: MP (milled surface), EP (epoxy-bonded surface) and SP (saturated surface). **Fig. 41b** shows a side view of the walls, including the finished frameworks, up to street level. Five stories are planned to be built above them, reaching a height of 16.5m.
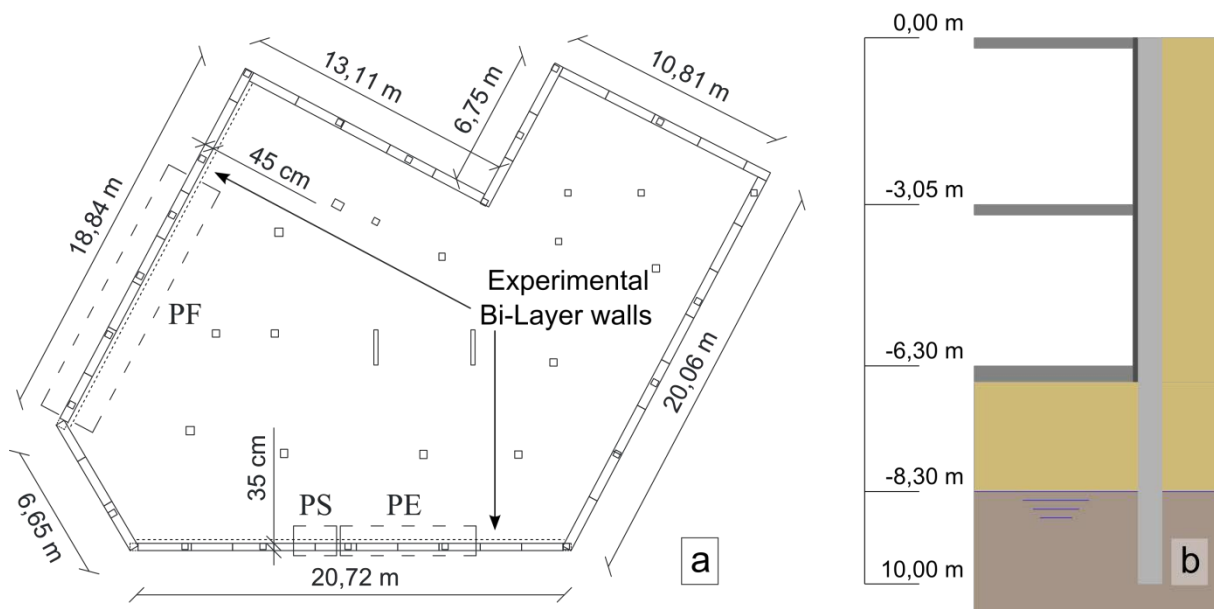
Fig. 41 - Details of diaphragm walls: (a) site plan; (b) side view.

5.2.1. Preparation of specimens

The first phase of the bi-layer walls was constituted by a conventional reinforced-concrete diaphragm wall with a compression strength at 28 days of f_c=30 MPa (UNE-EN 12390-3(UNE-EN 12390-3, 2003)), the mixture composition is given in **Table 19**. For the characterization of the concrete, samples were taken at the time of concreting the walls, with which the compressive strength of the first-phase concrete was determined (UNE-EN 12390-3(UNE-EN 12390-3, 2003)). Limestone-type aggregates were used (in both phases).

Table 19 - Concrete dosages.

Component	First-phase concrete	Second-phase concrete
Cement II/A-M 42.5 R (KG/m3)	365	
Cement I 52.5 R (KG/m3)		450
Corrector sand 0/2 (KG/m3)		355
Sand 0/4 (KG/m3)	970	975
Aggregate 4/12 (KG/m3)	200	300
Gravel 12/20 (KG/m3)	630	
Plasticizer (% cement, in kg)	0.8	
Nano-silica (% cement, in kg)		1.5
Superplasticizer (% cement, in kg)		1.5
Water/cement ratio	0.47	0.40
Metallic fibres (kg/m3)		30

Once the excavation was finished, cold milling of the exposed wall took place, in order to even out and prepare the surface and to increase its roughness, so as to improve the bond of the sprayed concrete layer. Milling was performed with a concrete miller attached to the end of a backhoe (**Fig. 42a**). A negative aspect of this type of mechanical treatment is that it can give rise to micro-cracks, which weaken the surface (Júlio et al., 2004; Talbot et al., 1994). **Fig. 42b** shows a photo of the surface finish, highlighting a specific area.

Subsequent to milling, one day before the second phase of concrete spraying, the wall was washed with a water-jet (**Fig. 42c**), which removes dust and loose particles produced in the milling process. Besides, this process also saturates the pores of the base concrete but, if performed long enough in advance, the surface has time to dry out, leaving a dry surface, but with saturated pores. This final preparatory work performed on the MP walls (milled surface) is considered the best surface moisture condition, though controversy persists over this point and contradictory results have emerged (Júlio et al., 2004).

The final step in the preparation of the EP walls (epoxy-bonded surface), prior to concrete spraying, was to place the bonding agent (**Fig. 42d**) on the wall. "Multitek Adhesive SDH" (a two-component, water-based epoxy adhesive for bonding concretes) was applied following the manufacturer's instructions.

Likewise, it is well known that moistening the surface before spraying is a technique that reduces the resistance of the bond, nevertheless pre-wetting the surface before applying the new concrete layer is common practice (Talbot et al., 1994). At the time of spraying, a localized water leakage occurred at the head of the SP walls (Saturated Surface); therefore, the surface of the diaphragm wall in this area was at all times totally saturated with water (**Fig. 42e**). As water leakage was present and with the intention of confirming that this is a harmful situation, an on-the-spot decision was taken to test this zone too.
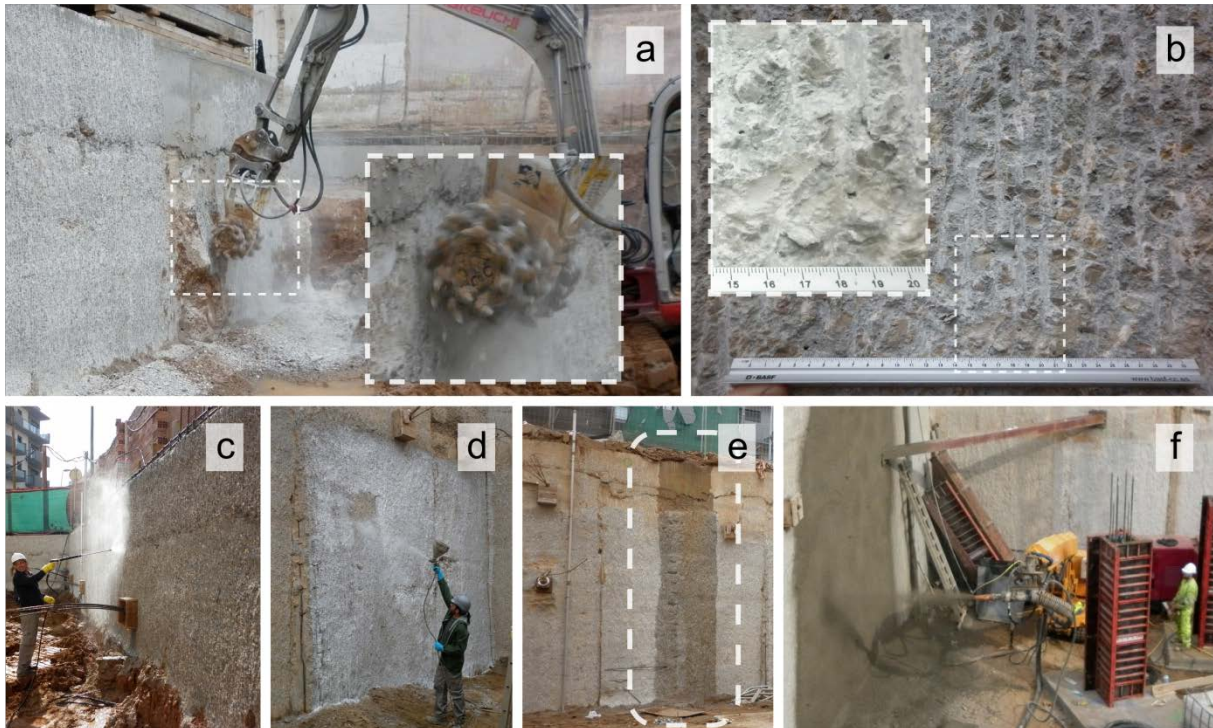
Fig. 42 - Main steps in the production of the specimens: (a) milling the wall built in the first phase; (b) finished surface; (c) water-jet washing; (d) placing the bonding agent; (e) area of water leakage; (f) spraying the second layer of concrete.

Table 20 summarizes the main processes characterizing the three types of surface preparation.

The second-phase concrete was sprayed with a dry-mix process (**Fig. 42f**), thereby completing the structural element. There is general agreement in the literature that a bond material with a modulus of elasticity similar to the adjacent concrete is desirable in the application and for the performance of concrete repairs (Simon Austin et al., 1999; Wall & Shrive, 1988). As the two phases are placed at different times, different moduli of elasticity develop in both concretes as they gain strength. Therefore, it is understood that equal moduli should be achieved throughout the service life of the structure. Various rules (including Eurocode 2 (EN, 2004b)) establish a relation between the modulus of elasticity and concrete strength. Therefore, the firms that supplied the concrete were asked to prepare dosages with the same characteristic strength at 28 days. The dosage of the sprayed concrete design (**Table 19**) was based on proposals made by García et. al. (García Vicente, Agulló Fité, Aguado de Cea, & Rodríguez Barboza, 2001) and the experience of the concrete manufacturer.

MEYCO MS 685, OPTIMA 209 nano-silica was used as a superplasticizer. The characteristics of the metallic fibres that reinforce the structural composition of the composite element were as follows : *Length: 35 mm, diameter: 0.55 mm, with hooked ends* (brand name: DRAMIX RC-65/35-BN).

The required thickness of the second layer was 10 cm but, due to the intrinsic irregularity of the spraying system, layer thicknesses ranging from 9 cm to 17 cm were detected in the subsequent extraction of cores. An Aliva 503 robot was used to for concrete spraying, once the base concrete was 84 (MP) and 86 (EP and SP) days old. After spraying, the surface was kept wet for a whole day. During the spraying of the second

layer, two casts were filled with the same concrete and the procedure outlined in UNE-EN 14488-1(UNE-EN 14488-1, 2006) was followed; cores were extracted from the casts and were used to determine their compressive strength (UNE-EN 12390-3(UNE-EN 12390-3, 2003)).

Table 20 - Types of surface preparation.

Name of preparation	Milled Surface (MP)	Surface with epoxy (EP)	Saturated Surface (SP)
Mechanical treatment	**Surface milling**	Surface milling	Surface milling
Surface moisture	Saturated and left to dry one day before second-stage concreting	Saturated and left to dry one day before second-stage concreting	**Saturated during** second-stage **concreting**
Bonding agent	No bonding agent	**Epoxy adhesive**	No bonding agent

Bold values indicate the distinctive preparation of each type of surface.

The cores for the study of bonding between the layers were extracted from the wall one day before the scheduled date for their test. They therefore retained the same curing conditions as the rest of the element for as long as possible. Since tests were planned at different ages, the extractions were also carried out at different ages. Core extraction was performed in the MP and EP areas, when the second-phase concrete was 1-day, 5-days and 34-days old.

5 cores from each of the areas were extracted at each age. In the SP area, only 4 cores were extracted at the age of 34 days. Some cores, mainly those extracted at the earliest ages, broke along the bond plane at the moment of extraction.

Various agents intervene in studies that take place under real working conditions on-site (e.g. Promoter, Constructor, Laboratories, Researchers). The circumstances under which this work was carried out made it very difficult to modify the experimental programme, as initially planned. In addition, especially at the first age (t=2 days), there was less than one day in which to perform the core extractions and the rest of the experimental measurements. At that age it was therefore not possible to extract more specimens to replace the six that debonded at the time of their extraction.

5.2.2. Shear test

The *modified LCB test* was chosen for the shear test from among those described in the introduction. **Fig. 43** shows a sketch of the device and a photograph of the test. This test was chosen for two reasons: on the one hand, it meant that a shear test could be performed on the extracted cores and, on the other hand, it made it easier to test irregular bonds between layers (a problem reported in the case of the "guillotine" test (Delatte Jr. et al., 2000)), as it leaves a small space between the load introduction edges. However, due to this separation, the bending component acting on the bond to be tested was higher.

The test is based on standard "NLT-328/08" (NLT-382/08, 2008), intended for the assessment of bonding in pavement layers made of bituminous materials (Miró Recasens et al., 2005), which are much more ductile materials than concrete, with much greater sensitivity to temperature variations. Because of this, the temperature control chamber was removed and the displacement speed of the loading piston was reduced from 2.5 mm/min to a value in the order of those used in shear tests on concrete: 0.25 mm/min (Mirsayah & Banthia, 2002; Ray, Davalos, & Luo, 2005; Wall & Shrive, 1988). A thin neoprene sheet was placed

between the device and the core, in order to reduce stress concentration in the supports. The test was performed using a hydraulic press with displacement control.
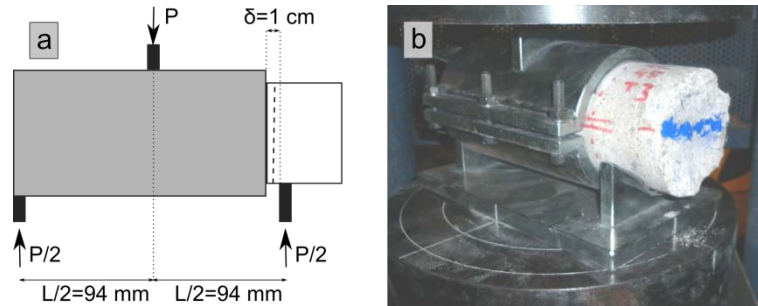
Fig. 43 - LCB shear test: (a) device sketch, (b) test configuration.

The shear stress which appears in the bonded interface is calculated according to the following formula:

$$\tau = (P/2)/S \qquad (7)$$

where, τ is the shear stress (MPa), P is the maximum load at failure (N), and S is the area of the cross section of the specimen (mm^2).

Prior to the extraction of the cores, a mark was made on the wall indicating its vertical direction, which coincided with the milling direction. Using this mark as a reference, the cores were oriented to perform shear stress in a direction perpendicular to milling (VM), parallel to milling (HM), and in a direction offset by 45º in relation to the previous ones (OM). **Fig. 44** shows a sketch of these positions. The core in **Fig. 43b** has a mark in the horizontal position; i.e. the stress runs perpendicular to the direction of milling.
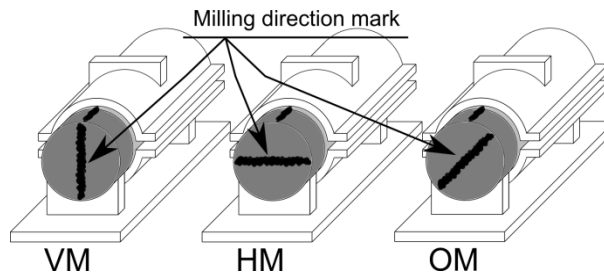
Fig. 44 - Core positions for shear test.

5.3. RESULTS AND DISCUSSION

5.3.1. Mechanical characterization results

Table 21 shows the evolution of strength as regards the age of both concrete phases. As can be seen, the strength values obtained for all concretes were above the expected design values, presented in section 5.2.1.

The last three lines of the table show the compressive strength of both concretes for the ages at which the shear tests were carried out. At these ages, the strength of the first-phase concrete was calculated on the basis of the results from earlier ages, using the concrete maturity formula (Neville & Brooks, 2010), assuming

constant average temperatures throughout the experimental campaign. This is a reasonable hypothesis, taking into account that the element is of little thickness and is in contact with the ground.

Table 21 - Compressive strength of concrete in both phases.

Age of 1st phase concrete, days	f_c, 1st phase concrete, N/mm2		Age of 2nd phase concrete, days	f_c, 2nd phase concrete, N/mm2
	MP walls	EP and SP walls		
7	26.29	30.26	-	-
28	33.89	34.82	-	-
56	36.83	37.37	-	-
87	39.28*	38.94*	2	30.99
91	39.51*	39.05*	6	39.22
120	40.94*	39.97*	35	45.40

* These values were calculated according to the concrete maturity equations (Neville & Brooks, 2010).

5.3.2. Shear test results

Among the correctly extracted specimens, three were not tested. This was due to a fault (described in 5.3.2.1) in the first two (MP-35 and SP-38) and due to an error in the load press in the third (MP-35). The results from the shear test are shown in **Table 22**. The following information is given for each series: name specifying surface preparation type and age at testing; number of cores debonded in extraction, rejected tests, and acceptable tests; test age; surface preparation; mean bond stress, calculated by means of formula (7); standard deviation; and, finally, the direction with regard to milling used in the tests. These results are examined in the following sections.

Table 22 - Shear test results.

Series	Number of Cores: extracted/debonded on extraction/rejected tests/acceptable tests	Age, days	Surface preparation	τ_m, MPa	Standard deviation, MPa	Milling direction: FV/FH/FO
MP-2	5/2/0/3	2	MP	1.04	0.160	1/1/1
EP-3	5/4/0/1	3	EP	1.43	-	1/0/0
MP-6	5/1/0/4	6	MP	1.18	0.181	2/2/0
EP-6	5/2/0/3	6	EP	1.18	0.681	1/1/1
MP-35	5/1/2/2	35	MP	1.63	0.046	1/1/0
EP-35	5/0/0/5	35	EP	1.04	0.109	2/2/1
SP-38	4/0/1/3	38	SP	1.01	0.401	-/-/-

5.3.2.1. Types of failure

As shown in **Fig. 45**, brittle failure was detected in all cases. Once the maximum load (P) was reached, there was an immediate drop in shear strength. Load P was used in formula (7) to assess the shear stress on the bond plane. The recorded displacement corresponds to the displacement of the piston by the loading press, which is therefore also affected by deformation or movements of the whole device, in addition to any deformation of the concrete under shear stress.

The graph shows a first non-linear stretch, which becomes progressively stiffer as deformation increases. So that the specimen moves in unison with the clamp, tension should be transferred between them, dispersed

throughout the neoprene sheeting. These sheets are regularly changed, as they are damaged in each test. Moreover, during the tests, a very slight rotation of the sample in the clamp could be observed. It is thought that the initial non-linear section is because of this slight rotation and the effect of the damaged neoprene.
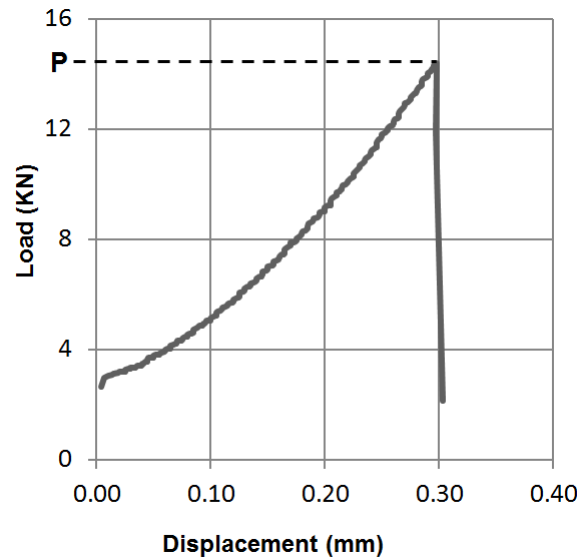
Fig. 45 - Typical shear test strength-displacement graph.

The failure plane tended to appear on the bond plane between the two concretes, due to the fact that this is weaker than any other plane within each of the concretes. There are nevertheless two mechanisms which can lead to failure on another plane.

Since there is a bending component between the separation of the supports, normal stresses appear on the bond plane; under compression in the upper area and under tension in the lower area (**Fig. 46a**). Normal compression on the bond plane increases the bonding value due to friction. On the other hand, a compressive strut is created on the plane between the load application points, where perpendicular tensile stresses, analogous to those in a splitting test, may occur (**Fig. 46b**). Therefore, failure will occur on this plane if the aforementioned stresses exceed the tensile strength of the concrete before the tangential strength is overcome on the bond plane.
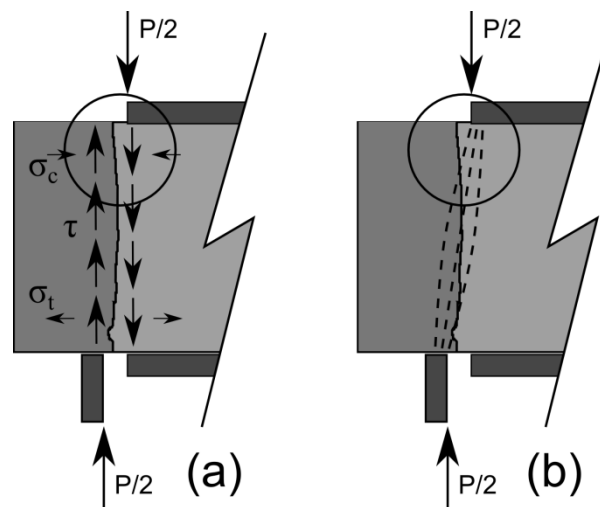
Fig. 46 - Failure mechanisms in the test.

This type of failure took place in some cases, for instance in the example shown in **Fig. 47a**. In other cases, failure occurred simultaneously on both planes (**Fig. 47b**). As this is an abrupt type of failure, the surface on which it first took place could not be determined. The chip was measured, shown as distance "s" in **Fig. 47a**, from its lower edge (perpendicular to the direction of the load) to the uppermost point of the core. When failure took place largely outside the bond plane of the two concretes ($s > 3$ cm), the test was declared null and the result was dismissed.

Fig. 47 - Atypical failure: (a) stone chip protruding on one side, (b) on two planes.

In order to reduce the influence of these secondary mechanisms, failure could be induced on the bond surface, producing notches on the edges of the bond surface, which leads to failure only along this plane; a strategy that has been validated in previous studies (Mirsayah & Banthia, 2002).

5.3.2.2. Shear stress depending on age

Fig. 48 shows a graph of the average value and represents the standard deviation for each age of the MP and SP series.
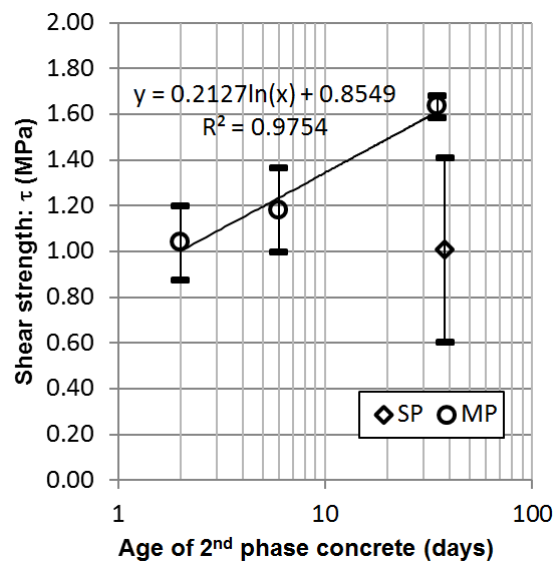
Fig. 48 - Shear stress vs. age of second-phase concrete: surface preparation with milling (MP) and saturated surface (SP).

In the case of MP, it can be clearly observed that the shear stress value increases with age. The linear regression line traced in **Fig. 48** shows an excellent fit with Plowman's modified function:

$$\tau = A + B \, log(maturity) \qquad\qquad (\, 8 \,)$$

where, A and B are constants to be determined and *maturity* is defined by the Nurse-Saul function:

$$maturity = \Sigma \, (T\text{-}T_0) \Delta t \qquad\qquad (\, 9 \,)$$

where, T_0 is the "datum" temperature, usually -10ºC, and Δt is a time interval.

Therefore, in agreement with Delatte's study (Delatte et al., 2000), the evolution of shear stress for the second phase carried out with sprayed concrete fits in with the maturity model, if it is assumed, once again, that the average temperature of concrete, for the period of time under study, is constant.

Homogeneous low variations of bond strength were obtained at several ages for the MP series (between 0.05 MPa and 0.18 MPa) and a higher variation was obtained (0.40 MPa) at only one age for the SP series.

5.3.2.3. Shear stress on saturated surfaces

The cores with SP preparation were only tested at 38 days. At this age, the bond values observed for the SP series were lower compared to the MP series. The only difference in the preparation of these series was surface wetting. The results indicate that total saturation of the surface at the time of concreting reduces the bonding capacity between the two concretes.

5.3.2.4. Shear stress on epoxy-bonded surfaces

**Fig. 49** shows a graph of the average values and represents the standard deviation at each age for the EP series. Only one core could be tested at the first age (t = 3 days); therefore, the dispersion for this time cannot be assessed. The variation differed greatly for the two other ages under consideration. The widest dispersion (0.68 MPa) was recorded at the second age (t = 6 days), and a much smaller standard deviation (0.11 MPa) was recorded at the third age (t=35 days).

The wider variability of the results for the EP series may be attributed to difficulties in the application of the bonding agent that is inherent to the work. After application of the product, one hour must elapse before proceeding to place the second-phase concrete. Likewise, the product must be applied within a period of approximately two hours; after that period it crystallizes, notably reducing the bonding capacity between concretes. If we take into account the difficulty of accurately predicting concreting times when spraying, it may be concluded that areas of varying strength in the bond will probably be found. On the other hand, since the product must be applied manually, its collocation depends on the experience of the worker applying it, which implies an additional factor adding more variation to the results.

Notwithstanding the scattered data, a decrease in strength with age is observed. Tu (Tu & Kruger, 1996) also noted a decrease in strength after 14 days, attributing it to the deterioration of epoxy caused by water that migrated from the fresh concrete and gradually accumulated at the epoxy-concrete interface.
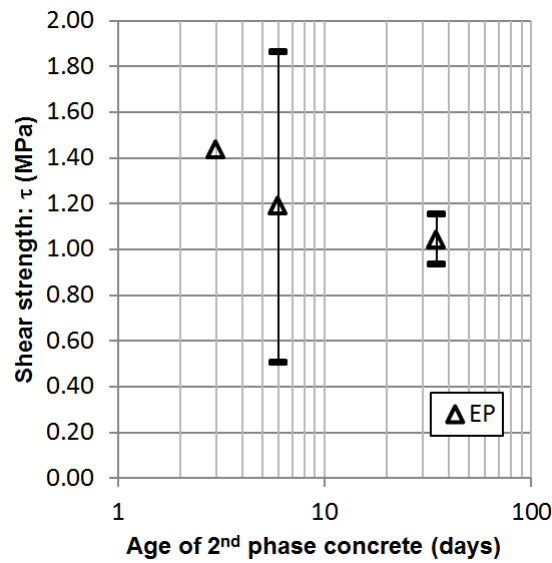
Fig. 49 - Shear stress vs. age of second-phase concrete, surface preparation with epoxy (EP).

5.3.2.5. Milling direction

Fig. 50 shows the graph for shear stress according to the age of second-phase concrete at the time of testing, grouped according to the direction in which the load was applied with regard to the milling direction. This graph only considers the results of the MP case. Conflicting results were obtained for different ages. At 2 days the strength of the HM case was higher; at 6 days, the results alternated; and at 35 days, the strength of the VM case was higher.
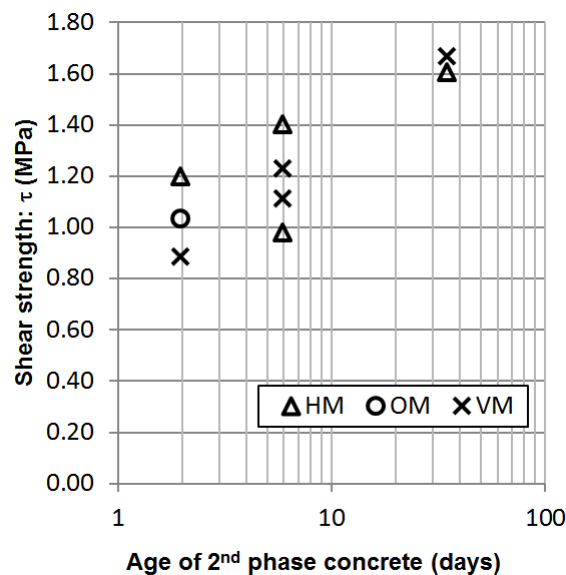
Fig. 50 - Direction of stress with regard to milling (MP case).

According to these results, there appears to be no connection between the milling direction and the direction in which the stress is applied, in terms of the strength of the specimen.

Examining the test specimens, it can be observed that the failure plane to a great extent follows the bond plane and the original milling marks are still visible in many of the specimens (**Fig. 51**).

Fig. 51 - Milling marks on tested cores.

Among the factors affecting bonding, the milling direction can mainly be associated with aggregate interlock. It is believed that, in the same way as the friction mechanism, this mechanism only contributes relevant strength where normal compression on the bond plane is able to mobilize it.

5.3.2.6. Shear angle

The first phase of concrete is cast on the ground, and the second phase, is sprayed. It is therefore extremely difficult if not impossible for the surfaces of both concrete phases to be plain and parallel to each other. This makes it impossible to extract a core with an axis that is perpendicular to the bond plane between the two concretes, which is in all cases the plane of failure.

It was investigated whether the failure angle has any influence on the results obtained. To that end, the average angle of the failure plane in the load application direction was measured ("α_m" in **Fig. 52**). For its calculation, the longitudinal difference between the upper and the lower points of the core (marked as "t" in **Fig. 52**) was measured. Then α_m was calculated by means of the following trigonometric expression:

$$\alpha_m = \text{arctg}(t/\phi_m)$$ (10)

where, ϕ_m is the average diameter of the contact surface, in mm, and t is the longitudinal difference previously described, also in mm.

Fig. 53 shows the graph for the shear strength value in relation to the failure angle of the core in the MP series. In these results, there is a noticeable tendency which fits in with the expected model, based on the concept of the bonding envelope (Simon Austin et al., 1999). The strength increased slightly for decreasing values of α_m.

Positive angles combine shear with tension, decreasing the value of the strength needed to reach failure stress. Negative angles combine shear with compression, increasing the value of that strength. In any case, the influence of the age of the second-phase concrete is greater than that of the angle of the failure plane.
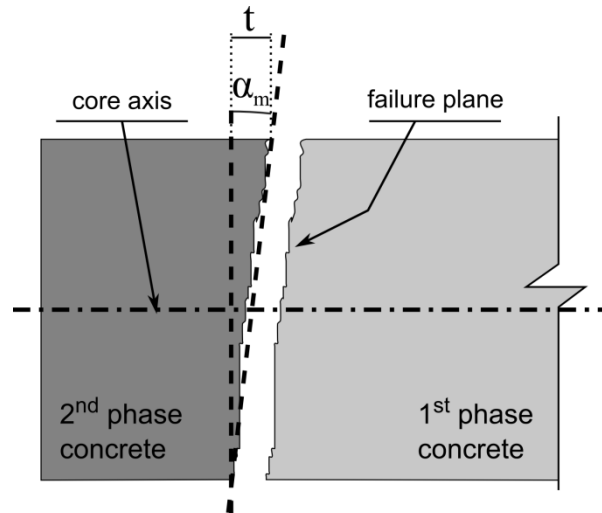
Fig. 52 - Failure plane angle.

In the future, with more experimental data, if this tendency is confirmed, a function could be determined that adjusts the values that are obtained with failure angles other than zero. In this way, validated test results could be used to evaluate extracted cores with irregular bond planes.
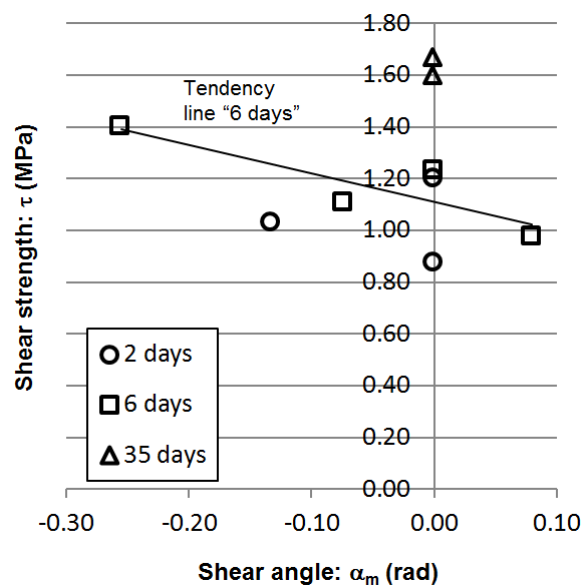
Fig. 53 - Influence of failure angle on shear strength.

5.3.2.7. Relationship between concrete shear strength and compressive strength

Fig. 54 shows the compressive strength of both concretes (first and second phase) depending on the shear strength in the MP series. First-phase concrete maintains almost constant values for compressive strength but, in accordance with the results obtained by (Júlio et al., 2006), there is an increase in bond strength as the second-phase concrete gains strength.

According to Eurocode 2 (EN, 2004b), the shear strength of bonds between concretes cast at different ages with no reinforcement is given by the following formula:

$$v_{Rdi} = cf_{ctd} + \mu\sigma_n$$

(11)

where, c and μ are factors which depend on the roughness of the substrate surface; f_{ctd} is the tensile strength of the concrete of lower strength; and σ_n is the stress caused by the lower normal strength through the surface that can act simultaneously with shear stress. As can be seen, only the concrete with the lowest strength is considered for the assessment of the shear strength.
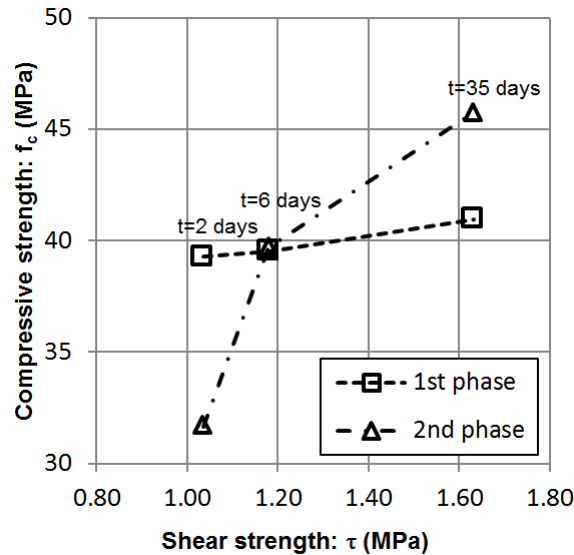
Fig. 54 - Influence of the strength of base concrete on shear strength (MP case).

According to the results obtained, for t = 6 days and t = 35 days the concrete with a lower strength (first phase) remained almost unchanged; however, the higher strength concrete (second phase) showed a considerable increase in strength, and at the same time the bond shear strength increased.

Additional research is necessary, but the experimental data and results suggest, as advanced by Júlio, that the formula to assess shear strength may be improved by incorporating higher concrete strengths.

5.4. CONCLUSIONS

This experimental study has studied bi-layer diaphragm concrete walls and, more particularly, the bond between the second phase of sprayed concrete placed over a first phase of surface-milled concrete. The following conclusions have been drawn:

- The test proposed for determining shear strength between concretes poured in different phases yielded valid results. With milled surfaces the coefficient of variation (CV) was lower than 15%;

- Shear strength on the milled surface increased with the age and the strength of the second-phase concrete, in line with the maturity formulas;

- Shear strength, when assessed with this test, was not dependent on the direction of the milling on the bond surface;

- Bonding capacity after spraying decreased on the surfaces that had previously been saturated with water;

- Finally, the results for *in situ* preparation of the surface with epoxy showed great variation, with a CV of up to 57% in the worst case.

In view of these results, it is not advisable to use epoxy products on bi-layer walls or large surfaces in general, unless the application and execution times of the bonding agent and the concrete spraying are rigorously controlled.

Improvements to the applied test have been proposed, so that it may potentially become a valid test for samples produced in the laboratory and for cores extracted on site. Future research work will focus on a) variations in the angle of the failure plane; and b) the production of notches in the cores and the way these may influence bond strength.

5.5. ACKNOWLEDGMENTS

CHAPTER 6.   CONCLUSIONS AND FUTURE PERSPECTIVES

6.1. INTRODUCTION

Underground space use is becoming vital to the developing of modern cities. The diaphragm wall technique (which causes a limited influence on existing infrastructure and also reduced interruptions to the daily life of the city during construction) is a viable solution to the construction of underground structures in a city scenario. A common problem associated with diaphragm walls is that they are frequently not fully watertight.

The aim of the research was to develop an innovative type of slurry wall: the bi-layer diaphragm wall, which will offer a new solution to the waterproof problem in diaphragm walls. The bi-layer walls are made of two bonded concrete layers, the first is a conventional reinforced concrete diaphragm wall, and the second is made spraying steel fibre reinforced concrete with a waterproof additive over the first layer.

A full scale experiment, where two bi-layer walls of different cross-sections were constructed, was performed and studied, followed by theoretical analysis to corroborate the advantages provided by the solution. The study was centred in three key aspects of this type of walls: the structural behaviour of the wall, the structural advantages provided by the collaboration of the steel fibre reinforced concrete (SFRC) layer,

and the bond between layers. General conclusion of the research is presented in the following section. Subsequently, specific conclusions in response to the different objectives are presented. Finally, general lines for future work needed in order to complete de development of the bi-layer diaphragm walls are introduced.

6.2. GENERAL CONCLUSIONS

In general terms it can be said that the research performed laid the foundation for the development of the bi-layer diaphragm wall technique, which is a promising solution for the leakage problem of diaphragm walls. The advantage of the method resides in the efficient use of the materials of a diaphragm wall that needs to be waterproof. A double function, structural and waterproofing, is assigned to the second layer, which, therefore, is able to collaborate with the overall structural response.

In this thesis, a complete flexural design method, based on an uncoupled structural-section analysis, was established (chapter 3). Furthermore, the structural model, based on a FEM model, was contrasted with the experimental walls (chapter 2). Various theoretical cases where analysed through this method to quantify the efficiency of the proposed solution.

For the geometrical ranges of the elements considered in the thesis (first layer between 55 cm and 60 cm, and second layer of 10 cm) the increase in the cross-section ultimate bending resistance when it is strengthened by the SFRC layer (i.e. when it changes from the simple cross-section (SS) to the compound cross-section (CS)) is between 8% and 15%. It follows that the main flexural resistance is provided by the first layer (the RC diaphragm wall), giving the SFRC layer a secondary flexural resistance.

This allows, in the first place, a reduction in the steel reinforcement of the first layer (up to 7.0% of the total flexural reinforcement, for the cases of chapter 4). Furthermore, in some extend, it also collaborates with a displacements reduction (reducing up to 7.3% of the maximum displacements in a 20 m high wall constructed with the Top-Down construction method. Case BL/55-10/TD/2u/2S/A of chapter 4).. It was also found that the spraying sequence is a crucial parameter to be able to take advantage of the SFRC collaboration. Specific indications are described in the following section.

The bonding capacity between layers, which is crucial for the development of the technique, was also analysed. A good bond level was obtained in a laboratory shear test over the cores extracted from the full scale experimental walls. The average shear strength value measured for each age, although depending on the surface preparation, was always above 1.0 MPa. The measures were obtained at 2, 6 and 35 days after the spraying of the SFRC layer for every preparation. This is a time lapse in the order of the needed for the wall construction.

Although the bonding strength depends on the test chosen to measure it, the magnitude obtained with the one used in this thesis is, according to preliminary estimations, an order of magnitude bigger than the shear stresses between layers that may be produced by the external forces. On the other hand, it is necessary a deeper study regarding shrinkage and creep in the second layer, which may lead to the need of improving the bonding to avoid the possibility of debonding of the second layer. Besides the shear test carried out, a monolithic behaviour was observed at global level in the experimental walls.

The material consumption (concrete and reinforcement steel) of two bi-layer diaphragm walls was also compared with an equivalent mono-layer diaphragm wall combined with an added waterproof system. It was found that the material used in both solutions was similar, in the best case, or larger in the bi-layer diaphragm walls (see chapter 3). Considering in addition that the technology to build it is more expensive (i.e. SFRC instead of RC and sprayed concrete instead of sprayed mortar), it follows that the construction costs should be higher in the bi-layer diaphragm wall technique.

However, it is an interesting option under particular circumstances, like space limitations or if continuous maintenance costs (due to drains and pump) should be avoided in future. It is also worth mentioning that the solution would be more effective if used on large construction sites, where the switch between excavation, temporary support, and spraying tasks is not a significant problem. A more detailed cost study and sustainability analysis should be performed to precisely quantify and compare the advantages of the solution.

In the authors' opinion, one drawback for the implementation of the technique is that it combines different relatively new structural technologies (sprayed concrete, SFRC, waterproof concrete) and methods of design (diaphragm wall design through FEM). Each one of them is somehow difficult to introduce as a standard technique. It is natural to think that, when the different techniques are combined, the difficulties increase accordingly. However, it can also be a competitive advantage for those companies having the know-how of this solution (theoretical analysis and construction).

6.3. SPECIFIC CONCLUSIONS

Seven objectives were established in the introductory chapter of this thesis to address the main aim of the project. Specific conclusions related to those objectives are established in this section. For each objective, the key contributions are highlighted. The dots are mainly textually extracted from the partial conclusions of the thesis main body chapters. The specific conclusions summarized in this section provide a general overview of the contributions in the different subjects.

6.3.1. Viability of the proposed solution.

- The construction of the experimental walls showed that the bi-layer diaphragm walls are viable with the present state of the construction technology.

- Besides the correct structural and bonding behaviour, more experiences are needed to corroborate the waterproofness and sectional response of the walls.

6.3.2. Bond strength reached between the concrete layers.

- A test was proposed for determining shear strength between concretes poured in different layers. The adopted test allows the testing of extracted cores, being therefore suitable to be used on real structures. It yields valid results, with a coefficient of variation lower than 15%.

- Shear strength in the milled surface increases with the age of second-layer concrete, fitting to the maturation formulas.

- Shear strength, assessed with the proposed test, is independent of the direction in which the milling of the bond surface is carried out.

- As expected, the saturation with water of the surface at the time of spraying the second phase diminishes the bonding capacity of the link.

- The *in situ* preparation of the surface with epoxy shows a wider dispersion of results (compared with the milled surface), with a coefficient of variation of up to 57% in the worst of cases. This behaviour may be attributed to the inherent difficulties in the application of the epoxy bonding agent.

- The pull-off test showed a wide range of results which arose from the experimental errors caused due the difficulties to perform the test on the irregular surfaces of both layers.

6.3.3. Structural behaviour of the bi-layer diaphragm walls.

- The experimental results of readings from inclinometers embedded in the walls were reproduced with a FEM numerical model running on the PLAXIS program. A comparison of the results from the calibrated model and from the experimental campaign demonstrated a very good correlation, which validated the model.

- The FEM model considered cross-sectional changes in the stages after spraying the second layer and reproduced both the qualitative and the quantitative displacements of the instrumented walls with a high degree of accuracy.

- The structural behaviour of bi-layer walls and mono-layer walls with the same first layer (SS) thickness is similar in relation to their total envelope of bending moments and deformations. This is because the increase in bending moments in the sprayed sections (CS) caused by the subsequent excavations are small compared with the change in moments that took place in the section not yet excavated (SS). Therefore, the first layer (SS) governs the general behaviour of the walls.

- The envelope of moments of the simple cross-section (i.e. the moment that have to be resisted by the SS cross-section) are smaller in the bi-layer than in the mono-layer alternatives (17% in the cases shown in chapter 2: 10 m high walls on heterogeneous soil with RC layer thickness of between 35 cm and 45 cm; and more than 20% in chapter 3: 20 m high walls on sandy soil with RC layer thickness of between 55 cm and 60 cm).

6.3.4. Overall flexural design model (structural and sectional level).

- A complete flexural design method was presented.

- The method is based on a FEM structural model developed with PLAXIS (a commercial geotechnical oriented FEM software) and the AES sectional model (a numerical model for the analysis, design and checking of composite sections developed in UPC).

- The complete reinforcement (bars of the first layer and fibres in the SFRC layer) can be designed and checked using this method.

- The smallest moments in the simple section and the collaboration of the SFRC layer afford a reinforcement reduction (2.1% and 2.5% in the chapter 3 cases, and up to 7%, if an adequate spraying sequence is used, in the chapter 4 cases. In both chapters 20 m high walls on sandy soil with RC layer thickness of between 55 cm and 60 cm were used).

6.3.5. Influence of the different constructions processes related to this type of walls.

- It is feasible for all final structural configurations and construction sequences to achieve a reinforcement steel reduction of the first layer by taking full advantage of the strength added by the SFRC layer.

- Using the adequate spraying sequence a first layer reinforcement reduction larger than 10 kg/m can be obtained in every configuration and sequence, reaching a reduction up to 21.7 kg/m in the best case. This represents a percentage reduction of 7.0% of the total bending reinforcements.

- The spraying sequence is a relevant parameter in the design of the bi-layer walls. In cases where moments do not increase after the excavation process is completed the spraying should be performed during the excavation. Otherwise, spraying must be done after finishing the excavation process. In every case, the sooner the spraying is performed, the larger the bending moments developed.

- It is confirmed that the displacements are governed by the thickness of the first layer, being practically identical for each combination of final structure configuration and construction sequence.

- A minor reduction in displacement is registered when the second layer is included. The maximum reduction obtained (0.6 mm) represented a percentage reduction of 7.3%. As it was said in section 6.3.3, the majority of the deflections (caused by the increase in the bending moments) have already taken place when the excavated sections are sprayed.

6.3.6. Efficiency of the bi-layer walls compared with equivalent conventional diaphragm wall alternatives.

- A comparison of different complete systems to deal with leakages (i.e. conventional diaphragm wall plus an independent waterproofing method) confirmed that the bi-layer walls are efficient only if waterproofness is needed. This is, a conventional diaphragm wall alone (without waterproofing) is always more economical than an equivalent bi-layer alternative.

- The comparison of the material consumption (concrete and reinforcement steel) of chapter 3 showed that the bi-layer system does not reduce the total use of materials of the complete waterproof systems, reaching, in the best cases, similar consumption of materials.

- Therefore, the final cost is probably still higher for the bi-layer system, as the material and labour costs per cubic meter of sprayed SFRC are higher than the cost of RC of the conventional diaphragm walls.

6.3.7. Dissemination of the results.

- Two papers were published, one accepted for publication, and one is under the second review in international journals (JCR JOURNALS – Q1) (each of them corresponding to each of the chapters of the thesis main body). With the followed strategy, feedback was obtained from the reviewers in the publishing process regarding the more advanced parts of the work, at the same time as the rest of the thesis work was being completed.

- One paper was published in a South-American international conference. It followed the strategy of making both the research and the PhD candidate known in the region where he intends to develop his career as university professor.

6.4. FUTURE PERSPECTIVES

Further research is necessary to complete the advances of the bi-layer diaphragm walls made in this thesis. This section is organized in two sub-sections. Firstly, crucial research lines are presented. These lines, in the author's opinion, are still needed to establish this type of solution as a regular option at the moment of choosing a waterproof diaphragm wall. Secondly, other possible research lines which would lead to an improvement of the technique are also highlighted.

6.4.1. Crucial research lines

First of all, more experimental results would be necessary to have more and better data to contrast models. Both structural and sectional measures would be needed to contrast the FEM and AES models respectively.

Particularly, it would be quite useful to test the bi-layer diaphragm wall up to failure, in order to analyze the possible failure modes and the limit states that the compound cross-section can reach.

Secondly, the differential time-dependent strains (creep and shrinkage) between both layers was left out of the model developed in this thesis (chapter 3). Although reasons were established to suppose that these effects would have a limited influence in the walls behaviour, this is a strong assumption that should be checked. Excessive shrinkage may lead to early debonding risk or to crack development that would be harmful for the waterproofness. In this sense, it would be necessary to evaluate the theoretical bond strength required for the correct behaviour of the walls, and compare it with the measured bond strength.

Additionally, although there are additives to make the concrete waterproof, a real measure of it would be needed for this application. It should be checked that a sufficient level of waterproofness can be achieved by the SFRC layer with the cracking levels expected after the differential time-dependent strains developed and the external forces were applied on the wall.

Finally, as it was seen, the analysis of final materials use revealed a similar material consumption for the different waterproof systems. It is interesting to perform a complete sustainability analysis (economic, social and environmental) to obtain a precise evaluation of the complete cost that allows a comparison of the different waterproofing systems.

6.4.2. Other research lines

It would be interesting to extend the parametric analysis to other relevant variables. For example, all along the thesis, a thickness of 10 cm was considered for the SFRC layer. It may be interesting to evaluate the viability of using other thickness or even a variable thickness for different heights of the wall.

Also, some aspects that are currently being investigated in diaphragm walls may also be investigated in the bi-layer diaphragm walls. For example, the 3D structural behaviour, which may be influenced in the bi-layer case by the horizontal connection provided by the SFRC layer. Or, the way of linking the walls with other structural elements (like base slabs) to avoid leakages in the connections.

REFERENCES

Abu-Tair, A., Rigden, S., & Burley, E. (1996). Testing the bond between repair materials and concrete substrate. *ACI Materials Journal*, *93*(6), 553–558. Retrieved from http://www.concrete.org/PUBS/JOURNALS/OLJDetails.asp?Home=MJ&ID=9861

ACI Committee 116. (2000). ACI 116R-00 Cement and Concrete Terminology, 1–73.

ACI Committee 212. (2010). *ACI 212.3R-10 Report on Chemical Admixtures for Concrete* (Vol. 1).

ACI Committee 544. (2002). *ACI 544.1R-96 State-of-the-Art Report on Fiber Reinforced Concrete* (Vol. 96, p. 66). American Concrete Institute.

AFTES, W. G. N. 6. (1996). AFTES recommendations on fibre-reinforced sprayed concrete technology and practice. *Tunnelling and Underground Space Technology*, *11*(2), 205–214. doi:10.1016/S0886-7798(96)90088-7

Aguado, A., Blanco, A., de la FUENTE, A., & Pujadas, P. (2012). *Manual Sobre el Hormigón con Fibras (In Spanish)* (p. 224). CEMEX-UPC.

ASTM. (2009). D4541 - Standard Test Method for Pull-Off Strength of Coatings Using Portable Adhesion Testers.

Austin, S. (2002). *Sprayed concrete technology* (p. 300). Chapman & Hall.

Austin, Simon, & Robins, P. J. (1995). *Sprayed Concrete – Properties, Design and Application*. Whittles Publishing Services.

Austin, Simon, Robins, P., & Pan, Y. (1995). Tensile bond testing of concrete repairs. *Materials and Structures*, *28*(5), 249–259. Retrieved from http://link.springer.com/article/10.1007/BF02473259

Austin, Simon, Robins, P., & Pan, Y. (1999). Shear bond testing of concrete repairs. *Cement and concrete research*, *29*, 1067–1076. Retrieved from http://linkinghub.elsevier.com/retrieve/pii/S0008884699000885

Bentur, A., & Mindess, S. (2007). *Fibre Reinforced Cementitious Composites* (p. 625). Taylor & Francis Group.

Blanco, A., Pujadas, P., de la Fuente, A., Cavalaro, S., & Aguado, A. (2013). Application of constitutive models in European codes to RC–FRC. *Construction and Building Materials*, *40*, 246–259. doi:10.1016/j.conbuildmat.2012.09.096

Bobylev, N. (2006). Strategic environmental assessment of urban underground infrastructure development policies. *Tunnelling and Underground Space Technology*, *21*(3-4), 469. doi:10.1016/j.tust.2005.12.106

Bonaldo, E., Barros, J., & Lourenco, P. (2005). Bond characterization between concrete substrate and repairing SFRC using pull-off testing. *International Journal of Adhesion and Adhesives*, *25*(6), 463–474. doi:10.1016/j.ijadhadh.2005.01.002

Bose, S. K., & Som, N. N. (1998). Parametric study of a braced cut by finite element method. *Computers and Geotechnics*, *22*(2), 91–107. doi:10.1016/S0266-352X(97)00033-5

Brinkgreve, R. (2002). *PLAXIS 2D, Version 8. A.A. Balkema Publishers, Lisse, The Netherlands* (p. 18). A.A. Balkema Publishers, Lisse, The Netherlands.

Brown, A. J., & Bruggemann, D. A. (2002). Arminou Dam, Cyprus, and construction joints in diaphragm cut-off walls. *Géotechnique*, *52*(1), 3–13. doi:10.1680/geot.2002.52.1.3

Bryson, L. S., & Zapata-Medina, D. G. (2012). Method for Estimating System Stiffness for Excavation Support Walls. *Journal of Geotechnical and Geoenvironmental Engineering*, *138*(9), 1104–1115. doi:10.1061/(ASCE)GT.1943-5606.0000683.

BS 8102. (1990). *Code of practice for protection of below ground structures against water from the ground* (p. 40). British Standard Institution.

BS 8102. (2009). *Code of practice for protection of below ground structures against water from the ground*. British Standard Institution.

Calvello, M., & Finno, R. J. (2004). Selecting parameters to optimize in model calibration by inverse analysis. *Computers and Geotechnics*, *31*(5), 410–424. doi:10.1016/j.compgeo.2004.03.004

Carrubba, P., & Colonna, P. (2000). A comparison of numerical methods for multi-tied walls. *Computers and Geotechnics*, *27*, 117–140. Retrieved from http://www.sciencedirect.com/science/article/pii/S0266352X00000070

Celestino, T. B., & Ishida, A. (2009). ACTIVITIES OF THE ITA WORKING GROUP ON SPRAYED CONCRETE USE. In ECI Symposium Series (Ed.), *Shotcrete for Underground Support XI*. Retrieved from http://dc.engconfintl.org/shotcrete/

Chan, R. W. M., Ho, P. N. L., & Chan, E. P. W. (1999). *Report on Concrete Admixtures for Waterproofing Construction* (p. 41). Retrieved from http://www.archsd.gov.hk/media/11756/c315.pdf

Clough, G. W., & O'Rourke., T. D. (1990). Construction induced movements of insitu walls. In *Design and performance of earth retaining structures (GSP 25)* (pp. 439–470). ASCE.

CNR. (2006). *CNR-DT 204/2006: Guide for the Design and Construction of Fiber-Reinforced Concrete Structures*.

Costa, P. A., Borges, J. L., & Fernandes, M. M. (2007). Analysis of A Braced Excavation In Soft Soils Considering The Consolidation Effect. *Geotechnical and Geological Engineering*, *25*(6), 617–629. doi:10.1007/s10706-007-9134-7

CPH. (2008). *EHE-08: Instrucción del Hormigón Estructural (in Spanish).*

CYPE Ingenieros. (2011). Software for Architecture, Engineering & Construction. Retrieved from http://www.cype.es/

DBV. (2001). *Guide to Good Practice "Steel Fibre Concrete", German Society for Concrete and Construction Technology.* Berlin.

De la Fuente, A., Aguado de Cea, A., & Molins, C. (2008). Numerical model for the nonlinear analysis of precast and sequentially constructed sections (in Spanish). *Hormigón & Acero*, *57*(247), 69–87.

De la Fuente, A., Aguado de Cea, A., Molins, C., & Armengou, J. (2012). Numerical model for the analysis up to failure of precast concrete sections. *Computers & Structures*, *106-107*, 105–114. doi:10.1016/j.compstruc.2012.04.007

De la Fuente, A., Escariz, R. C., de Figueiredo, A. D., Molins, C., & Aguado de Cea, A. (2012). A new design method for steel fibre reinforced concrete pipes. *Construction and Building Materials*, *30*, 547–555. doi:10.1016/j.conbuildmat.2011.12.015

Delatte Jr., N. J., Wade, D. M., & Fowler, D. W. (2000). Laboratory and field testing of concrete bond development for expedited bonded concrete overlays. *Materials Journal*, *97*(3), 272–280. Retrieved from http://www.concrete.org/PUBS/JOURNALS/AbstractDetails.asp?ID=4622

Delatte, N. J., Williamson, M. S., & Fowler, D. W. (2000). Bond strength development with maturity of high-early-strength bonded concrete overlays. *ACI Materials Journal*, *97*(2), 201–207. Retrieved from http://www.concrete.org/PUBS/JOURNALS/OLJDetails.asp?Home=MJ&ID=824

Delattre, L. (2001). A century of design methods for retaining walls – The French point of view, 33–52.

Di Prisco, M., Plizzari, G., & Vandewalle, L. (2009). Fibre reinforced concrete: new design perspectives. *Materials and Structures*, *42*(9), 1261–1281. doi:10.1617/s11527-009-9529-4

Duncan, J., & Chang, C. (1970). Nonlinear analysis of stress and strain in soils. *Journal of the Soil Mechanics and Foundations Division*, *96*(5), 1629–1653. Retrieved from http://cedb.asce.org/cgi/WWWdisplay.cgi?17188

Dunnicliff, J. (1993). *Geotechnical instrumentation for monitoring field performance.* New York: John Wiley & Sons.

Durmisevic, S. (1999). The future of the underground space. *Cities*, *16*(4), 233–245. doi:10.1016/S0264-2751(99)00022-0

El Hussieny, O. M. (1992). A study of different aspects of diaphragm walls. *Tunnelling and Underground Space Technology*, *7*(1), 55–58. doi:10.1016/0886-7798(92)90113-V

El-Razek, M. E. A. (1999). New method for construction of diaphragm walls. *Journal of Construction Engineering and Management*, *125*(4), 233–241. Retrieved from http://ascelibrary.org/doi/pdf/10.1061/(ASCE)0733-9364(1999)125%3A4(233)

EN. (2004a). *Eurocode 7: Geotechnical design — Part 1: General rules*. European Committee for Standardization.

EN. (2004b). *Eurocode 2: Design of Concrete Structures - Part 1-1: General Rules and Rules for Buildings*. European Committee for Standardization.

EN 1538. (2010). Execution of special geotechnical work - Diaphragm walls. European Committee for Standardization (CEN).

Fang, H.-Y. (1995). *Foundation Engineering Handbook* (p. 942). Chapman & Hall.

FIB. (2010). *Fédération Internationale du Béton. Model Code 2010 – first complete draft, vol. 1. Bulletin 55. Lausanne (Switzerland)*.

Foye, K. C., & Jaoude, G. A. (2004). *Limit States Design of Deep Foundations. … on Design and Construction of Deep Foundations, …* (p. 245). doi:10.5703/1288284313262.This

Franzén, T. (1992). Shotcrete for underground support: a state-of-the-art report with focus on steel-fibre reinforcement. *Tunnelling and Underground Space Technology*, *7*(4), 383–391. doi:10.1016/0886-7798(92)90068-S

Gaba, A., Simpson, B., Powrie, W., & Beadman, D. (2003). *CIRIA C580 - Embedded retaining walls: guidance for economic design. Proceedings of the Institution of Civil Engineers-Geotechnical engineering* (Vol. 156, p. 390). London: CIRIA. Retrieved from http://cat.inist.fr/?aModele=afficheN&cpsidt=17373224

Gallovich Sarzalejo, A., Rossi, B., Perri, G., Winterberg, R., & Perri Aristeguieta, R. E. (2005). *Fibras como elemento estructural para el refuerzo del hormigón - Manual Técnico. (In Spanish)* (p. 251). Maccaferri do Brasil Ltd.

Galobardes, I. (2013). *Characterization and control of wet-mix sprayed concrete with accelerators, Doctoral thesis*. Univesidad Politécnica de Catalunya.

García Vicente, T., Agulló Fité, L., Aguado de Cea, A., & Rodríguez Barboza, J. U. (2001). Propuesta metodológica para dosificación del hormigón proyectado. *HORMIGÓN Y ACERO*, *220*, 43–56. Retrieved from http://dialnet.unirioja.es/servlet/articulo?codigo=292793

Goodier, C. I. (2000). *Wet-Process Sprayed Mortar and Concrete for Repair. Doctoral dissertation*. Loughborough University.

Hashash, Y. M. A., Levasseur, S., Osouli, A., Finno, R., & Malecot, Y. (2010). Comparison of two inverse analysis techniques for learning deep excavation response. *Computers and Geotechnics*, *37*(3), 323–333. doi:10.1016/j.compgeo.2009.11.005

Hoseini, M., Bindiganavile, V., & Banthia, N. (2009). The effect of mechanical stress on permeability of concrete: A review. *Cement and Concrete Composites*, *31*(4), 213–220. doi:10.1016/j.cemconcomp.2009.02.003

Hsiung, B.-C. B. (2009). A case study on the behaviour of a deep excavation in sand. *Computers and Geotechnics*, *36*(4), 665–675. doi:10.1016/j.compgeo.2008.10.003

ICE. (2007). *Specification for Piling and Embedded Retaining Walls, 2nd edition* (p. 242). Thomas Telford Ltd. doi:10.1680/sfpaerw.33580

ITA, W. G. (1993). Shotcrete for rock support: a summary report on the state of the art in 15 countries. *Tunnelling and Underground Space Technology*, *8*(4), 441–470. doi:10.1016/0886-7798(93)90006-H

Júlio, E., Branco, F., & Silva, V. D. (2004). Concrete-to-concrete bond strength. Influence of the roughness of the substrate surface. *Construction and Building Materials*, *18*(9), 675–681. doi:10.1016/j.conbuildmat.2004.04.023

Júlio, E., Branco, F., & Silva, V. D. (2005). Concrete-to-concrete bond strength: influence of an epoxy-based bonding agent on a roughened substrate surface. *Magazine of Concrete Research*, *57*(8), 463–468. Retrieved from http://www.icevirtuallibrary.com/content/article/10.1680/macr.2005.57.8.463?crawler=true

Júlio, E., Branco, F., Silva, V. D., & Lourenco, J. (2006). Influence of added concrete compressive strength on adhesion to an existing concrete substrate. *Building and Environment*, *41*(12), 1934–1939. doi:10.1016/j.buildenv.2005.06.023

Khoiri, M., & Ou, C.-Y. (2013). Evaluation of deformation parameter for deep excavation in sand through case histories. *Computers and Geotechnics*, *47*, 57–67. doi:10.1016/j.compgeo.2012.06.009

Kung, G. T. C., Juang, C. H., Hsiao, E. C. L., & Hashash, Y. M. A. (2007). Simplified Model for Wall Deflection and Ground-Surface Settlement Caused by Braced Excavation in Clays. *Journal of Geotechnical and Geoenvironmental Engineering*, *133*(6), 731–747. doi:10.1061/(ASCE)1090-0241(2007)133:6(731)

Kung, G. T.-C. (2009). Comparison of excavation-induced wall deflection using top-down and bottom-up construction methods in Taipei silty clay. *Computers and Geotechnics*, *36*(3), 373–385. doi:10.1016/j.compgeo.2008.07.001

Kurk, F., & Eagan, P. (2008). The value of adding design-for-the-environment to pollution prevention assistance options. *Journal of Cleaner Production*, *16*(6), 722–726. doi:10.1016/j.jclepro.2007.02.022

Li, K., Ju, Y., Han, J., & Zhou, C. (2008). Early-age stress analysis of a concrete diaphragm wall through tensile creep modeling. *Materials and Structures*, *42*(7), 923–935. doi:10.1617/s11527-008-9432-4

Lim, A., Ou, C.-Y., & Hsieh, P.-G. (2010). Evaluation of clay constitutive models for analysis of deep excavation under undrained conditions. *Journal of GeoEngineering*, *5*(1), 9–20. Retrieved from http://yo-1.ct.ntust.edu.tw/jge/files/articlefiles/v5i120100525218817485.pdf

Long, M. (2001). Database for retaining wall and ground movements due to deep excavations. *Journal of Geotechnical and Geoenvironmental Engineering*, *127*(3), 203–224.

Malmgren, L. (2007). Strength, ductility and stiffness of fibre-reinforced shotcrete. *Magazine of Concrete Research*, *59*(4), 287–296. doi:10.1680/macr.2007.59.4.287

Martinola, G., Meda, A., Plizzari, G. a., & Rinaldi, Z. (2010). Strengthening and repair of RC beams with fiber reinforced concrete. *Cement and Concrete Composites*, *32*(9), 731–739. doi:10.1016/j.cemconcomp.2010.07.001

Meyerhof, G. G. (1994). Evolution of safety factors and geotechnical limit state design. *Texas USA*. Texas A&M University. Retrieved from https://ceprofs.civil.tamu.edu/briaud/buchanan web/Lectures/Second Buchanan Lecture.pdf

Miró Recasens, R., Martínez, A., & Pérez Jiménez, F. (2005). Assessing heat-adhesive emulsions for tack coats. *Proceedings of the Institution of Civil Engineers Transport*, *158*(1), 45–51. doi:10.1680/tran.158.1.45.57833

Mirsayah, A. A., & Banthia, N. (2002). Shear strength of steel fiber-reinforced concrete. *ACI Materials Journal*, *99*(5), 473–479. Retrieved from http://www.concrete.org/PUBS/JOURNALS/OLJDetails.asp?Home=MJ&ID=12326

Momayez, A., Ehsani, M., Ramezanianpour, A. A., & Rajaie, H. (2005). Comparison of methods for evaluating bond strength between concrete substrate and repair materials. *Cement and Concrete Research*, *35*(4), 748–757. doi:10.1016/j.cemconres.2004.05.027

Moormann, C. (2004). Analysis of wall and ground movements due to deep excavations in soft soil based on a new worldwide database. *Soils and foundations*, *44*(1), 87–98.

Neville, A. M., & Brooks, J. J. (2010). *CONCRETE TECHNOLOGY* (p. 442). Prentice Hall.

Newman, J., & Choo, B. S. (2003). *Advanced Concrete Technology - Processes* (p. 699). Elsevier Ltd.

NLT-382/08. (2008). Evaluación de la adherencia entre capas de firme, mediante ensayo de corte. *CEDEX, Madrid*.

Ou, C.-Y. (2006). *Deep excavation: theory and practice* (p. 532). London: Taylor & Francis Group.

Ou, C.-Y., Chiou, D.-C., & Wu, T.-S. (1996). Three-dimensional finite element analysis of deep excavations. *Journal of Geotechnical Engineering*, *122*(5), 337–345.

Ou, C.-Y., & Hsieh, P.-G. (2011). A simplified method for predicting ground settlement profiles induced by excavation in soft clay. *Computers and Geotechnics*, *38*(8), 987–997. doi:10.1016/j.compgeo.2011.06.008

Ou, C.-Y., & Lai, C. (1994). Finite-element analysis of deep excavation in layered sandy and clayey soil deposits. *Canadian geotechnical journal*, *31*, 204–214. Retrieved from http://www.nrcresearchpress.com/doi/abs/10.1139/t94-026

Ou, C.-Y., & Lee, K. H. (1987). Watertightness of the diaphram wall at vertical joints. In *Proceedings of the Eighth Asian Regional Conference on Soil Mechanics and Foundation Engineering* (pp. 309–312). Kyoto, Japan.

PLAXIS 2D. (2010a). Reference Manual. Retrieved from http://www.plaxis.nl/files/files/2D2010-2-Reference_02.pdf

PLAXIS 2D. (2010b). Tutorial Manual. Retrieved December 01, 2011, from http://www.plaxis.nl/files/files/2D2010-2-Reference_02.pdf

Potts, D. M., & Zdravković, L. (1999). *Finite Element Analysis in Geotechnical Engineering: Theory*. London: Telford.

Puller, M. (1994). The waterproofness of structural diaphragm walls. *Proceedings of the ICE - Geotechnical Engineering*, *107*(1), 47–57. doi:10.1680/igeng.1994.25720

Ramachandran, V. S. (1995). *Concrete Admixtures Handbook - Properties, Science, and Technology (2nd edition)* (p. 1180). Noyes Publications.

Ray, I., Davalos, J., & Luo, S. (2005). Interface evaluations of overlay-concrete bi-layer composites by a direct shear test method. *Cement and Concrete Composites*, *27*(3), 339–347. doi:10.1016/j.cemconcomp.2004.02.048

RILEM TC 162-TDF. (2003). σ-ε-Design Method. *Materials and Structures*, *36*(8), 560–567. doi:http://dx.doi.org/10.1007/BF02480834 PB

Rodriguez Liñan, C. (1995). *Pantallas para excavaciones profundas. Construcción y Cálculo* (p. 160). Sevilla: Escuela Técnica Superior de Arquitectura de Sevilla.

Rönkä, K., Ritola, J., & Rauhala, K. (1998). Underground space in land-use planning. *Tunnelling and Underground Space Technology*, *13*(1), 39–49. doi:10.1016/S0886-7798(98)00029-7

Roscoe, K. H., & Burland, J. B. (1968). On the generalized stress-strain behaviour of wet clay. In *Engineering plasticity* (pp. 535–609). Cambridge: Heyman and Leckie.

Sanhueza Plaza, C. X., & Oteo, C. (2007). Estudio Comparativo sobre Diferentes Modelos de Cálculo Aplicados a la Construcción de Muros Pantalla. *Revista de la Construcción*, *6*(1), 13–27.

Saucier, F., Bastien, J., Pigeon, M., & Fafard, M. (1991). A combined shear-compression device to measure concrete-to-concrete bonding. *Experimental Techniques*, *15*(5), 50–55. Retrieved from http://onlinelibrary.wiley.com/doi/10.1111/j.1747-1567.1991.tb01214.x/abstract

Schanz, T., Vermeer, P. A., & Bonnier, P. G. (1999). The hardening soil model: formulation and verification. In *Beyond 2000 in computational geotechnics —10 years of PLAXIS* (pp. 1–16). Rotterdam: Balkema.

Schneebeli, G. (1981). *Muros pantalla : técnicas de realización : métodos de cálculo*. Editores Técnicos Asociados.

Segura-Castillo, L., & Aguado, A. (2011). *2011NT06(V2) - Análisis final de la experiencia edificio Aprestadora. [in Spanish]* (p. 119). Barcelona.

Segura-Castillo, L., Aguado, A., de la Fuente, A., & Josa, A. (2013). Bi-layer diaphragm walls: Structural and sectional analysis. *Journal of Civil Engineering and Management (Accepted for publication).*

Segura-Castillo, L., Aguado, A., & Josa, A. (2013). Bi-layer diaphragm walls: Experimental and numerical structural analysis. *Engineering Structures*, *56*, 154–164. doi:10.1016/j.engstruct.2013.04.018

Segura-Castillo, L., & Aguado de Cea, A. (2012a). Bi-layer diaphragm walls: Evolution of concrete-to-concrete bond strength at early ages. *Construction and Building Materials*, *31*(1), 29–37. doi:10.1016/j.conbuildmat.2011.12.090

Segura-Castillo, L., & Aguado de Cea, A. (2012b). Bi-layer diaphragm walls: Early ages concrete-to-concrete bond strength assessed through shear and pull-off tests. [in spanish]. In *XXXV Jornadas Sudamericanas de Ingeniería Estructural*. Río de Janeiro: ASAEE.

Segura-Castillo, L., Josa, A., & Aguado, A. (n.d.). Bi-layer diaphragm walls: Parametric study of construction processes. *Engineering Structures (Submitted).*

Sherif, A. S., & Kudsi, T. N. (1975). Reliability of underground concrete structures under water ingress attack. In *Fourth International Symposium on Uncertainty Modeling and Analysis, 2003. ISUMA 2003.* (Vol. 52, pp. 40–44). IEEE. doi:10.1109/ISUMA.2003.1236138

Shohet, I. M., & Galil, I. (2005). Decision Support System for Waterproofing of Below-Grade Structures. *Computer-Aided Civil and Infrastructure Engineering*, *20*(3), 206–220. doi:10.1111/j.1467-8667.2005.00388.x

Talbot, C., Pigeon, M., Beaupré, D., & Morgan, D. (1994). Influence of surface preparation on long-term bonding of shotcrete. *ACI Materials Journal*, *91*(6), 560–566. Retrieved from http://www.concrete.org/PUBS/JOURNALS/AbstractDetails.asp?ID=1376

Terzaghi, K., Peck, R. B., & Mesri, G. (1996). *Soil mechanics in engineering practice* (p. 592). New York: John Wiley & Sons.

Tu, L., & Kruger, D. (1996). Engineering properties of epoxy resins used as concrete adhesives. *ACI Materials Journal*, *93*(1), 26–35. Retrieved from http://www.concrete.org/PUBS/JOURNALS/OLJDetails.asp?Home=MJ&ID=9793

UNE-EN 12390-3. (2003). *Ensayos de Hormigón Endurecido - Parte 3: Determinación de la resistencia a compresión de probetas.* Madrid: AENOR, Asociación Española de Normalización y Certificación. Retrieved from http://www.aenor.es/aenor/normas/normas/fichanorma.asp?tipo=N&codigo=N0043808&PDF =Si#.UkGkxtKno8o

UNE-EN 14488-1. (2006). *Ensayos de hormigón proyectado. Parte 1: Toma de muestras de hormigón fresco y endurecido.* Madrid: AENOR; Asociación Española de Normalización y Certificación. Retrieved from http://www.aenor.es/aenor/normas/normas/fichanorma.asp?tipo=N&codigo=N0035682&PDF =Si#.UkGkRdKno8o

Wall, J., & Shrive, N. (1988). Factors affecting bond between new and old concrete. *ACI Materials Journal*, *85*(2). Retrieved from http://www.concrete.org/PUBS/JOURNALS/OLJDetails.asp?Home=MJ&ID=2329

Wang, J. H., Xu, Z. H., & Wang, W. D. (2010). Wall and Ground Movements due to Deep Excavations in Shanghai Soft Soils. *Journal of Geotechnical and Geoenvironmental Engineering*, *136*(7), 985–994. doi:10.1061/(ASCE)GT.1943-5606.0000299

Whittle, A. J. (1987). *A constitutive model for overconsolidated clays with application to the cyclic loading of friction piles*. Massachusetts Institute of Technology.

Wong, I. (1997). Experience with waterproofness of basements constructed of concrete diaphragm walls in Singapore. *Tunnelling and Underground Space Technology*, *12*(4), 491–495. Retrieved from http://linkinghub.elsevier.com/retrieve/pii/S088677989800008X

Xanthakos, P. P. (1979). *Slurry walls* (p. 622). New York: McGraw-Hill.

Zollo, R. F. (1997). Fiber-reinforced concrete: an overview after 30 years of development. *Cement and Concrete Composites*, *19*(2), 107–122. Retrieved from http://linkinghub.elsevier.com/retrieve/pii/S0958946596000467

Se abre el telón: Un cubo de hormigón
¿Cómo se llama la obra?
-Atracción fatal-

APPENDIX 1. Early ages concrete-to-concrete bond strength assessed through shear and pull-off tests[5]

ABSTRACT: Leakage represents a widespread problem in diaphragm walls built under certain conditions, such as enclosures in water-bearing ground. An innovative structural element typology is proposed, referred to as a bi-layer diaphragm wall. Its two layers are poured and sprayed, respectively, in two phases; the first layer is a standard reinforced-concrete diaphragm wall, while the second consists of a layer of sprayed concrete with steel fibers, which performs a dual waterproofing and structural role. The bond between both concretes plays an important role in the performance of the structure. If bond strength is sufficiently high, the structure behaves monolithically. Through an experimental campaign, our research aims to study the evolution of bond strength between the two concretes at early ages (2, 6 and 35 days). Two preparation techniques were studied: milled surfaces and milled and epoxy-bonded surfaces. The bond strength was assessed through shear and pull-off tests. The results reveal that the shear strength of milled surfaces follows a typical maturity law. In contrast, a wide range of results is evident for in situ epoxy-bonded surface preparations. Pull-off tests show, in every case, a wide range of results.

Keywords: diaphragm wall, bi-layer, waterproof, bond, shear, pull-off, concrete, fibers.

---

[5] Segura-Castillo, L., & Aguado de Cea, A. (2012). Bi-layer diaphragm walls: Early ages concrete-to-concrete bond strength assessed through shear and pull-off tests. [in spanish]. In XXXV Jornadas Sudamericanas de Ingeniería Estructural. Río de Janeiro: ASAEE.

A1.1.   INTRODUCCIÓN

A1.1.1.   Impermeabilización en pantallas continuas

La aparición de filtraciones de agua es un problema habitual en las pantallas continuas realizadas en terrenos con un nivel freático elevado. Desde la aparición de esta técnica, la impermeabilidad de las pantallas continuas ha sido motivo de debate, dando lugar a la aparición de diversas técnicas para reparar las filtraciones cuando estas ocurren, o prevenir su aparición (Puller, 1994). En la **Fig. 55** se muestran algunos ejemplos típicos de defectos ocurridos en pantallas continuas.

Fig. 55 - Defectos usuales en pantallas continuas: a- Diferencias de posición entre bataches adyacentes, b-Pérdidas entre juntas durante construcción, c- Pérdidas que aparecen ya en servicio

Una técnica habitualmente utilizada en la construcción de pantallas continuas consiste en reparar las zonas defectuosas luego de que se detectan las pérdidas, repicando estas áreas y restituyéndolas con un mortero expansivo impermeable. Dado que las pérdidas suelen aparecer en diversas áreas de las pantallas, en tiempos distintos (incluso luego de finalizadas las obras), esta solución puede extenderse por períodos indefinidos y requerir varias sesiones de trabajo. Por ello, esta técnica es un gran inconveniente tanto para el propietario como para la constructora que se tiene que encargar de las reparaciones.

Otra solución consiste en realizar una capa de mortero (u hormigón) impermeable en todo el paramento interior de estos muros. Al revestirse la totalidad del paramento, esta se vuelve una solución efectiva pero costosa (Wong, 1997). Un ejemplo de esta solución fue utilizado por (Li et al., 2008) para estudiar el comportamiento de la fluencia a tracción del hormigón a edades tempranas.

En 1990 se publicó una norma "British Standard Code of Practice, BS 8102"(1990) que definió grados de estanqueidad. Luego de esta publicación, la práctica común en UK consistió en hacer una cavidad drenada (cámara bufa) con una bomba permanente en un sumidero en el nivel más bajo. Por lo tanto, el volumen con que se diseña las bases es reducido por el volumen de la cavidad de drenado, el volumen de los muros de revestimiento y el volumen de las tolerancias de construcción de los muros pantalla (El Hussieny, 1992). Todo ello conduce a una pérdida de espacio que puede tener una repercusión negativa con respecto a la función requerida del espacio.

A1.1.2.   Marco general del proyecto

Este trabajo forma parte de la tesis doctoral del primer autor que se está realizando en la Universidad Politécnica de Catalunya (UPC). El objetivo central planteado para esta tesis es el desarrollar (evaluando su

viabilidad, modelando numéricamente, contrastando experimentalmente, e indicando el modo de diseño) un elemento estructural nuevo de características innovadoras: el Muro Pantalla Bi-Capa.

Estos muros, presentan una sección compuesta por dos hormigones: a) hormigón realizado mediante el sistema de muro pantalla tradicional; y b) una segunda capa de hormigón proyectado con fibras e impermeabilizante; que suma a las características propias de los muros pantallas (contención del terreno y capacidad portante) la propiedad de ser impermeable de por sí. Un esquema de la solución se puede ver en la **Fig. 56**.
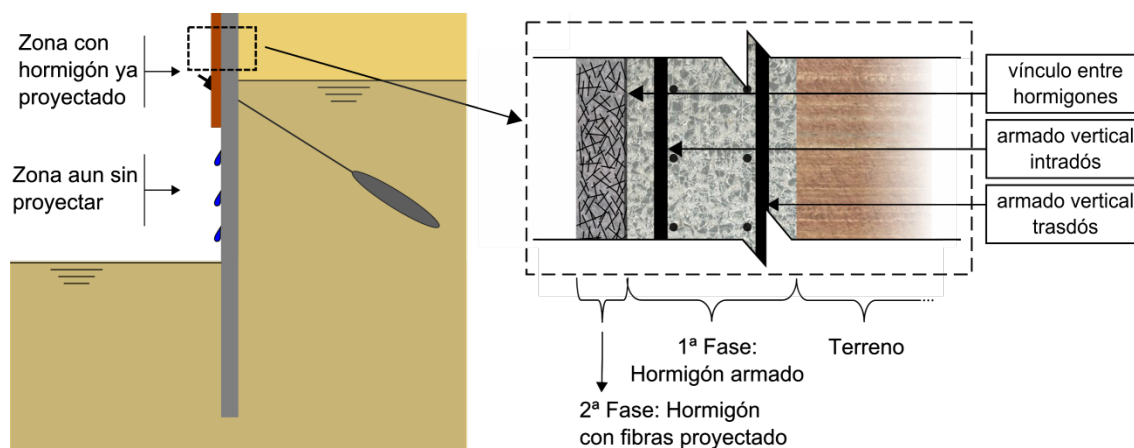

Fig. 56 - Esquema de la solución por muro Bi-Capa. Vista general y vista de una sección

La solución se basa en la idea ya descrita de realizar una 2ª capa en todo el interior del paramento. El elemento innovador consiste en que se espera maximizar la utilización de la segunda capa de hormigón, dándole un fin estructural, además de la finalidad original (impermeabilidad) con la que fue pensada. El aporte estructural de la segunda capa se brindará mediante la utilización de hormigón fibro reforzado (FRC) en su construcción. De este modo, se espera poder reducir el espesor de la primera capa, lo suficiente para volver viable la solución conjunta.

A1.1.3. Adherencia entre hormigones

El desempeño del vínculo entre ambos hormigones cumple un rol importante en el desempeño del conjunto estructural. Si se logra suficiente adherencia, la estructura reforzada se comporta monolíticamente, siendo los materiales efectivamente movilizados (Bonaldo et al., 2005).

Este comportamiento es necesario en el campo de la reparación y refuerzo de estructuras de hormigón, donde la práctica común consiste en, en primer lugar, incrementar la rugosidad de la capa base; en algunos casos, aplicar un puente de adherencia y/o conectores de acero; y posteriormente colocar la capa de refuerzo (Júlio et al., 2006). Ejemplos habituales de esta aplicación incluyen puentes construidos en varias etapas o técnicas de refuerzo de pavimentos (Delatte Jr. et al., 2000) o técnicas más complejas como la NSM (Near Surface Mounted) (Bonaldo et al., 2005).

Entre otros autores, (Talbot et al., 1994), en refuerzo con hormigón proyectado, y (Delatte et al., 2000) en refuerzo para puentes, estudiaron la durabilidad y maduración del vínculo con la edad.

Los valores obtenidos de la resistencia del vínculo dependen fuertemente del método de ensayo elegido (Momayez et al., 2005). Varios autores han realizado diferentes estudios que, por un lado, describen y clasifican los métodos y, por otro, relacionan los resultados por ellos obtenidos (Abu-Tair et al., 1996; Simon Austin et al., 1999; Júlio et al., 2004; Momayez et al., 2005)

El slant shear test (Wall & Shrive, 1988) se ha convertido en el ensayo más ampliamente aceptado, y ha sido adoptado por varias normas internacionales como ensayo para evaluar la adherencia de materiales de conglomerante orgánico (resinas) al hormigón base (Abu-Tair et al., 1996). Sin embargo, no hay acuerdo entre investigadores sobre la idoneidad en materiales de conglomerantes hidráulicos (base cemento) (Momayez et al., 2005).

Los métodos más difundidos para el ensayo a corte están diseñados para ensayar probetas elaboradas en laboratorio. Como ensayos apropiados para aplicar en testigos obtenidos en campo, podemos mencionar el ensayo LCB (Miró Recasens et al., 2005), y el ensayo a corte directo "guillotina" (Delatte et al., 2000). Como ensayo para realizar in-situ, se puede mencionar el ensayo pull-off (Simon Austin, Robins, & Pan, 1995). Mediante el mismo se es capaz de evaluar la adherencia de la unión sometida a esfuerzos de tracción. En particular, (Júlio et al., 2005) examinaron la correlación entre la adherencia a corte, medida con el ensayo a corte oblicuo, y la adherencia a tracción obtenida con el ensayo pull-off, registrando una correlación linear.

A1.2.   OBJETIVOS

Los objetivos buscados en la realización de este trabajo son dos:

- Estudiar la evolución a tempranas edades (2, 6, y 35 días) de la resistencia del vínculo alcanzada entre el hormigón proyectado sobre el hormigón base, previamente fresado, que conforman el muro Bi-Capa.

- Buscar un ensayo práctico para caracterizar la adherencia entre capas, factible de ser utilizado como control rutinario en la implementación de esta tipología de elementos.

Se analiza además, la influencia de las condiciones de contacto, para lo que se ha analizado también la alternativa de realizar el vínculo mediante una capa de imprimación con resina epoxi. Todo ello es estudiado experimentalmente en una actuación real en un edificio.

A1.3.   METODOLOGÍA

A1.3.1.   Programa experimental

La tipología de pantallas descrita fue utilizada en un edificio ubicado en Barcelona. Para el propósito de este artículo, se extrajeron testigos de las pantallas experimentales para la realización de ensayos de corte, y a su vez, se realizaron ensayos pull-off in-situ, como se describe a continuación.

En la **Fig. 57a** se presenta el plano de la planta de la obra. Las pantallas corresponden a todo el perímetro de la obra, habiéndose construidos por los métodos usuales. Por otro lado, en dicha figura se presentan las distintas zonas utilizadas para analizar las condiciones adherentes, con la siguiente nomenclatura: PF

(Superficie Fresada), PE (Superficie con epoxi). En la **Fig. 57b** se muestra un esquema de la vista lateral de los mismos.

La primera fase de las pantallas Bi-Capa está constituida por una pantalla convencional de hormigón armado con una resistencia a compresión a 28 días de f_c=30 MPa. Al finalizar la excavación se realizó el fresado de la pared expuesta con el objeto de, por un lado, regularizar y preparar la superficie y, por otro lado, mejorar la textura cara a favorecer la adherencia de la capa de hormigón proyectado. El fresado se realizó con una fresadora de hormigón colocada en la punta de una retroexcavadora.
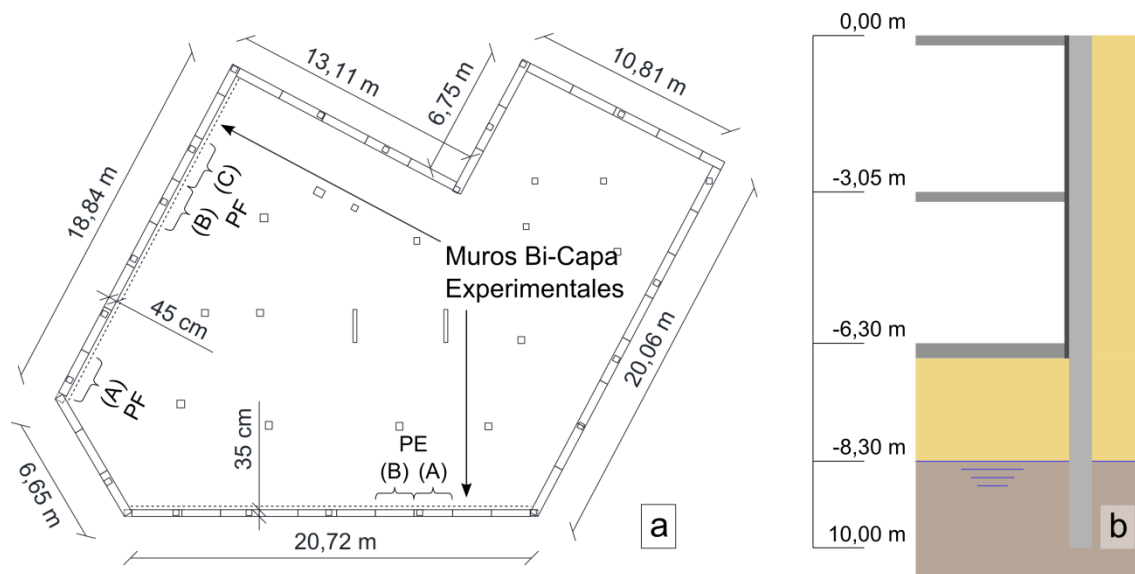

Fig. 57 - Detalle de las pantallas: a) Plano del sitio de obra; b) corte lateral

Con posterioridad al fresado, el día anterior a la colocación del hormigón proyectado de segunda etapa se realizó una limpieza con chorro de agua. Mediante esta limpieza, se elimina el polvo y partículas sueltas que se producen en el proceso de fresado. Además, este proceso satura los poros del hormigón base, pero, al ser realizado con la suficiente antelación, permite el secado superficial, obteniendo una superficie con poros saturados, pero seca superficialmente. Esta es considerada la mejor situación con respecto a la humedad superficial, si bien aún hay controversia y resultados contradictorios al respecto (Júlio et al., 2004). En las pantallas denominadas PF (Superficie Fresada), esta fue la última tarea de preparación de superficie que se realizó.

En las pantallas denominadas PE (Superficie con Epoxi) se colocó, antes de que se realizara el proyectado, el puente de adherencia. Se utilizó el adhesivo epoxi bi-componente de base acuosa para unión de hormigones: "Multitek Adhesivo SDH", dispuesto de acuerdo a las indicaciones del fabricante.

El hormigón de segunda fase fue proyectado por vía húmeda, completando el elemento estructural. La dosificación utilizada para este tipo de hormigón se diseñó buscando que hormigones de ambas fases tuviesen características mecánicas lo más similares posibles.

Los testigos para estudiar la adherencia entre capas se extrajeron del muro un día antes de la fecha prevista para su ensayo. De esta forma éstos tienen, durante el mayor tiempo posible, las mismas condiciones de curado que el resto del elemento. Ya que se planeó realizar ensayos a diferentes edades, la extracción

también se realizó en diferentes edades. Cuando el hormigón de segunda fase tenía 1 día, 5 días y 34 días de edad se realizaron extracciones de testigos en las zonas PF y PE. Para cada edad se extrajeron 5 testigos de cada una de las zonas.

Se cuenta con series parcialmente incompletas para ambos tipos de ensayos. La razón principal es que algunos testigos, tanto para el ensayo de corte como para el pull-off, y principalmente los extraídos en las edades más tempranas, se rompieron por el plano de unión en el momento de realizar la extracción, o la perforación parcial. Información complementaria sobre el programa experimental se puede obtener en (Segura-Castillo & Aguado de Cea, 2012a).
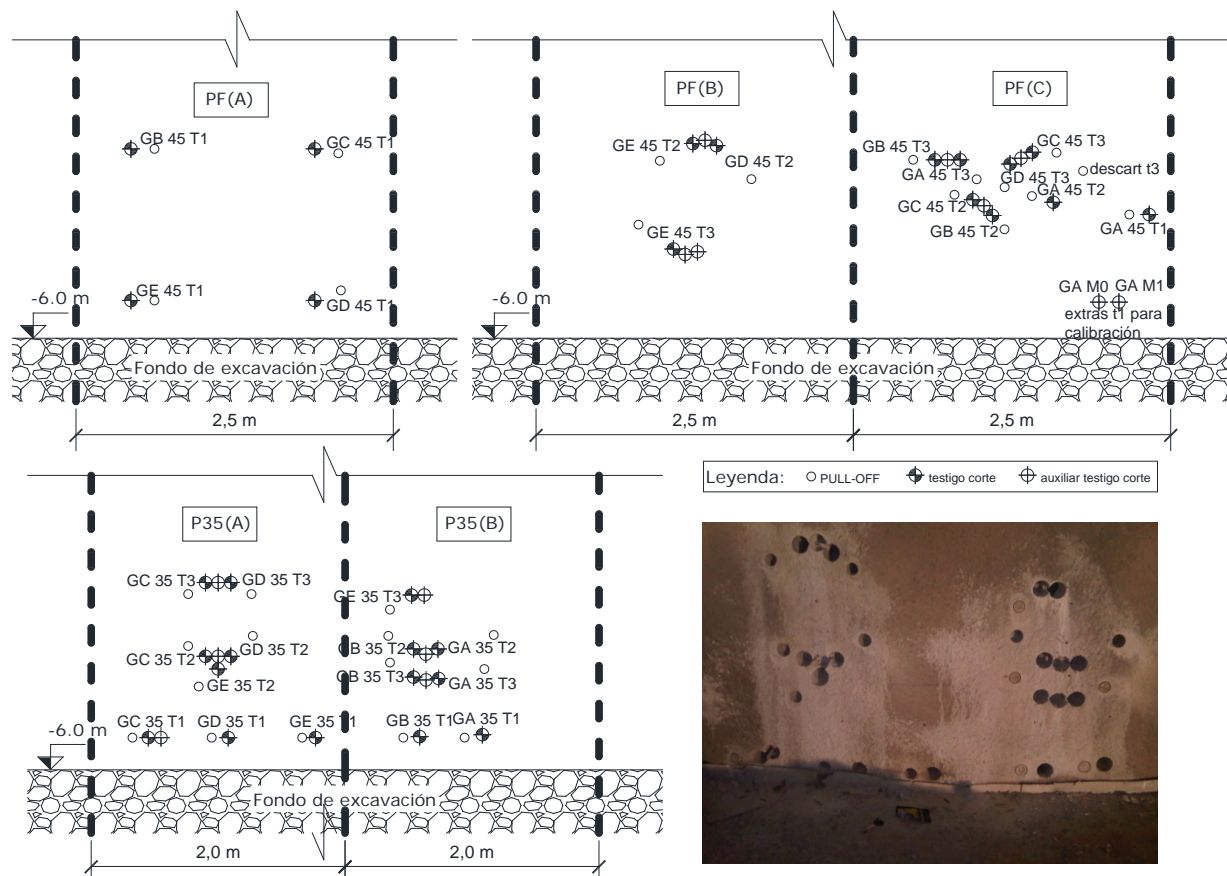

Fig. 58 - Esquema de posiciones de extracción de testigos para el ensayo de corte y de realización de ensayos pull-off in-situ para las distintas preparaciones, e imagen de la pantalla luego de realizadas las extracciones

A1.3.2.   Zonas de extracción de testigos

Para poder relacionar los resultados de ambos ensayos se extrajeron, en cada zona y para cada tiempo, el testigo necesario para el ensayo de corte junto al lugar donde se realizó el ensayo pull-off. En la **Fig. 58** se pueden observar las posiciones en las que se realizaron las extracciones y los ensayos. Si bien originalmente se eligió una distribución regular para realizar los ensayos (ver la distribución de los ensayos "T1", correspondientes a la primera edad.), debido que el paramento no era completamente plano, sino que presentaba un relieve con suaves protuberancias generadas por el proyectado, fue necesario extraer los testigos con una distribución irregular. Se eligieron estas zonas para disponer la máquina de extracción de testigos, lo más perpendicular al plano medio del paramento del muro.

A1.3.3. Ensayo a corte

De los ensayos descriptos en la introducción se eligió, para el ensayo a corte, el ensayo LCB-modificado. En la **Fig. 59** se observa un esquema del dispositivo y una fotografía del ensayo. El ensayo se basa en la norma (NLT-382/08, 2008), pensada para la evaluación de la adherencia en capas de firme compuestas por materiales bituminosos (Miró Recasens et al., 2005), materiales mucho más dúctiles que el hormigón y cuyas propiedades son mucho más sensibles a las variaciones de temperatura.

Por tal motivo, se suprimió la cámara de control de temperatura y se redujo la velocidad de desplazamiento del pistón de carga, de 2,5 mm/mm, a un valor en el orden de los usados para ensayos de corte en hormigón: 0,25 mm/min (Mirsayah & Banthia, 2002; Ray et al., 2005; Wall & Shrive, 1988). Para reducir la concentración de tensiones en los apoyos, se colocó una lámina fina de neopreno entre el dispositivo y el testigo. En la realización de los ensayos se ha utilizado una prensa hidráulica con control de desplazamientos.
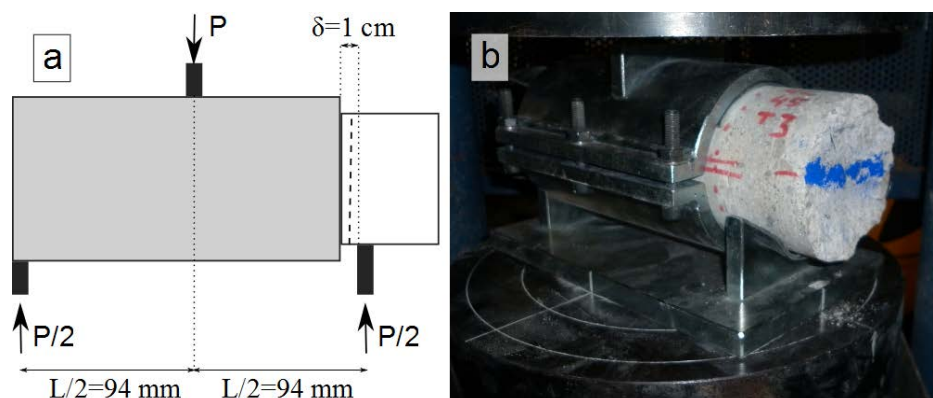

Fig. 59 - Ensayo de Corte LCB: (a) Esquema del dispositivo, (b) Configuración del ensayo

La razón de ser de la elección de este ensayo responde a dos motivos: por un lado, permite ensayar a corte testigos extraídos, por otro lado, permite ensayar más fácilmente uniones irregulares entre capas (problema reportado para el ensayo "gillotina" (Delatte Jr. et al., 2000)) ya que deja un pequeño espacio entre los bordes de introducción de carga. Sin embargo, al tener esta separación, la componente de flexión que actúa en la unión a ensayar es mayor.

La tensión rasante que aparece en la zona de la interfase correspondiente a la junta se calcula según la fórmula:

$$\tau = (P/2)/S \qquad\qquad (12)$$

dónde: τ = tensión de corte (en MPa)

P = fuerza máxima de falla (en N)

S = área de la sección transversal del espécimen (en mm2)

A1.3.4. Ensayo pull-off

El ensayo pull-off es uno de los métodos de ensayo a tracción más comúnmente utilizados para evaluar la adherencia entre dos hormigones. De acuerdo a la norma (ASTM, 2009), el procedimiento de ensayo

consiste en pegar, mediante un adhesivo, un disco de carga a la superficie de la segunda capa. Luego de que el adhesivo se ha endurecido, un dispositivo de carga se fija al disco de carga y se alinea, de forma de que la fuerza se ejerza en dirección perpendicular a la superficie a ser evaluada. La fuerza aplicada por el dispositivo se va aumentando gradualmente y de la forma más homogénea y continua posible, de acuerdo a un ritmo de carga previamente estipulado. La falla ocurre en el plano más débil del sistema compuesto por el disco de carga, el adhesivo, ambas capas de hormigones, y cada una de las interfaces entre los componentes anteriores. En la **Fig. 60** se puede ver una foto y esquema del mismo.

Una limitación de este tipo de ensayo, es su relativamente poca precisión, evidenciada por las grandes variaciones de resultados que se obtienen con diferentes dispositivos (Bonaldo et al., 2005). Además, los resultados dependen de algunos factores como la profundidad del testigo dentro de la capa base, el espesor de la segunda capa y la excentricidad de la carga (Simon Austin et al., 1995). En este sentido, si no se garantiza la ortogonalidad de la perforación, la excentricidad de la carga aumentará con la profundidad de perforación. También se cree que aumentando la profundidad de excavación, aumenta el daño al testigo generado por las vibraciones de la broca de corte. Además de los aspectos señalados, (Simon Austin et al., 1995) describen otras cuestiones relativas al ensayo, como propiedades de los materiales ensayados, condiciones de superficie, geometría, carga, y efectos de disparidad de materiales.
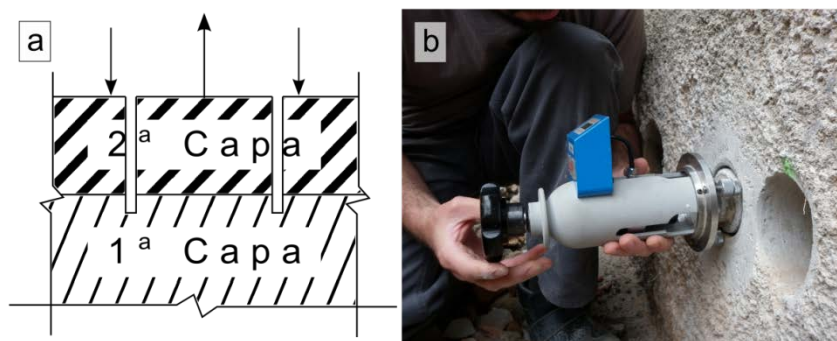

Fig. 60 - Ensayo Pull-off: (a) Esquema del ensayo, (b) Configuración del ensayo

A1.4.   RESULTADOS Y ANALISIS

Los resultados se presentan en los tres apartados siguientes, pudiéndose consultar la totalidad de los resultados referidos al ensayo de corte (Apartado A1.4.1), así como un análisis de los mismos, en Segura-Castillo & Aguado (2012).

A1.4.1.   Resultados principales del ensayo de corte

En la **Fig. 61** se grafica el valor medio obtenido para cada edad, de ambas preparaciones superficiales. En la **Fig. 62** se grafica la dispersión estándar calculada para cada edad de ambas preparaciones superficiales.

A1.4.1.1.   *Preparación por fresado*

Para las distintas edades se obtuvieron dispersiones homogéneas (entre 0.05 MPa y 0.18 MPa). Se puede observar claramente el aumento del valor de la resistencia a corte al aumentar la edad. En la **Fig. 61** se traza a su vez la curva de mejor ajuste, se presenta la ecuación de dicha curva y su valor de R^2. Dicha ecuación es de la forma de la función de Plowman modificada:

$$\tau = A + B * log \ (madurez) \tag{13}$$

dónde: τ = tensión de corte

       A, B = constantes a determinar

       madurez = término definido por la función de Nurse-Saul:

$$madurez = \Sigma(T\text{-}T_0) \ \Delta t \tag{14}$$

dónde: T_0 = temperatura "datum", usualmente -10ºC

       Δt = intervalo de tiempo

Por lo que, en concordancia con el estudio de (Delatte et al., 2000), la evolución de la resistencia a corte, para la segunda fase realizada con hormigón proyectado, se ajusta perfectamente al modelo de maduración si se supone que la temperatura media del hormigón, para el transcurso de tiempo estudiado, es constante. Esta es una hipótesis razonable si se considera que el elemento es de un espesor pequeño y está en contacto con el terreno.
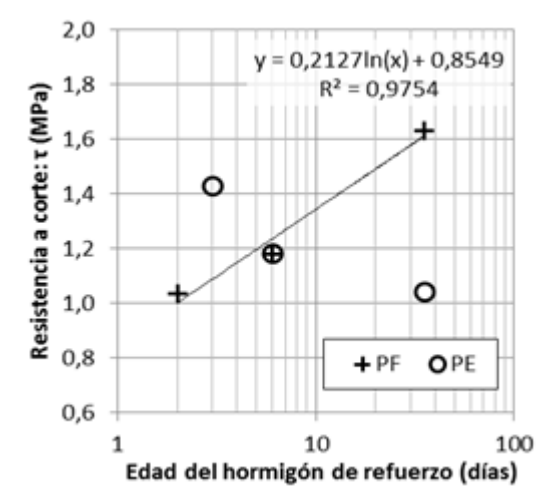

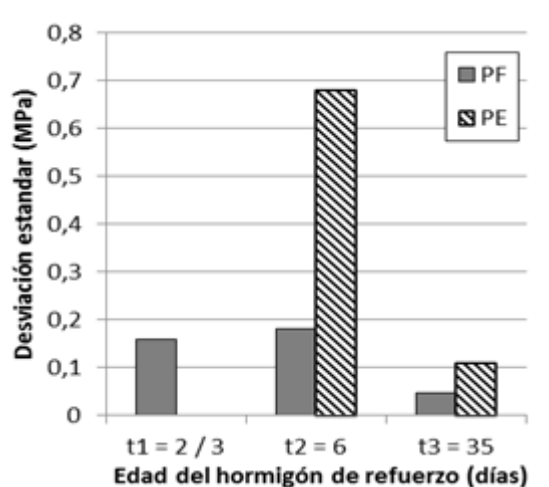**Fig. 61 - Resistencia a corte vs edad del hormigón de 2ª fase**

Fig. 62 - Desviación estándar obtenida para las distintas edades

A1.4.1.2.   Preparación con puente de adherencia epoxi

En la primer edad (t=3 días) solo se pudo ensayar un testigo, por lo que no se puede evaluar la dispersión para este tiempo. Para las otras dos edades consideradas, se obtuvieron dispersiones muy diferentes. En la segunda edad (t=6 días) se registró la mayor dispersión (0.68 MPa), y en la tercer edad, una dispersión mucho menor (0.11 MPa).

Se adjudica la mayor variabilidad de los resultados del caso PE a las dificultades de aplicación del vínculo de adherencia inherentes de la obra. Luego de aplicar el producto, se debe esperar una hora antes de poder colocar el hormigón de segunda etapa. A su vez, se dispone de un lapso de aproximadamente dos horas para aplicar el producto, luego del cual, el mismo cristaliza, reduciendo notablemente la capacidad adherente entre hormigones. Si se considera la dificultad de prever con precisión los tiempos de hormigonado cuando se realiza mediante proyectado, se puede concluir que es probable que se encuentren zonas de muy variada resistencia en el vínculo. Por otro lado, al ser un producto de aplicación manual, se depende de la experiencia del operario para su colocación, lo que añade un factor extra que añade más dispersión a los resultados.

Se observa un descenso de la resistencia al aumentar la edad. (Tu & Kruger, 1996) también registraron una caída de la resistencia luego de 14 días, adjudicando la misma, al deterioro que causa en el epoxi el agua que migra desde el hormigón fresco, y se acumula gradualmente en la interface unida por el epoxi.

A1.4.2.   Resultados pull-off

En la **Table 23**, incluida en el Anexo, se presentan los resultados obtenidos para el ensayo pull-off. Los resultados válidos para nuestro estudio, es decir, aquellos con rotura en la interfase entre capas (R.I. en la **Table 23**), se grafican en las **Fig. 63** y **Fig. 64**, para la preparación superficial por fresado y con Epoxi respectivamente.
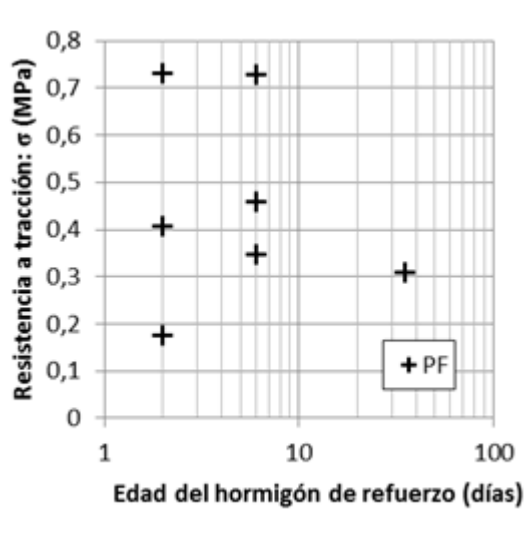

Fig. 63 - Resistencia a tracción vs edad del hormigón de 2ª fase para preparación por Fresado

Se puede observar la gran dispersión en los resultados obtenidos para todas las edades y en ambos tipos de preparaciones. Se adjudica principalmente a dos motivos la existencia de estas grandes dispersiones. Por un

lado, al gran espesor de la 2ª capa de hormigón (teniendo en cuenta el espesor previsto en el diseño), y por otro, a las desviaciones angulares registradas entre elemento de extracción, eje del testigo, y dirección perpendicular al paramento. Como se ha comentado en la introducción de este artículo, ambos sucesos son comunes en este tipo de ensayo pero, por los motivos que se indican a continuación, parecen agravarse notoriamente en este caso concreto.
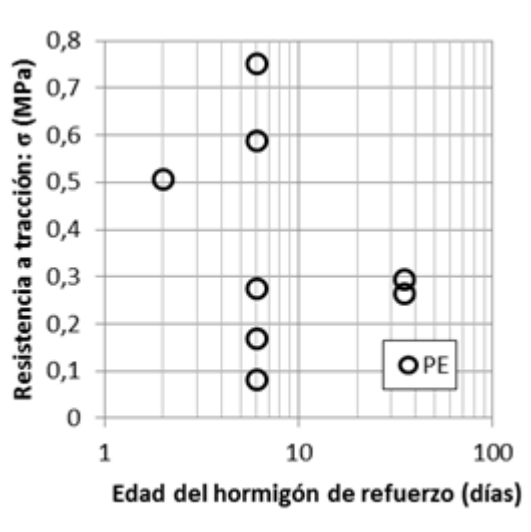

Fig. 64 - Resistencia a tracción vs edad del hormigón de 2ª fase para preparación con adhesivo Epoxi

El espesor previsto en diseño para la segunda capa de hormigón era de 10cm. Por las heterogeneidades propias del sistema de proyección, resulta difícil lograr un espesor homogéneo, dependiendo en gran medida de la habilidad del operario realizando la tarea. Como se puede observar en la **Table 23 (ver Anexo)**, los espesores registrados para la segunda capa van desde 8,5 cm a 16,0 cm, que es, en algunos casos, un aumento considerable si se compara con los usualmente utilizados en los trabajos de referencia (Simon Austin et al., 1995; Bonaldo et al., 2005; Delatte Jr. et al., 2000; Júlio et al., 2005; Momayez et al., 2005; Talbot et al., 1994), que van hasta 10 cm como máximo.

Por otro lado, por el sistema de construcción de los muros pantalla bi-capa, es difícil controlar los ángulos que forman el paramento, la unión entre capas, el eje de perforación del testigo y el eje de esfuerzo del dispositivo de carga.

En la **Fig. 65** se observa un esquema de una sección del muro. La primera capa de hormigón es formada por el sistema tradicional de construcción de los muros continuos. Por lo tanto, la forma de la superficie exterior queda determinada por la forma en la que se ha escavado el terreno. La homogeneidad del plano exterior depende en gran medida de la maquinaria con la que se ha realizado la excavación y del tipo de suelo en el que esta se inserta. Dependiendo de estas variables es común, en mayor o menor medida, el desprendimiento de parte del suelo de los paramentos de la excavación, dando lugar luego del hormigonado a la formación de "barrigas". En la cara interior del muro, una vez expuesta luego de realizada la excavación interior, es común la realización de un fresado de homogenización, en donde se eliminan estas "barrigas". De todos modos, aún pueden permanecer variaciones más suaves a lo largo del paramento. En la **Fig. 65** se denotó como α_1 al ángulo producido entre el plano promedio del muro y el plano en una posición específica.
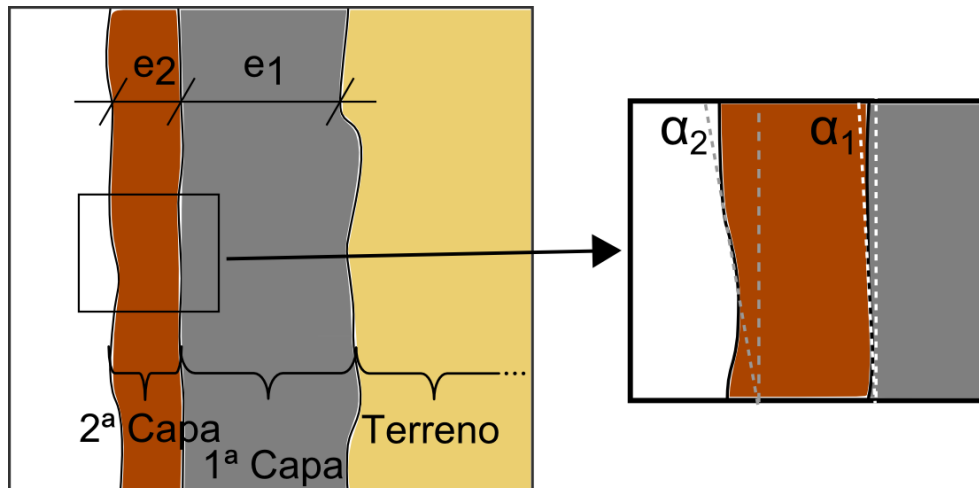
Fig. 65 - Esquema de irregularidades en la interfase entre capas y superficie de pantallas

La segunda capa es formada mediante hormigón proyectado. Lo dicho anteriormente respecto a la dificultad en controlar es espesor de la capa de proyectado implica directamente la formación de un nuevo ángulo del paramento respecto al plano medio de la pantalla. En la **Fig. 65** se denotó como α_2 a dicho ángulo. En la **Fig. 66** se ve una foto de la obra experimental luego de acabo el proyectado. Se puede observar claramente el acabado con superficie irregular.

Para realizar correctamente el ensayo, sería necesario alinear perpendicularmente al plano determinado por α_1 la máquina para realizar la perforación parcial del testigo. En la experiencia realizada no hemos logrado encontrar una forma de realizar eficientemente esta alineación. Cabe mencionar que se debieron realizar un conjunto grande de ensayos en un período limitado de tiempo, disponiendo de poco margen (tanto de tiempo, como de recursos humanos) para solucionar los problemas que surgían en el transcurso de la experimentación.

Fig. 66 - Foto del acabado final del proyectado en los muros Bi-Capa

Viendo los resultados obtenidos y considerando los comentarios anteriormente realizados, se puede afirmar que, claramente, durante el diseño de la campaña experimental se subestimó la influencia de los aspectos

negativos que afectan al ensayo pull-off para la utilización en este caso. Como caso extremo de estas desalineaciones, en la **Fig. 67** se observa la imagen de uno de los testigos extraídos mediante el ensayo pull-off.

Fig. 67 - Ejemplo de desalineaciones sufridas durante la realización del ensayo pull-off

A1.4.3. Relación corte/pull-off

Se ha indicado anteriormente que varios resultados de cada serie debieron ser descartados. En este apartado se analizan los resultados para los cuales se obtuvo un ensayo válido para ambos tipos de ensayos. Las parejas válidas se grafican en las **Fig. 68** y **Fig. 69**, para la preparación superficial por fresado y con Epoxi, respectivamente. Las gráficas relacionan la resistencia a tracción alcanzada por el ensayo pull-off y la resistencia obtenida mediante el ensayo de corte, y en cada una se discrimina a su vez la edad en la que se ha realizado el ensayo.
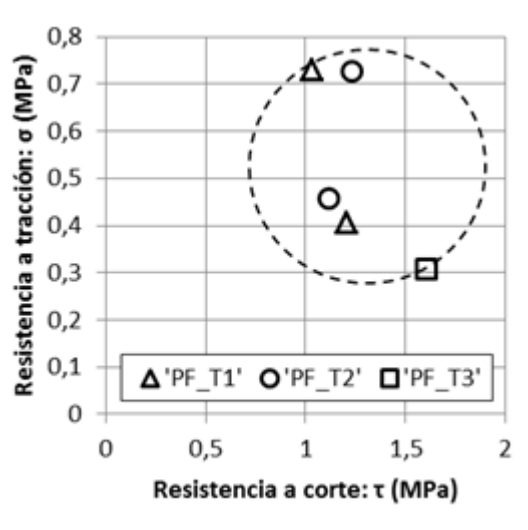
Fig. 68 - Resistencia a tracción vs Resistencia a corte para preparación por Fresado

En la **Fig. 69** se incluye línea de mejor ajuste para la totalidad de los valores (es decir, sin diferenciar por edad de ensayo). A pesar de la dispersión mencionada en el apartado anterior, se observa una leve correlación para los ensayos realizados en la superficie con epoxi. Que ambos ensayos brinden resultados correlacionados, induce a pensar que la dispersión obtenida es producida por las dispersiones en el valor de

la adherencia, y no a que son producto del ensayo utilizado, confirmando lo planteado en el apartado A1.4.1.2 referido a la variabilidad de la respuesta del epoxi cuando es utilizado en esta aplicación.
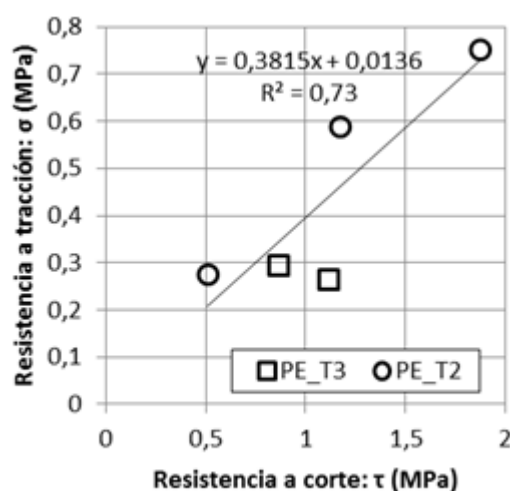

Fig. 69 - Resistencia a tracción vs Resistencia a corte para preparación con adhesivo Epoxi

Para las parejas relacionando las resistencias obtenidas para la superficie fresada, la correlación entre ambos ensayos se pierde, pudiéndose observar simplemente una zona de concentración de valores.

A1.5.   CONCLUSIONES

El presente estudio experimental analiza los muros pantalla bi-capa, particularmente, la adherencia alcanzada entre el hormigón de la segunda capa, colocado mediante proyectado, y el de la primera capa, perteneciente a una pantalla continua, previamente fresada; y la búsqueda de un ensayo factible de ser utilizado para el control rutinario de dichas pantallas. Las siguientes conclusiones pueden ser extraídas:

- La resistencia al corte con la superficie tratada con fresado aumenta con la edad del hormigón de segunda fase, ajustándose a las fórmulas de maduración. Para el mismo ensayo, la preparación de la superficie con Epoxi en obra presenta gran dispersión de resultados, con un CV de hasta 57% en el peor de los casos.

- Debido a las características del elemento propuesto, principalmente el espesor de la segunda capa y las variaciones del plano de interfase y del paramento interior con el plano medio de la pantalla, el ensayo pull-off registra una gran dispersión de valores.

- No se puede por lo tanto, en las condiciones en las que se realizó esta experiencia, recomendar la utilización de este ensayo para el control rutinario de la adherencia.

- A la vista de los resultados obtenidos, para la utilización en muros bi-capa o grandes superficies en general, salvo que se realicen controles rigurosos en los tiempos de disposición y ejecución del puente de adherencia y del proyectado del hormigón, no es aconsejable la utilización de productos epoxi.

Debido a la gran dispersión obtenida en las distintas series para el ensayo pull-off, consideramos que la correlación analizada en este apartado debe ser tomada como un resultado meramente orientativo, siendo necesario repetir la experiencia, tomando precauciones especiales para el control de la perpendicularidad y el espesor de capa, para poder extraer conclusiones generales sobre la relación entre ambos ensayos.

A1.6.   AGRADECIMENTOS

A1.7.   ANEXO – Resultados experimentales del ensayo pull-off

Table 23 - Resultados ensayo pull-off.

Descripción	Pantalla	Preparación superficial	Nombre Edad	Valor Edad (días)	Validez	Forma de rotura	Espesor capa proyectado (cm)	Fuerza de rotura (Kg)	Área de sección de rotura (cm2)	Carga de rotura (Kg/cm2)
GA-35-t1	35	PE	T1	2	Rech.	R.S.		191,0	20	9,55
GB-35-t1	35	PE	T1	2	Rech.	R.S.		98,0	20	4,9
GE-35-t1	**35**	**PE**	**T1**	**2**	**Acept.**	**R.I.**	**15,0**	**210,9**	**41,51**	**5,08**
GD-35-t1	35	PE	T1	2	Rech.*	R.I.	9,2	---	41,51	---
GC-35-t1	35	PE	T1	2	Rech.	R.S.		264,0	20	13,2
GA-45-t1	45	PF	T1	2	Rech.	R.S.		196,0	20	9,8
GC-45-t1	**45**	**PF**	**T1**	**2**	**Acept.**	**R.I.**	**16,0**	**303,9**	**41,51**	**7,32**
GB-45-T1	**45**	**PF**	**T1**	**2**	**Acept.**	**R.I.**	**12,9**	**168,9**	**41,51**	**4,07**
GE-45-t1	45	PF	T1	2	Rech.	R.S.		22,2	20	1,11
GD-45-t1	**45**	**PF**	**T1**	**2**	**Acept.**	**R.I.**	**8,5**	**73,1**	**41,51**	**1,76**
GA-35-t2	**35**	**PE**	**T2**	**6**	**Acept.**	**R.I.**	**11,0**	**313,0**	**41,51**	**7,54**
GB-35-t2	**35**	**PE**	**T2**	**6**	**Acept.**	**R.I.**	**9,5**	**244,1**	**41,51**	**5,88**
GC-35-t2	**35**	**PE**	**T2**	**6**	**Acept.**	**R.I.**	**8,5**	**34,0**	**41,51**	**0,82**
GD-35-t2	**35**	**PE**	**T2**	**6**	**Acept.**	**R.I.**	**12,6**	**70,2**	**41,51**	**1,69**
GE-35-t2	**35**	**PE**	**T2**	**6**	**Acept.**	**R.I.**	**11,2**	**114,2**	**41,51**	**2,75**
GA-45-t2	**45**	**PF**	**T2**	**6**	**Acept.**	**R.I.**	**16,0**	**144,0**	**41,51**	**3,47**
GB-45-t2	**45**	**PF**	**T2**	**6**	**Acept.**	**R.I.**	**15,7**	**302,2**	**41,51**	**7,28**
GC-45-t2	**45**	**PF**	**T2**	**6**	**Acept.**	**R.I.**	**14,3**	**190,1**	**41,51**	**4,58**
GD-45-t2	45	PF	T2	6	Rech.	R.S.		180,0	20	9
GE-45-t2	45	PF	T2	6	Rech.	R.S.		186,0	20	9,3
GC-35-t3	**35**	**PE**	**T3**	**35**	**Acept.**	**R.I.**	**10,7**	**94,9**	**32,17**	**2,95**
GD-35-t3	**35**	**PE**	**T3**	**35**	**Acept.**	**R.I.**	**13,0**	**84,9**	**32,17**	**2,64**
GE-35-t3	35	PE	T3	35	Rech.	R.A.		233,0	20	11,65
GB-35-t3	35	PE	T3	35	Rech.	R.A.		223,0	20	11,15
GA-35-t3	35	PE	T3	35	Rech.	R.A.		263,0	20	13,15
GC-45-t3	**45**	**PF**	**T3**	**35**	**Acept.**	**R.I.**	**14,4**	**99,1**	**32,17**	**3,08**
GD-45-t3	45	PF	T3	35	Rech.	R.A.		58,0	20	2,9
GA-45-t3	45	PF	T3	35	Rech.	R.A.		167,0	20	8,35
GB-45-t3	45	PF	T3	35	Rech.	R.A.		157,0	20	7,85
GE-45-t3	45	PF	T3	35	Rech.	R.A.		85,0	20	4,25

Códigos de tipos de Rotura:
R.S.   = Rotura interna superficial del hormigón proyectado.
R.I.   = Rotura por la interfase entre el hormigón proyectado y el hormigón de pantalla
R.A.   = Rotura por la interfase entre el adhesivo y el hormigón proyectado.
Comentarios:
* Rechazado debido a rotura defectuosa